5-2022

The Impacts of Increased Precipitation Intensity on Dryland Ecosystems in the Western United States

Martin C. Holdrege
Utah State University

THE IMPACTS OF INCREASED PRECIPITATION INTENSITY ON DRYLAND ECOSYSTEMS IN THE WESTERN UNITED STATES

by

Martin C. Holdrege

A dissertation submitted in partial fulfillment
of the requirements for the degree

of

DOCTOR OF PHILOSOPHY

in

Ecology

Approved:

_____ Andrew Kulmatiski, Ph.D. Co-Major Professor	_____ Karen H. Beard, Ph.D. Co-Major Professor
_____ Peter B. Adler, Ph.D. Committee Member	_____ Kyle A. Palmquist, Ph.D. Committee Member
_____ D. Richard Cutler, Ph.D. Committee Member	_____ D. Richard Cutler, Ph.D. Interim Vice Provost of Graduate Studies

UTAH STATE UNIVERSITY
Logan, Utah

2022

ABSTRACT

The Impacts of Increased Precipitation Intensity on Dryland Ecosystems in the Western United States

by

Martin C. Holdrege, Doctor of Philosophy

Utah State University, 2022

Major Professors: Dr. Andrew Kulmatiski and Dr. Karen H. Beard
Department: Wildland Resources

Increases in precipitation intensity have been predicted and observed as a result of global warming. However, disagreement exists regarding how different ecosystems will respond to such changes, and studies are lacking in many ecosystem types. My dissertation addresses how increased precipitation intensity affects soil water availability, and how plants responds to any such changes. I address these questions in the context of big sagebrush ecosystems (Chapters 2 & 4) and dryland winter wheat production (Chapter 3). I used both experimental (Chapters 2 & 3) and ecohydrological modeling (Chapter 4) approaches. In all cases treatments created fewer but larger precipitation events, without changing total annual precipitation. The results suggest that these fewer larger storms will decrease evaporation, and increase percolation depth and deep drainage. In agreement with the two-layer hypothesis, both the field experiment and simulations showed that shrubs preferentially benefited from the increases in water availability in deeper soil layers. In contrast, more shallowly rooted grasses and forbs had

little increase in water uptake from deep soils and did not exhibit consistent changes in transpiration or biomass. Therefore, this change in the soil water profile provides a mechanism for greater shrub dominance, which suggests that increases in precipitation intensity may contribute to globally observed woody plant encroachment. However, the simulations suggest that the positive effect on water availability and shrub growth should not be expected in mesic sites, where the biggest effect of larger precipitation events was to cause more water losses to deep drainage. Similar to herbaceous plant growth in sagebrush ecosystems, production of dryland winter wheat was not affected by increased precipitation intensity. This may be in part because winter wheat is a crop that matures early in the growing season, which is before the impacts of the treatments on soil moisture were most apparent. The results from this research underscore that responses to increased precipitation intensity are likely to differ between plant functional types and, more broadly, that it is important to account for climatic variability when forecasting ecological responses to climate change.

(201 pages)

PUBLIC ABSTRACT

The Impacts of Increased Precipitation Intensity on Dryland Ecosystems in the Western United States

Martin C. Holdrege

As the atmosphere warms, precipitation events become larger, but less frequent. Such increases in precipitation intensity are expected regardless of changes in total annual precipitation. Despite strong evidence for increases in precipitation intensity, disagreement exists regarding how these changes will impact plants, and studies are lacking in many types of ecosystems. This dissertation addresses how increased precipitation intensity affects soil water availability, and how plants respond to any such changes. I address this question in the context of big sagebrush ecosystems and dryland winter wheat agriculture, which are both environments that can be sensitive to changes in water availability. Results from two field experiments (Chapters 2 & 3) and modelling (Chapter 4) indicate that fewer larger precipitation events cause water to be 'pushed' deeper into the ground. In sagebrush ecosystems this benefitted shrubs, because they tend to have deeper roots and could preferentially access the deeper soil water. The model simulations indicate that these positive effects on shrub growth should be expected in dry climates, but not in wetter climates where larger precipitation events caused more water to be lost to deep drainage. By comparison, increased precipitation intensity had little effect on more shallowly rooted herbaceous plants in sagebrush ecosystems. Similarly, production of winter wheat was not affected by increased precipitation intensity, potentially because this crop matures early in the growing season, while changes in soil

moisture were most apparent only later in the summer. My research shows that responses to increased precipitation intensity are likely to differ between plant types and that larger precipitation events may contribute to patterns of increasing dominance of woody plants that can be observed globally. More broadly, these results stress the importance of accounting for climatic variability when forecasting ecological responses to climate change.

ACKNOWLEDGMENTS

Firstly, I would like to thank my two advisors, Dr. Andrew Kulmatiski and Dr. Karen Beard. They have been dedicated mentors throughout my time as a graduate student. Without their continued support this dissertation would not have been possible. I would also like to thank my committee members, Drs. Peter Adler, Richard Cutler, and Kyle Palmquist. Peter taught me to think carefully and critically about hard ecological questions, Richard was instrumental in furthering my passion for data analytics, and without Kyle's expertise and excellent mentorship I would not have been able to use ecohydrological modelling in my research. Thank you to Marsha Bailey for always having answers to a myriad of questions about graduate school. For their funding support, I would like to thank the Utah Agricultural Experiment Station, the Ecology Center, and the Department of Wildland Resources.

I would like to thank the many technicians who over the years have spent countless hours in the field with me in all types of weather. More personally, I am thankful to all the people in the Utah State graduate student community who make it a welcoming place to be. Thank you to Kendall Becker, Erika Blomdahl, Gwendŵr Meredith, David Soderberg, and most importantly my partner Hope Braithwaite, for friendship, adventures, and discussions on science and life. Lastly, I am eternally grateful to my parents and two sisters for supporting me and always being only a phone call away.

Martin C. Holdrege

CONTENTS

Page

LIST OF TABLES

LIST OF FIGURES

CHAPTER 1

INTRODUCTION

Changes in both the mean and variability of temperature and precipitation are expected with climate change. Older studies on the ecological impacts of altered precipitation regimes focused on changes in the total amount of precipitation (e.g., Arkin et al., 1976), and until more recently there has been little emphasis on changes in precipitation variability. Both increases and decreases in total precipitation are anticipated depending on region (Sharma & Ojha, 2019). However, increases in the variability of precipitation are expected regardless of changes in total precipitation (Donat et al., 2016). Increases in precipitation variability range from the multi-year scale (e.g., multi-year droughts followed by wet years), to the individual precipitation event (e.g., change in size and frequency). In this dissertation I focus on the ecological effects of increased precipitation intensity. "Increased precipitation intensity," as I use the phrase here, refers to a decrease in the number of days that receive precipitation and an increase in the amount of precipitation received on those days, without necessarily a change in total precipitation.

While increases in precipitation intensity are nearly universally anticipated, the magnitude of these changes and how the shape of the distribution of event sizes will be altered, remains uncertain (Herold et al., 2017). The Clausius-Clapeyron relation shows that there is a 7%/°C increase in water holding capacity of air (i.e., saturation vapor pressure), and this rate has been used as a prediction for increased precipitation intensity (O'Gorman & Muller, 2010). As the atmosphere warms, a larger pool of water can be stored in the atmosphere, thereby creating larger precipitation events. In addition to this

thermodynamic component (i.e., changes in the amount of atmospheric water vapor), complex dynamic factors also play a role in the intensification of precipitation, including changes in the vertical motion of air in the atmosphere (Chou et al., 2012). Therefore, actual changes in precipitation intensity vary from the 7%/°C rate (Pendergrass, 2018).

Historical precipitation data from the United States indicates there has been a 16%/°C increase in mean precipitation event size (Myhre et al., 2019). Modeling and observational results suggest that most extreme (rare) events will increase at a faster rate than 7%/°C, with remainder of the distribution shifting more slowly (Fischer & Knutti, 2016; Pendergrass & Knutti, 2018). These increases in intensity happen in two ways, big events becoming more frequent (e.g., more days that receive 3 cm events), and big events becoming bigger (e.g., the biggest event of the year going from 4 cm to 5 cm). Greater changes in the former (frequency) are expected relative to the latter (size) (Pendergrass & Hartmann, 2014). Du et al. (2019) present results from global climate models showing that the annual precipitation maximum (biggest precipitation event of the year) may increase roughly 25% by the end of the century under representative concentration pathway (RCP) 8.5 and 10% under RCP 4.5. Observational and modeling results differ in the magnitude of changes in precipitation intensity (Myhre et al., 2019), and uncertainties exist in both approaches (Pendergrass & Hartmann, 2014). However, the overall message is clear: We should expect fewer and larger precipitation events in the future.

Despite the strong evidence of increased precipitation intensity, disagreement exists in the literature regarding how different ecosystems will respond, and studies are limited or lacking in many ecosystem types. Knapp et al. (2008) suggested that increased precipitation intensity could have either positive or negative impacts on plants, depending

on how specific climatic and edaphic conditions affect water fluxes. While this hypothesis has been frequently suggested, it has rarely been tested directly (Hou et al., 2021).

Water entering an ecosystem as precipitation is lost in one of four ways: evaporation (from plants, litter, or surface soils), run-off, deep drainage, or transpiration. The role of these fluxes is well understood, but good estimates of their relative magnitudes can be challenging to make (Sun et al., 2019). Without a change in total precipitation, changes in transpiration must be caused by changes in partitioning of water to evaporation, run-off, and drainage. Fewer larger precipitation events may reduce evaporation because a lower proportion of the water is intercepted by vegetation, and the water percolates deeper into the ground where it can escape evaporation (Knapp et al., 2008). However, this deeper percolation may in turn lead to increased water losses to deep drainage past the rooting zone. If events are sufficiently large, or if soils limit infiltration, then increased precipitation intensity could also cause increased run-off (Knapp et al., 2008).

Responses to increased precipitation intensity may vary with climate due to differential impacts on evaporation or drainage (Heisler-White et al., 2008; Liu et al., 2020). Studies are generally in agreement that increased precipitation intensity tends to benefit plant productivity in arid areas but decrease productivity in mesic areas (Liu et al., 2020; Wilcox et al., 2015; Zeppel et al., 2014). However, many of these studies have focused on temperate grasslands with warm-season precipitation regimes or on subtropical savannahs (but see Ritter et al., 2020). It is unclear whether the same general response is likely to occur in shrublands or croplands in temperate climates with winter-

dominated precipitation regimes. While experiments have also been conducted in agricultural systems, they have mostly been in mesic locations (e.g., Drebenstedt, Hart, et al., 2020; Drebenstedt, Schmid, et al., 2020; Poll et al., 2013), and less is known about potential responses in drier locations.

In addition to differences in climate, the effects of increased precipitation intensity are also likely to depend on vegetation characteristics. Walter's two layer hypothesis states that niche partitioning between woody and herbaceous plants occurs, at least in part, because of differential access to shallow and deep soil water resources (Walter, 1971; Ward et al., 2013). Therefore, increased precipitation intensity may preferentially benefit more deeply rooted woody plants through deeper percolation of soil water. This expectation is consistent with experiments that increased precipitation intensity in a savannah (Kulmatiski & Beard, 2013) and interannual precipitation variability in a desert shrubland (Gherardi & Sala, 2015), both of which found positive growth responses of woody but not herbaceous plants. However, some observational studies have found negative woody plant responses to increased intensity (Good & Caylor, 2011; Ritter et al., 2020; Xu et al., 2018). There remains, therefore, disagreement about how and under what conditions increased precipitation intensity might change woody dominance.

The research presented in this dissertation broadly pertains to dryland ecosystems, and specifically focuses on big sagebrush dominated ecosystems (Chapters 2 & 4) and dryland winter wheat production (Chapter 3) in the Western United States. Understanding the impacts of increased precipitation intensity is especially important in these water limited or 'dryland' ecosystems, because they are most sensitive to changes in soil

moisture (Noy-Meir, 1973). Dryland ecosystems, which include both unmanaged ecosystems and rain-fed agricultural systems, are defined as having an annual precipitation to evapotranspiration ratio of less than 0.65, and represent over 40% of global land cover (Prăvălie, 2016). Big sagebrush ecosystems are dominant in drylands of the western United States (Rigge et al., 2020). Understanding how sagebrush ecosystems will respond to changes in the climate is especially important, because they have already declined over 45% from their original distribution, and many obligate species rely on these ecosystems (Remington et al., 2021). Despite their importance, little is known about how these types of ecosystems will respond to increased precipitation intensity (but see Ritter et al. [2020] and Sala et al., [2015], who incorporated some climate data from the region). A key aspect of the ecohydrology of sagebrush ecosystems, and of dryland agriculture in this region, is that deep recharge of soil water occurs in late winter and spring due to rainfall and snowmelt, and plants access this stored water during the growing season (Lauenroth et al., 2014; Schlaepfer et al., 2012). This makes these ecosystems ecohydrologically different from those in which several previous manipulative experiments have been conducted, which more strongly rely on water pulses during the growing season (e.g., Wilcox et al., 2015).

No single type of study can fully assess ecosystem responses to increased precipitation intensity and therefore applying more than one approach can be useful. Observational studies can address questions at large spatial and temporal scales; however, it can be challenging to isolate the mechanisms driving observed patterns. Assessing causal effects of climate variables using observational studies is especially challenging due to often strong correlations between the variables (Dolby, 2021). By comparison,

manipulative field experiments are the gold standard for addressing causal links. However, field experiments are costly, which creates limitations on the number of scenarios that can be tested, and inference is often constrained to a limited spatial extent or ecosystem type. Process-based modeling approaches do not have these shortcomings because such models can be applied at broad spatial and temporal scales, and across many climate scenarios. However, there is uncertainty in how well underlying processes are represented in models, as well as uncertainty in the estimates of parameters used (Turley & Ford, 2009). Therefore, there are very real limitations to how accurately such models can estimate ecosystem responses.

To overcome some of these limitations, my collaborators and I conducted two field experiments (Chapters 2 & 3) and one ecohydrological modeling study (Chapter 4) that were broadly meant to help answer 1) how increased precipitation intensity will affect soil water availability, and 2) how plants will respond to any such changes. These questions were asked in the context of big sagebrush (Chapters 2 & 4) and dryland winter wheat (Chapter 3) systems. Both field experiments used the same experimental design and were conducted in sites with very similar climates. This allows for direct comparisons of how different vegetation types (cropland vs. shrubland), respond to increased precipitation intensity. To augment these experiments, the ecohydrological modelling study was used to assess the effects of increased intensity across sites spanning the climate envelope of big sagebrush ecosystems with a large number of treatments (increased precipitation intensity, warming, and soil texture). Because increases in precipitation intensity are near universally expected, but impacts under-studied, these three chapters provide a valuable contribution to our understanding of the effects of this

important component of climate change.

References

Arkin, G. F., Ritchie, J. T., Thompson, M., & Chaison, R. (1976). A Rainout Shelter Installation for Studying Drought Stress 1. *Agronomy Journal*, *68*(2), 429–431. https://doi.org/10.2134/agronj1976.00021962006800020060x

Chou, C., Chen, C. A., Tan, P. H., & Chen, K. T. (2012). Mechanisms for global warming impacts on precipitation frequency and intensity. *Journal of Climate*, *25*(9), 3291–3306. https://doi.org/10.1175/JCLI-D-11-00239.1

Dolby, G. A. (2021). Towards a unified framework to study causality in Earth–life systems. *Molecular Ecology*, *July*, 1–15. https://doi.org/10.1111/mec.16142

Donat, M. G., Lowry, A. L., Alexander, L. V., O'Gorman, P. A., & Maher, N. (2016). More extreme precipitation in the world's dry and wet regions. *Nature Climate Change*, *6*(5), 508–513. https://doi.org/10.1038/nclimate2941

Drebenstedt, I., Hart, L., Poll, C., Marhan, S., Kandeler, E., Böttcher, C., Meiners, T., Hartung, J., & Högy, P. (2020). Do soil warming and changes in precipitation patterns affect seed yield and seed quality of field-grown winter oilseed rape? *Agronomy*, *10*(4). https://doi.org/10.3390/agronomy10040520

Drebenstedt, I., Schmid, I., Poll, C., Marhan, S., Kahle, R., Kandeler, E., & Högy, P. (2020). Effects of soil warming and altered precipitation patterns on photosynthesis, biomass production and yield of barley. *Journal of Applied Botany and Food Quality*, *93*, 44–53. https://doi.org/10.5073/JABFQ.2020.093.006

Du, H., Alexander, L. V., Donat, M. G., Lippmann, T., Srivastava, A., Salinger, J., Kruger, A., Choi, G., He, H. S., Fujibe, F., Rusticucci, M., Nandintsetseg, B.,

Manzanas, R., Rehman, S., Abbas, F., Zhai, P., Yabi, I., Stambaugh, M. C., Wang, S., … Wu, Z. (2019). Precipitation from persistent extremes is increasing in most regions and globally. *Geophysical Research Letters*, *46*(11), 6041–6049. https://doi.org/10.1029/2019GL081898

Fischer, E. M., & Knutti, R. (2016). Observed heavy precipitation increase confirms theory and early models. *Nature Climate Change*, *6*(11), 986–991. https://doi.org/10.1038/nclimate3110

Gherardi, L. A., & Sala, O. E. (2015). Enhanced precipitation variability decreases grass- and increases shrub-productivity. *Proceedings of the National Academy of Sciences*, *112*(41), 12735–12740. https://doi.org/10.1073/pnas.1506433112

Good, S. P., & Caylor, K. K. (2011). Climatological determinants of woody cover in Africa. *Proceedings of the National Academy of Sciences*, *108*(12), 4902–4907. https://doi.org/10.1073/pnas.1013100108

Heisler-White, J. L., Knapp, A. K., & Kelly, E. F. (2008). Increasing precipitation event size increases aboveground net primary productivity in a semi-arid grassland. *Oecologia*, *158*(1), 129–140. https://doi.org/10.1007/s00442-008-1116-9

Herold, N., Behrangi, A., & Alexander, L. V. (2017). Large uncertainties in observed daily precipitation extremes over land. *Journal of Geophysical Research: Atmospheres*, *122*(2), 668–681. https://doi.org/10.1002/2016JD025842

Hou, E., Litvak, M. E., Rudgers, J. A., Jiang, L., Collins, S. L., Pockman, W. T., Hui, D., Niu, S., & Luo, Y. (2021). Divergent responses of primary production to increasing precipitation variability in global drylands. *Global Change Biology*, *July*, gcb.15801. https://doi.org/10.1111/gcb.15801

Knapp, A. K., Beier, C., Briske, D. D., Classen, A. T., Luo, Y., Reichstein, M., Smith, M. D., Smith, S. D., Bell, J. E., Fay, P. a., Heisler, J. L., Leavitt, S. W., Sherry, R., Smith, B., & Weng, E. (2008). Consequences of more extreme precipitation regimes for terrestrial ecosystems. *BioScience*, *58*(9), 811–821. https://doi.org/10.1641/B580908

Kulmatiski, A., & Beard, K. H. (2013). Woody plant encroachment facilitated by increased precipitation intensity. *Nature Climate Change*, *3*(9), 833–837. https://doi.org/10.1038/nclimate1904

Lauenroth, W. K., Schlaepfer, D. R., & Bradford, J. B. (2014). Ecohydrology of Dry Regions: Storage versus Pulse Soil Water Dynamics. *Ecosystems*, *17*(8), 1469–1479. https://doi.org/10.1007/s10021-014-9808-y

Liu, J., Ma, X., Duan, Z., Jiang, J., Reichstein, M., & Jung, M. (2020). Impact of temporal precipitation variability on ecosystem productivity. *Wiley Interdisciplinary Reviews: Water*, *7*(6), 1–22. https://doi.org/10.1002/wat2.1481

Myhre, G., Alterskjær, K., Stjern, C. W., Hodnebrog, Ø., Marelle, L., Samset, B. H., Sillmann, J., Schaller, N., Fischer, E., Schulz, M., & Stohl, A. (2019). Frequency of extreme precipitation increases extensively with event rareness under global warming. *Scientific Reports*, *9*(1), 16063. https://doi.org/10.1038/s41598-019-52277-4

Noy-Meir, I. (1973). Desert Ecosystems: Environment and Producers. *Annual Review of Ecology and Systematics*, *4*, 25–51.

O'Gorman, P. A., & Muller, C. J. (2010). How closely do changes in surface and column water vapor follow Clausius-Clapeyron scaling in climate change simulations?

Environmental Research Letters, *5*(2). https://doi.org/10.1088/1748-9326/5/2/025207

Pendergrass, A. G. (2018). What precipitation is extreme? *Science*, *360*(6393), 1072–1073. https://doi.org/10.1126/science.aat1871

Pendergrass, A. G., & Hartmann, D. L. (2014). Changes in the distribution of rain frequency and intensity in response to global warming. *Journal of Climate*, *27*(22), 8372–8383. https://doi.org/10.1175/JCLI-D-14-00183.1

Pendergrass, A. G., & Knutti, R. (2018). The uneven nature of daily precipitation and its change. *Geophysical Research Letters*, 1–9. https://doi.org/10.1029/2018GL080298

Poll, C., Marhan, S., Back, F., Niklaus, P. A., & Kandeler, E. (2013). Field-scale manipulation of soil temperature and precipitation change soil CO2 flux in a temperate agricultural ecosystem. *Agriculture, Ecosystems and Environment*, *165*, 88–97. https://doi.org/10.1016/j.agee.2012.12.012

Prăvălie, R. (2016). Drylands extent and environmental issues. A global approach. *Earth-Science Reviews*, *161*, 259–278. https://doi.org/10.1016/j.earscirev.2016.08.003

Remington, T. E., Deibert, P. A., Hanser, S. E., Davis, D. M., Robb, L. A., & Welty, J. L. (2021). *Sagebrush conservation strategy-- challenges to sagebrush conservation* (U.S. Geological Survey Open-File Report 2020-1125). https://doi.org/10.3133/ofr20201125.

Rigge, M., Homer, C., Cleeves, L., Meyer, D. K., Bunde, B., Shi, H., Xian, G., Schell, S., & Bobo, M. (2020). Quantifying western U.S. rangelands as fractional components with multi-resolution remote sensing and in situ data. *Remote Sensing*, *12*(3), 1–26. https://doi.org/10.3390/rs12030412

Ritter, F., Berkelhammer, M., & Garcia-Eidell, C. (2020). Distinct response of gross primary productivity in five terrestrial biomes to precipitation variability. *Communications Earth & Environment*, *1*(1), 1–8. https://doi.org/10.1038/s43247-020-00034-1

Sala, O. E., Gherardi, L. A., & Peters, D. P. C. (2015). Enhanced precipitation variability effects on water losses and ecosystem functioning: differential response of arid and mesic regions. *Climatic Change*, *131*(2), 213–227. https://doi.org/10.1007/s10584-015-1389-z

Schlaepfer, D. R., Lauenroth, W. K., & Bradford, J. B. (2012). Ecohydrological niche of sagebrush ecosystems. *Ecohydrology*, *5*, 453–466. https://doi.org/10.1002/eco.23

Sharma, & Ojha. (2019). Changes of Annual Precipitation and Probability Distributions for Different Climate Types of the World. *Water*, *11*(10), 2092. https://doi.org/10.3390/w11102092

Sun, X., Wilcox, B. P., & Zou, C. B. (2019). Evapotranspiration partitioning in dryland ecosystems: A global meta-analysis of in situ studies. *Journal of Hydrology*, *576*(June), 123–136. https://doi.org/10.1016/j.jhydrol.2019.06.022

Turley, M. C., & Ford, E. D. (2009). Definition and calculation of uncertainty in ecological process models. *Ecological Modelling*, *220*(17), 1968–1983. https://doi.org/10.1016/j.ecolmodel.2009.04.046

Walter, H. (1971). *Ecology of tropical and subtropical vegetation.* Oliver & Boyd.

Ward, D., Wiegand, K., & Getzin, S. (2013). Walter's two-layer hypothesis revisited: Back to the roots! *Oecologia*, *172*(3), 617–630. https://doi.org/10.1007/s00442-012-2538-y

Wilcox, K. R., von Fischer, J. C., Muscha, J. M., Petersen, M. K., & Knapp, A. K. (2015). Contrasting above- and belowground sensitivity of three Great Plains grasslands to altered rainfall regimes. *Global Change Biology*, *21*(1), 335–344. https://doi.org/10.1111/gcb.12673

Xu, X., Medvigy, D., Trugman, A. T., Guan, K., Good, S. P., & Rodriguez-Iturbe, I. (2018). Tree cover shows strong sensitivity to precipitation variability across the global tropics. *Global Ecology and Biogeography*, *27*(4), 450–460. https://doi.org/10.1111/geb.12707

Zeppel, M. J. B., Wilks, J. V., & Lewis, J. D. (2014). Impacts of extreme precipitation and seasonal changes in precipitation on plants. *Biogeosciences*, *11*(11), 3083–3093. https://doi.org/10.5194/bg-11-3083-2014

CHAPTER 2

WOODY PLANT GROWTH INCREASES WITH PRECIPITATION INTENSITY IN A COLD SEMI-ARID SYSTEM[1]

Abstract

As the atmosphere warms, precipitation events become larger, but less frequent. Yet, there is fundamental disagreement about how increased precipitation intensity will affect vegetation. Walter's two-layer hypothesis and experiments testing it have demonstrated that precipitation intensity can increase woody plant growth. Observational studies have found the opposite pattern. Not only are the patterns contradictory, but inference is largely limited to grasslands and savannas. We tested the effects of increased precipitation intensity in a shrub-steppe ecosystem that receives >30% of its precipitation as snow. We used 11 (8 m x 8 m) shelters to collect and redeposit rain and snow as larger, more intense events. Total annual precipitation was the same in all plots, but each plot received different precipitation event sizes ranging from 1 mm to 18 mm. Over three growing seasons, larger precipitation event sizes increased soil water availability, sagebrush (*Artemisia tridentata*) stem radius, and canopy greenness, decreased new root growth in shallow soils, and had no effect on herbaceous plant cover. Thus, we found that increased precipitation intensity can increase soil water availability and woody plant growth in a cold semi-arid system. Assuming that stem growth is positively correlated with shrub reproduction, establishment and spread, results suggest that increasing precipitation intensity may have contributed to the woody plant encroachment observed

[1] Holdrege, M. C., K. H. Beard, and A. Kulmatiski. 2021. Woody plant growth increases with precipitation intensity in a cold semiarid system. Ecology 102(1):e03212. 10.1002/ecy.3212

around the world in the past 50 years. Further, continuing increases in precipitation intensity caused by atmospheric warming are likely to continue to contribute to shrub encroachment in the future.

Introduction

As the atmosphere warms, precipitation intensity has been predicted (Trenberth 2011, Pendergrass and Knutti 2018) and observed to increase around the world (Donat et al. 2016, Fischer and Knutti 2016). Increased precipitation intensity has the potential to affect water cycling, plant growth, community composition, and biosphere-atmosphere feedbacks, particularly in semi-arid systems (Wilcox et al. 2015). Yet, there is fundamental disagreement in the literature about whether increased precipitation intensity will increase or decrease woody plant growth (Good and Caylor 2011, Soliveres et al. 2013, Kulmatiski and Beard 2013, Case and Staver 2018).

Covering more than one-third of land area globally and inhabited by more than one billion people, arid and semi-arid ecosystems are both ecologically and economically important (Safriel et al. 2005, Prăvălie 2016). Over the past 50 years, woody plant encroachment has caused large-scale changes in semi-arid systems, with important management consequences (Archer et al. 2017). In North America, woody plant encroachment is occurring at rates of $< 0.1\%$ to 2.3% yr^{-1}, depending on the ecoregion (Barger et al. 2011). Understanding this transition is important because it can decrease livestock production (Anadon et al. 2014), increase soil erosion, and decrease plant diversity (Lett and Knapp 2005).

Many factors from grazing and fire management to CO_2 fertilization have been found to contribute to woody plant encroachment (Archer et al. 2017, Bestelmeyer et al.

2018), but the role of increasing precipitation intensity remains poorly understood (Kulmatiski and Beard 2013, Case and Staver 2018, Venter et al. 2018). Much of the research on the effects of precipitation intensity on vegetation has been conducted in temperate grasslands and sub-tropical savannas, with the latter studies being more relevant to woody plant growth. Walter's two-layer hypothesis suggests that conditions that increase the depth of water infiltration into the soil, such as increasing precipitation intensity, will benefit woody plants (Walter 1971, Ward et al. 2013). Where increased individual growth is positively correlated with reproduction and establishment (Cawker 1980, Evans and Black 1993, Perryman et al. 2001), deeper infiltration can be expected to contribute to shrub encroachment (Meyer et al. 2007, Caracciolo et al. 2016, Stevens et al. 2017).

Consistent with this hypothesis, an experiment in a xeric, subtropical savanna on clay soils found that increased precipitation intensity 'pushed' water deeper into the soil and increased woody plant growth (Kulmatiski and Beard 2013, Berry and Kulmatiski 2017). But, the opposite pattern has been generally recorded in large-scale observational studies, where woody plant cover tends to decrease with increasing precipitation intensity (Good and Caylor 2011, Case and Staver 2018, Xu et al. 2018), an exception being coarse-textured soils where positive woody cover responses were observed (Case and Staver 2018). Without an understanding of whether increasing precipitation intensity will increase or decrease woody plant growth, it is difficult to apply effective management approaches in semi-arid systems (e.g., for soil conservation or forage production).

Especially little is known about the effects of precipitation intensity in ecosystems that receive large amounts of snow (Zeppel et al. 2014, Lubetkin et al. 2017). Snowy

systems may respond differently than tropical and sub-tropical systems because deep percolation during snowmelt may increase vertical niche partitioning for soil water resources (Schlaepfer et al. 2012, Kulmatiski et al. 2020). Where species composition is a function of vertical niche partitioning, deeper soil water infiltration can be expected to benefit deeply-rooted species (Ward et al., 2013). Many studies have manipulated snowpack, but these studies have focused on increasing or decreasing total snowpack and extending or shortening the snow-free period and not on changing the intensity of snow events (e.g. Wipf and Rixen 2010, Li et al. 2016, Sherwood et al. 2017). Tests of the effects of precipitation intensity in 'snowy' systems have the potential to help explain woody plant encroachment in temperate systems.

Because it is reasonable to expect that plant growth will increase with precipitation intensity in some systems and decrease in others (Knapp et al. 2008), experiments are needed to better constrain the conditions under which precipitation intensity may increase or decrease woody plant growth (Case and Staver 2018). The overarching goal of this research was to test woody and herbaceous plant growth responses to a range of precipitation intensities in a shrub-steppe ecosystem that receives over a third of its precipitation as snow. We hypothesized that shrub growth would increase with precipitation intensity because larger precipitation events would 'push' soil water deeper into the soil providing a competitive advantage to woody plants with deeper roots (Kulmatiski et al. 2020). To test this hypothesis, we collected and redeposited both rain and snowfall as fewer, larger precipitation events while maintaining the same total precipitation. We measured above- and belowground plant growth and soil moisture during three growing seasons after treatment.

Methods

Study site

Research was conducted at the Hardware Ranch Wildlife Management Area (41° 36’ 53” N, 111° 34’ 1” W; 1760 m), Utah, USA (Fig. 2.1). Mean annual precipitation is 468 mm, with 170 mm (36%) falling as snow, primarily between December and March (Menne et al. 2012). On days with rain, mean rainfall event size is 5.3 mm. Mean monthly temperatures range from -4 °C in January to 23 °C in July (Menne et al. 2012). While mid-winter thaw events do occur, the ground is typically covered by snow from December to March: median snow depth at the nearest snow depth measurement station (38 km away) with a similar elevation (1820 m) is greater than zero from 9 November to 4 May (Ben Lomond Trail station; https://www.wcc.nrcs.usda.gov/snow/snow_map.html). Soils are derived from quartzite and sandstone and are in the Yeates Hollow series (well-drained, cobbly silty clay loam; Soil Survey Staff, 2018). This soil type has a cobbly (15-35% rock fragments) A horizon (~ 0-28 cm) and a very cobbly (35-60% rock fragments) B horizon (~ 28-46 cm)(Soil Survey Staff, 2018). Shallow soils (< 15 cm) are sandier (22% sand, 66% silt, 12% clay) than deeper soils (>15 cm; 6% sand, 60% silt, 34% clay).

Common plant species in this sagebrush-dominated rangeland include shrubs: big sagebrush (*Artemisia tridentata* Nutt. ssp. *vaseyana* [Rydb.] Beetle; 25% cover), bitterbrush (*Purshia tridentata* [Pursh] DC.; 4% cover), rabbitbrush (*Chrysothamnus viscidiflorus* [Hook.] Nutt.; 2% cover), and grasses: meadow brome (*Bromus commutatus* Schrad., 10 % cover), bluebunch wheatgrass (*Pseudoroegneria spicata* [Pursh] Á. Löve; 6% cover), and prairie Junegrass (*Koeleria macrantha* [Ledeb.] Schult.; 1 % cover).

Aboveground net primary productivity at the site is approximately 145 g m^{-2} $year^{-1}$, with 58% coming from shrub growth, 17% from grasses, and 25% from forbs. With 70% vegetative ground cover including shrubs that are roughly 1 m tall, and 3% exposed mineral soil, direct impact of rain on soil is uncommon. Cattle were excluded during the experiment, but livestock had grazed the site for over 100 years. Native ungulates (elk and deer), rabbits, and rodents are common and were able to access the plots.

Experimental treatments

In June 2015, 14 plots, each 8 m x 8 m in size, were established in a grid with at least 15 m between plots. All plots were on a 4-6 degree, south-facing slope. Washes, areas with exposed rock, and areas that did not include at least one *P. tridentata* and five *A. tridentata* were not included so that all plots had similar soils and vegetation. Pre-treatment vegetation surveys and soil moisture measurements were taken until January 2016, when treatments were assigned randomly and applied through July 2018. Three plots were shelter-free controls and used to describe shelter effects (Appendix S2.1). The remaining 11 plots were covered with 8 m x 8 m x 2.5 m (w x l x h) shelters (Fig. 2.1). To allow a regression of vegetation responses across a wide range of precipitation event sizes, seven plots were assigned to different treatment levels (described below; Smith et al. 2014). Two additional replicate plots were assigned to each of two treatment levels (Control plots, in which precipitation was immediately redeposited onto plots, and '4 mm' plots in which precipitation events were equal to or greater than 4 mm; described below). To allow a categorical comparison of treatments, plots were split into low-treatment levels and high-treatment levels (described below) so that tests with a treatment sample size of five or six could be performed.

Shelters were open on all sides with a clear Plexiglass® acrylic (6.35 mm thick, 92% light transmittance) roof that collected 100% of precipitation (Fig. 2.1). Rainwater from roofs was collected in two holding tanks per shelter. Tanks ranged from 75 L to 1,100 L depending on treatments. Float switches and water pumps sprayed collected water through six sprinkler heads (1 m height) at a rate of 26 mm $hour^{-1}$, which is a higher rate than natural precipitation (the 99^{th} percentile of natural precipitation rate measured at 15-minute intervals at the site is 8 mm $hour^{-1}$). Sprinklers with similar irrigation rates as those used here have been found to produce similar kinetic energy distribution as natural rainfall events (Ge et al. 2016). Treatments, therefore, created precipitation events that were more intense at both hourly and daily timescales. Despite the high irrigation rate from the sprinklers, runoff was not observed.

For a range of mean hypothetical temperature scenarios associated with climate change, we expect different degrees of precipitation intensification, which form the basis for the choice of treatment levels. Treatment levels were designed to create precipitation event sizes that could be expected with temperature changes from -1 to +10 °C relative to current temperatures. Consistent with the Clausius-Clapeyron relationship, precipitation event sizes were designed to increase by 7% per 1 °C of warming (O'Gorman & Muller, 2010; Appendix S2.2). This method resulted in minimum precipitation event sizes of 2, 3, 4, 8 and 18 mm for hypothetical temperature increases of 1 °C, 2 °C, 3 °C, 5 °C and 10 °C (see Appendix S2.2 for additional details). To further expand our inference, one treatment designed to reflect precipitation intensity associated with -1 °C temperature change was added. In this treatment, irrigation was triggered manually multiple times per growing season depositing additional 1 mm events (hereafter referred to as the 1 mm

treatment). All these treatments received the same total precipitation, and only differed in event size and frequency.

Snow addition frequencies were based on the historical distribution of snow events >4 cm (Menne et al. 2012). A 7% change in precipitation event size for each 1 °C was estimated to result in a median of 14, 13, 11, 10, 8, 7 and 4 snow events per year for the 1, control, 2, 3, 4, 8, and 18 mm treatments (Appendix S2.2). Across the three winters of the experiment (2016, 2017, 2018), which were not identical to long-term means, the treatments received a mean of 11, 10, 9, 8, 6, 4, and 3 snow additions per plot, respectively. In control plots, snow (>4 cm) was scraped off the roofs and immediately shoveled back onto the plot. For treatments to receive fewer larger snow events, snow was removed off the shelter roofs and allowed to accumulate on plastic sheeting adjacent to plots before being shoveled onto the plots. For the -1 °C treatment, one large snow event was deposited as two smaller events resulting in one extra snow event each season. To limit water loss due to snowmelt, accumulated snow was shoveled onto plots before warm spells. As with rain, all treatments received the same amount of total snow, and only differed in the timing and magnitude of the events.

Abiotic treatment responses

Measurements of soil moisture were taken roughly every two weeks in every plot during the growing season using capacitance sensors in PVC access tubes which were installed in June 2015, before treatment applications (Diviner 2000, Sentek Pty Inc., Stepney, Australia). In addition, soil water potential was recorded hourly at six depths using pre-calibrated heat dissipation sensors in one 4 mm treatment plot and one control plot (229L heat dissipation sensors, Campbell Scientific, Logan, UT, USA; Flint et al.

2002). Soil water potential data was converted to volumetric water content using site-specific soil characteristic curves for shallow (0-30 cm) and deep (30-60 cm) soils. To provide an index of soil water availability and flow through the soil, volumetric soil moisture data was used to calculate the sum of positive increments of soil water through each soil depth (i.e., soil water flux; Berry and Kulmatiski 2017).

Biotic treatment responses

Each June (peak growing season), percent cover by plant species was determined using visual estimation in nine, permanent 1 m x 1 m subplots in each plot. Shrub stem radius was measured on the main stems of the three *A. tridentata* closest to the center of the plot using point dendrometers mounted 10 cm from the ground (spring return linear position sensor BEI 9605, BEI Sensors, Thousand Oaks, CA, USA; Wang and Sammis 2008). To limit damage caused by mounting sensors onto stems, only stems with a radius > 3.5 cm were used. Stem radial growth was recorded hourly to 0.1 mm (CR10X; Campbell Scientific, Logan, Utah, USA). Dendrometers were installed at the end of the first treated growing season, so dendrometer growth data reflects only growth during the second and third treated years.

If a dendrometer failed, growth during the period of no measurement was assumed equal to mean growth measured by the other two dendrometers in that plot (13% of data). For replicated plots, missing data was interpolated from mean values from other plots of that same treatment (8% of data). Data smoothing to remove spurious values was performed using a moving 10^{th} percentile or 90^{th} percentile 'window' and a 24-hour wide bin.

To provide another measure of aboveground plant growth, vegetation greenness (Normalized Difference Vegetation Index; NDVI) was measured in every plot, once every two weeks during the growing season (SRS-NDVI Sensor, Meter Group, Inc., Pullman, WA, USA). In addition, mid-day (1000 to 1400 h) NDVI was measured every 15 minutes in one control and one 4 mm treatment plot. Because sensors were mounted 2.4 m aboveground with an oblique field of view of 3.1 m^2, we presume that NDVI data largely reflects the greenness of the shrub canopy with less influence from the subtending herbaceous canopy.

To measure belowground responses, one 2-m long and 5-cm wide acrylic plastic tube was installed at a 30° angle in each plot in June 2015 before the start of the experiment. Images were collected every 5.2 cm down one side of the tube using a video microscope camera (Bartz Technology Co, Carpinteria, CA, USA). Images were collected every two weeks in May and June, and monthly in July and August. Root length, width, area and number of new roots were measured using Rootfly software (version 2.0.2, Wells and Birchfield, Clemson University, SC, USA). Root data were binned into 10-cm vertical increments (0-10, 10-20, 20-30, 30-40, and 40-50 cm). Data from below 50 cm are reported but were not analyzed statistically because not all tubes extended beyond 50 cm depths before hitting parent material.

Statistical analysis

Broadly, regression models were used to analyze data collected annually. For more complex datasets, generalized additive mixed models (GAMMs) were used to model non-linear responses to date or depth. All analyses were done using R version 3.5.1 (R Core Team 2018).

Change in shrub, grass, and total herbaceous (grass and forb) cover and mean growing season NDVI were analyzed using ordinary least squares regression models (lm function in base R). Predictor variables were treatment (i.e., mean precipitation event size; Fig. 2.2), year, and treatment x year interaction. To account for initial plot differences, response variables were the difference between the treatment for that year and the first year of the experiment.

Shrub stem radius (daily mean values), NDVI and soil volumetric water content (twice monthly values), and new root growth and root area data (annual means) were analyzed using GAMMs (mgcv package; Wood 2011). Soil volumetric water content from three depths (10-30 cm, 40-60 cm, 70-100 cm) were analyzed separately. For each dataset, three GAMMs were fit that contained the fixed effect of either date (shrub, NDVI, and soil moisture data) or depth (root data): 1) a null model where a single spline was fit to depth or date (no treatments distinguished), 2) a model that grouped treatments into two levels: low intensity (1 mm, control, 2 mm, and 3 mm treatments: six plots total) and high intensity (4 mm, 8 mm, and 18 mm treatments: five plots total), and 3) a model that separated all treatments. All GAMMs treated plot as a random effect and were fit using a first-order auto-regression structure (AR1) to account for temporal or depth autocorrelation between observations.

Daily mean water potential and daily mid-day NDVI in one control and one 4 mm treatment plot were also analyzed using GAMMs. While not taken in replicate plots, these measurements are included because continuous measurements show daily resolution and provide valuable supporting information. For water potential, measurements in shallow (10-30 cm) and deep (60-100 cm) soils were analyzed

separately (three sensors in each of these two depth categories). Two GAMMs were fit: 1) a null model where a single spline was fit to date (the two plots not distinguished), and 2) a model that separated the two plots.

For regression models, variables were considered significant if $P < 0.05$, and for GAMMs top models were those with the lowest Akaike's information criterion (AIC) and models were considered similar if $\Delta AIC < 2$ (Burnham and Anderson 2002).

Results

Abiotic effects

For biweekly measurements of soil water content, both the low vs. high and all separate treatment models outperformed the null model at all depths, reflecting that there was more water in high intensity treatments than in the low intensity treatments at all depths (Fig. 2.3, Appendix S2.3). This was supported by the continuous measurements of soil water potential in one control and one 4 mm treated plot (Fig. 2.4). Water potential differed over time between the two plots (Fig. 2.4), with the control plot having more 'dry days' (i.e., water potentials < -1.5 MPa) than the 4 mm treatment plot; this difference was greatest in the deepest soils (Appendix S2.3). When soil water potential values were used to calculate water flux, more water flowed through most soil depths in the 4 mm treatment plot than the control plot (Appendix S2.3).

Biotic effects

Grass (22.0 ± 2.9 %; mean ± standard error), forb (17.0 ± 2.2 %) and shrub cover (30.6 ± 2.8 %) did not change with treatment (grass, $F_{1,10} = 0.24$, $P = 0.64$; grass and forb, $F_{1,10} = 0.81$, $P = 0.39$; and shrub, $F_{1,10} = 0.003$, $P = 0.95$) and there were no

treatment by year interactions ($P > 0.05$). For stem radius growth over time (Fig. 2.5a), the best GAMM model separated all treatments (Appendix S2.4). There was a positive linear relationship between total change in stem radius and treatment (Fig. 2.5b).

For the change in mean growing season NDVI, there was also a positive relationship with treatment ($F_{1,10} = 6.0$, $P = 0.034$) indicating that vegetation greenness increased with treatment intensity, and there was no treatment by year interaction ($F_{1,10} = 0.55$, $P = 0.48$). However, for the twice-monthly NDVI measurements, the null model outperformed the 'all separate' or 'high vs. low' models (Appendix S2.5). For continuous measurements, growing-season NDVI was higher in the 4 mm treatment plot than the control plot (Appendix S2.5).

For new root growth, the best model separated low and high precipitation intensity treatments (Appendix S2.6). The difference between low and high intensity treatments reflected less new root growth in shallow soils with the high intensity than with low intensity treatments, with no difference in deeper soils (Figs. 2.6a and 2.6b). Root area did not differ between high intensity and low intensity plots (Figs. 2.6c and 2.6d, Appendix S2.6).

Discussion

There is fundamental disagreement in the literature about how woody plants will respond to increased precipitation intensity (Good and Caylor 2011, Kulmatiski and Beard 2013, Case and Staver 2018). Even less is known about how precipitation intensity will affect woody plant growth in 'snowy' ecosystems (Lubetkin et al. 2017). Using large shelters needed to manipulate precipitation over potentially-wide shrub rooting areas, we collected both rain and snow, and redeposited that precipitation as fewer, larger events.

Our treatments spanned a large range of precipitation intensities, outside historical and expected values, and woody plant growth increased even in the most intense treatments (Fig. 2.5). This positive effect was observed in stem radial growth and supported by NDVI data, though visual estimates did not detect changes in shrub or herbaceous plant cover. Results were consistent with the hypothesis that larger precipitation events increase woody plant growth by increasing water availability, and by 'pushing' water deeper into the soil. These results are important because they extend inference about the role of precipitation intensity on woody growth from sub-tropical to temperate ecosystems. Assuming that stem growth is positively correlated with shrub reproduction, establishment and spread (Cawker 1980, Perryman et al. 2001, Caracciolo et al. 2016), results suggest that increasing precipitation intensity has and will continue to contribute to woody plant encroachment in both subtropical (Meyer et al. 2007, Stevens et al. 2017, Case and Staver 2018) and temperate climates.

Why shrubs may increase

Greater precipitation intensity treatments moved more water into the soil. We assume more water moved into the soil because interception and evaporation decreased with increased precipitation intensity. In this water-limited system, more soil water should allow greater stomatal conductance, plant growth and a competitive advantage to taller plants (i.e., woody plants) that can outcompete shorter plants for light (Knapp et al. 2008). Consistent with this idea, we observed that woody plant growth increased in treatments that increased soil water. Similarly, woody stem diameter increased more in the wetter growing season than in the drier growing season: shrub stem growth increased roughly 1.5 mm and 0.5 mm across treatments in the 2017 (635 mm annual precipitation)

and 2018 growing seasons (400 mm annual precipitation), respectively. We also observed that shallow root growth decreased with precipitation intensity. We could not distinguish grass from shrub roots, but an increase in the ratio of aboveground to belowground growth is consistent with a shift to woody dominance (Van Wijk 2011).

In addition to increased total soil moisture, treatments increased deep soil moisture. Greater deep soil moisture should benefit plants with deeper or more flexible rooting strategies (Canadell et al. 1996, Schenk and Jackson 2002, Berry and Kulmatiski 2017). Deep soil moisture has been found to be important for *A. tridentata* abundance (Kulmatiski et al. 2020) and reproduction (Evans and Black 1993).

Manipulating both rain and snow intensity provided insight into yearlong effects of increased precipitation intensity, but prevented us from isolating the effects of increased rain intensity from those of increased snow intensity. Previous research has shown that plant growth in shrub-steppe ecosystems is strongly tied to soil water recharge from spring snowmelt so it is reasonable to expect that our snow treatments increased shrub growth (Poore et al. 2009, Lauenroth and Bradford 2012, Lubetkin et al. 2017). Consistent with this, treatments appeared to have a large positive effect on soil moisture in the winter and spring, but not in the summer (Figs. 2.3 and 2.4), suggesting that snow manipulations contributed to shrub growth responses. Additional treatments would be necessary to fully dissect the effects of snow and rain manipulations, but even without these treatments, it is clear that increasing both snow and rain intensity increased shrub growth.

Shrub growth is notoriously difficult to assess and many different approaches have been developed to measure it, such as destructive sampling, allometry, and LiDAR

(Fahey and Knapp 2007). Point dendrometers are a relatively new tool that provided nearly-continuous, non-destructive measurements of small changes in shrub radial growth. It was possible, for example, to detect increases in stem radius caused by individual precipitation events and stem shrinkage during dry periods. These precise growth responses were corroborated by NDVI data, but were not detected by visual estimation of species percent cover. While very sensitive, we believe the point dendrometers produced biologically-relevant measurements because they revealed a doubling of stem radius increment in the largest treatment relative to controls (i.e., 2 mm vs. 1 mm; Fig. 2.5).

While it is important to note that different techniques were used to detect shrub and herbaceous growth, it appeared that larger storms increased water availability, but that only shrubs were able to convert this increased soil water into greater growth. If these increases in shrub stem diameter are correlated with increases in fecundity and establishment (Cawker 1980, Perryman et al. 2001), then it is likely that increased precipitation intensity may contribute to shrub encroachment. Increased shrub encroachment can be expected to decrease forage production and increase fire return intervals, but may also result in greater primary productivity (Archer et al. 2017). Again, it will be important to test the link between individual growth and shrub expansion because, it is possible, for example, that greater precipitation intensity increases growth of mature shrubs, but decreases seedling establishment.

The importance of site conditions

Site conditions provide important context for our results. Our site was on relatively shallow (4–6 degree) slopes and overland flow was not evident. In sites with

steeper slopes, greater precipitation intensity may decrease woody plant growth by increasing overland flow and soil erosion. Our site had silty, clay-loam soils that typically have slow hydraulic conductivity and percolation rates, and have been suggested to produce negative woody plant growth responses to increased precipitation intensity (Case and Staver 2018). However, large rock content at the site likely increased percolation rates, and as a result, the soils likely behave more like sandy soils than the soil texture would suggest. Because we observed positive woody plant growth responses to increased precipitation intensity on silty, clay-loam soils, it is possible that percolation rates and not just soil texture are critical in determining ecosystem responses to precipitation intensity (Case and Staver 2018). With an aridity index of ~0.48, our site is semi-arid. In more mesic sites, if precipitation intensity increases above percolation rates, or percolation rates are greater than plant uptake rates, then greater runoff and water percolation below the rooting zone would be more likely and expected to decrease both herbaceous and woody plant growth (Knapp et al. 2008).

This research isolated the effects of precipitation intensity from other climate change effects, such as temperature, CO_2 fertilization, and mean annual precipitation. As a result, the net effects of these different changes remain unknown. Increasing temperatures may increase plant growth in systems where water is relatively abundant during the growing season (Schwinning et al. 2005, Del Grosso et al. 2008) or decrease plant growth where water is more limited during the growing season (Schwinning et al. 2005, Poore et al. 2009). In this system, most stem growth occurred during the cool spring when soil moisture was abundant. Results are consistent with previous studies reporting that sagebrush responds positively to winter but not summer water additions

(Germino and Reinhardt 2014) suggesting that shrub growth in this system is not sensitive to midsummer drought (Bates et al. 2006). While it is not clear from this research what the net effect of increased temperatures and increased precipitation intensity will be, results suggest that increasing precipitation intensity will not exacerbate water stress caused by increased temperatures at this site. Further, it remains possible that greater temperatures, atmospheric CO_2 concentrations, and precipitation intensity will each increase shrub growth, particularly in the spring and fall.

Conclusions

Woody plant encroachment and increased precipitation intensity have been observed around the world (Eldridge et al. 2011, Odorico et al. 2012, Bestelmeyer et al. 2018). Understanding the grass to shrub transition is important because woody encroachment can decrease livestock production (Anadon et al. 2014), increase soil erosion, and decrease plant diversity (Lett and Knapp 2005). Our research supports the hypothesis that increased precipitation intensity increases woody plant growth (and potentially encroachment if there is a link between stem growth, reproduction and spread) by pushing water deeper into the soil, even in systems with snow, clay loam soils, and gentle slopes. Our findings help expand our inference about the effects of precipitation intensity on woody plants from sub-tropical climates to temperate climates, but additional research will be needed to further constrain the climate, soil, and slope conditions under which this effect occurs. Additionally, the relative importance of precipitation intensity and other factors (i.e., fire, grazing, and CO_2 fertilization) on woody plant growth and reproduction remains to be determined.

Data availability

Data are available in Beard and Kulmatiski (2020) on the USU Digital Commons at https://doi.org/10.26078/5b85-m736.

References

Anadon, J. D., O. E. Sala, B. L. Turner, and E. M. Bennett. 2014. Effect of woody-plant encroachment on livestock production in North and South America. Proceedings of the National Academy of Sciences 111:12948–12953.

Archer, S. R., E. M. Anderson, K. I. Predick, S. Schwinning, R. J. Steidl, and S. R. Woods. 2017. Woody plant encroachment: Causes and consequences. Pages 25–84 *in* D. D. Briske, editor. Rangeland systems: Processes, management and challenges. Springer, Cham.

Barger, N. N., S. R. Archer, J. L. Campbell, C. Y. Huang, J. A. Morton, and A. K. Knapp. 2011. Woody plant proliferation in North American drylands: A synthesis of impacts on ecosystem carbon balance. Journal of Geophysical Research: Biogeosciences 116:1–17.

Bates, J. D., T. Svejcar, R. F. Miller, and R. A. Angell. 2006. The effects of precipitation timing on sagebrush steppe vegetation. Journal of Arid Environments 64:670–697.

Berry, R. S., and A. Kulmatiski. 2017. A savanna response to precipitation intensity. PLoS ONE 12:1–18.

Bestelmeyer, B. T., D. P. C. Peters, S. R. Archer, D. M. Browning, G. S. Okin, R. L. Schooley, and N. P. Webb. 2018. The grassland–shrubland regime shift in the southwestern United States: Misconceptions and their implications for management. BioScience 68:678–690.

Burnham, K. P., and D. R. Anderson. 2002. Model selection and inference: A practical information-theoretic approach. 2nd edition. Springer, New York.

Canadell, J., R. B. Jackson, J. R. Ehleringer, H. A. Mooney, O. E. Sala, and E. D. Shulze. 1996. Maximum rooting depth of vegetation types at the global scale. Oecologia 108:583–595.

Caracciolo, D., E. Istanbulluoglu, L. V. Noto, and S. L. Collins. 2016. Mechanisms of shrub encroachment into Northern Chihuahuan Desert grasslands and impacts of climate change investigated using a cellular automata model. Advances in Water Resources 91:46–62.

Case, M. F., and A. C. Staver. 2018. Soil texture mediates tree responses to rainfall intensity in African savannas. New Phytologist 219:1363–1372.

Cawker, K. B. 1980. Evidence of climatic control from population age ttructure of Artemisia tridentata Nutt. in southern British Columbia. Journal of Biogeography 7:237–248.

Donat, M. G., A. L. Lowry, L. V. Alexander, P. A. O'Gorman, and N. Maher. 2016. More extreme precipitation in the world's dry and wet regions. Nature Climate Change 6:508–513.

Eldridge, D. J., M. A. Bowker, F. T. Maestre, E. Roger, J. F. Reynolds, and W. G. Whitford. 2011. Impacts of shrub encroachment on ecosystem structure and functioning: Towards a global synthesis. Ecology Letters 14:709–722.

Evans, R. D., and R. A. Black. 1993. Growth, photosynthesis, and resource investment for vegetative and reproductive modules of Artemisia tridentata. Ecology 74:1516–1528.

Fahey, T. J., and A. K. Knapp. 2007. Principles and standards for measuring primary production. Oxford University Press, Oxford.

Fischer, E. M., and R. Knutti. 2016. Observed heavy precipitation increase confirms theory and early models. Nature Climate Change 6:986–991.

Flint, A. L., G. S. Campbell, K. M. Ellett, and C. Calissendorff. 2002. Calibration and temperature correction of heat dissipation matric potential sensors. Soil Science Society of America Journal 66:1439–1445.

Ge, M., P. Wu, D. Zhu, and D. P. Ames. 2016. Comparison between sprinkler irrigation and natural rainfall based on droplet diameter. Spanish Journal of Agricultural Research 14:e1201.

Germino, M. J., and K. Reinhardt. 2014. Desert shrub responses to experimental modification of precipitation seasonality and soil depth: Relationship to the two-layer hypothesis and ecohydrological niche. Journal of Ecology 102:989–997.

Good, S. P., and K. K. Caylor. 2011. Climatological determinants of woody cover in Africa. Proceedings of the National Academy of Sciences 108:4902–4907.

Del Grosso, S., W. Parton, T. Stohlgren, D. Zheng, D. Bachelet, S. Prince, K. Hibbard, and R. Olson. 2008. Global potential net primary production predicted from vegetation class, precipitation, and temperature. Ecology 89:2117–2126.

Knapp, A. K., C. Beier, D. D. Briske, A. T. Classen, Y. Luo, M. Reichstein, M. D. Smith, S. D. Smith, J. E. Bell, P. a. Fay, J. L. Heisler, S. W. Leavitt, R. Sherry, B. Smith, and E. Weng. 2008. Consequences of more extreme precipitation regimes for terrestrial ecosystems. BioScience 58:811–821.

Kulmatiski, A., P. B. Adler, and K. M. Foley. 2020. Hydrologic niches explain species

coexistence and abundance in a shrub–steppe system. Journal of Ecology 108:998–1008.

Kulmatiski, A., and K. H. Beard. 2013. Woody plant encroachment facilitated by increased precipitation intensity. Nature Climate Change 3:833–837.

Lauenroth, W. K., and J. B. Bradford. 2012. Ecohydrology of dry regions of the United States: Water balance consequences of small precipitation events. Ecohydrology 5:46–53.

Lett, M. S., and A. K. Knapp. 2005. Woody plant encroachment and removal in mesic grassland: Production and composition responses of herbaceous vegetation. The American Midland Naturalist 153:217–231.

Li, W., J. Wu, E. Bai, D. Guan, A. Wang, F. Yuan, S. Wang, and C. Jin. 2016. Response of terrestrial nitrogen dynamics to snow cover change: A meta-analysis of experimental manipulation. Soil Biology and Biochemistry 100:51–58.

Lubetkin, K. C., A. L. Westerling, and L. M. Kueppers. 2017. Climate and landscape drive the pace and pattern of conifer encroachment into subalpine meadows. Ecological Applications 27:1876–1887.

Menne, M. J., I. Durre, B. Korzeniewski, S. McNeal, K. Thomas, X. Yin, S. Anthony, R. Ray, R. S. Vose, B. E. Gleason, and T. G. Houston. 2012. Global Historical Climatology Network - Daily (GHCN-Daily), Version 3. https://www.ncdc.noaa.gov/cdo-web/datasets/GHCND/stations/GHCND:USC00425186/detail.

Meyer, K. M., K. Wiegand, D. Ward, and A. Moustakas. 2007. SATCHMO: A spatial simulation model of growth, competition, and mortality in cycling savanna patches.

Ecological Modelling 209:377–391.

O'Gorman, P. A., and C. J. Muller. 2010. How closely do changes in surface and column water vapor follow Clausius-Clapeyron scaling in climate change simulations? Environmental Research Letters 5.

Odorico, P. D., G. S. Okin, and B. T. Bestelmeyer. 2012. A synthetic review of feedbacks and drivers of shrub encroachment in arid grasslands. Ecohydrology 5:520–530.

Pendergrass, A. G., and R. Knutti. 2018. The uneven nature of daily precipitation and its change. Geophysical Research Letters:1–9.

Perryman, B. L., A. M. Maier, A. L. Hild, and R. A. Olson. 2001. Demographic characteristics of 3 Artemisia tridentata Nutt. subspecies. Journal of Range Management 54:166–170.

Poore, R. E., C. A. Lamanna, J. J. Ebersole, and B. J. Enquist. 2009. Controls on radial growth of mountain big sagebrush and implications for climate change. Western North American Naturalist 69:556–562.

Prăvălie, R. 2016. Drylands extent and environmental issues. A global approach. Earth-Science Reviews 161:259–278.

R Core Team. 2018. R: A Language and Environment for Statistical Computing. Vienna, Austria.

Safriel, U., Z. Adeel, N. David, P. Juan, W. Robin, L. Rattan, W. Mark, J. Ziedler, P. Stephen, A. Emma, K. Caroline, S. Barry, W. Konrad, N. Thomas, P. Boris, R. Inbal, T. Jillian, L. Esther, and D. McNab. 2005. Dryland Systems. Pages 623–662 *in* H. Rashid, S. Robert, and A. Neville, editors. Millennium Ecosystems Assessment--Ecosystems and Human Well-Being. Island Press, Washington DC.

Schenk, H. J., and R. B. Jackson. 2002. Rooting depths, lateral root spreads and belowground aboveground allometries of plants in water limited ecosystems. Journal of Ecology 90:480–494.

Schlaepfer, D. R., W. K. Lauenroth, and J. B. Bradford. 2012. Consequences of declining snow accumulation for water balance of mid-latitude dry regions. Global Change Biology 18:1988–1997.

Schwinning, S., B. I. Starr, and J. R. Ehleringer. 2005. Summer and winter drought in a cold desert ecosystem (Colorado Plateau) part II: Effects on plant carbon assimilation and growth. Journal of Arid Environments 61:61–78.

Sherwood, J. A., D. M. Debinski, P. C. Caragea, and M. J. Germino. 2017. Effects of experimentally reduced snowpack and passive warming on montane meadow plant phenology and floral resources. Ecosphere 8:e01745.

Smith, N. G., V. L. Rodgers, E. R. Brzostek, A. Kulmatiski, M. L. Avolio, D. L. Hoover, S. E. Koerner, K. Grant, A. Jentsch, S. Fatichi, and D. Niyogi. 2014. Toward a better integration of biological data from precipitation manipulation experiments into Earth system models. Reviews of Geophysics 52:412–434.

Soil Survey Staff. 2018. Natural Resrouces Conservation Service, United States Department of Agriculture: Web Soil Survey. https://websoilsurvey.sc.egov.usda.gov/.

Soliveres, S., P. García-Palacios, F. T. Maestre, A. Escudero, and F. Valladares. 2013. Changes in rainfall amount and frequency do not affect the outcome of the interaction between the shrub Retama sphaerocarpa and its neighbouring grasses in two semiarid communities. Journal of Arid Environments 91:104–112.

Stevens, N., C. E. R. Lehmann, B. P. Murphy, and G. Durigan. 2017. Savanna woody encroachment is widespread across three continents. Global Change Biology 23:235–244.

Trenberth, K. E. 2011. Changes in precipitation with climate change. Climate Research 47:123–138.

Venter, Z. S., M. D. Cramer, and H. J. Hawkins. 2018. Drivers of woody plant encroachment over Africa. Nature Communications 9:1–7.

Walter, H. 1971. Ecology of tropical and subtropical vegetation. Oliver & Boyd, Edinburgh.

Wang, J., and T. W. Sammis. 2008. New automatic band and point dendrometers for measuring stem diameter growth. Applied Engineering in Agriculture 24:731–742.

Ward, D., K. Wiegand, and S. Getzin. 2013. Walter's two-layer hypothesis revisited: Back to the roots! Oecologia 172:617–630.

Van Wijk, M. T. 2011. Understanding plant rooting patterns in semi-arid systems: An integrated model analysis of climate, soil type and plant biomass. Global Ecology and Biogeography 20:331–342.

Wilcox, K. R., J. C. von Fischer, J. M. Muscha, M. K. Petersen, and A. K. Knapp. 2015. Contrasting above- and belowground sensitivity of three Great Plains grasslands to altered rainfall regimes. Global Change Biology 21:335–344.

Wipf, S., and C. Rixen. 2010. A review of snow manipulation experiments in Arctic and alpine tundra ecosystems. Polar Research 29:95–109.

Wood, S. N. 2011. Fast stable restricted maximum likelihood and marginal likelihood estimation of semiparametric generalized linear models. Journal of the Royal

Statistical Society: Series B (Statistical Methodology) 73:3–36.

Xu, X., D. Medvigy, A. T. Trugman, K. Guan, S. P. Good, and I. Rodriguez-Iturbe. 2018. Tree cover shows strong sensitivity to precipitation variability across the global tropics. Global Ecology and Biogeography 27:450–460.

Zeppel, M. J. B., J. V. Wilks, and J. D. Lewis. 2014. Impacts of extreme precipitation and seasonal changes in precipitation on plants. Biogeosciences 11:3083–3093.

Figures

Figure 2.1 Shelters (8 m x 8 m) were constructed in a sagebrush-dominated system to collect and redistribute rain and snow as fewer, larger events in (a) winter and (b) summer, in Utah, USA.

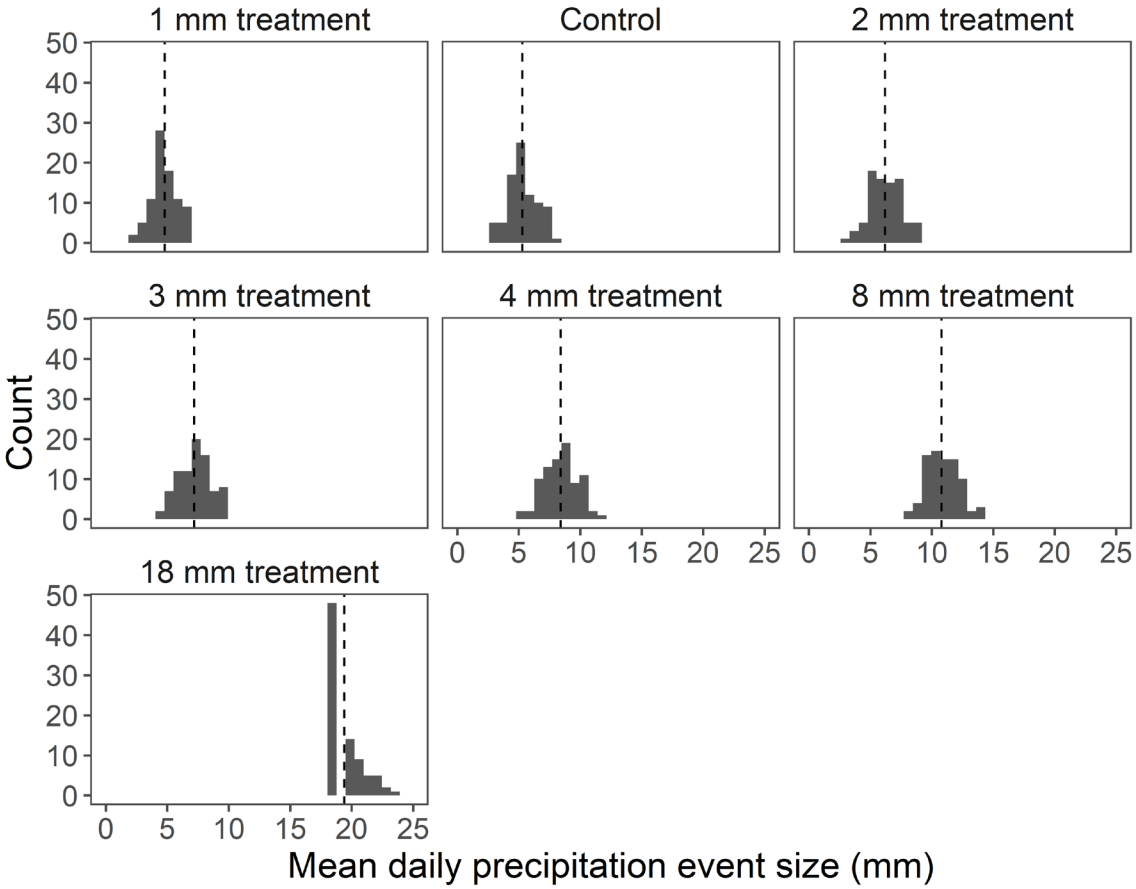

Figure 2.2 A tipping bucket model was applied to the historical precipitation record (daily precipitation from 1928-2018) to simulate the effects of applied treatments and to determine the mean daily precipitation event sizes for each year. The figure shows the distribution of mean daily event sizes for the 90 years. Dotted line shows distribution mean. Annual precipitation is the same in each treatment.

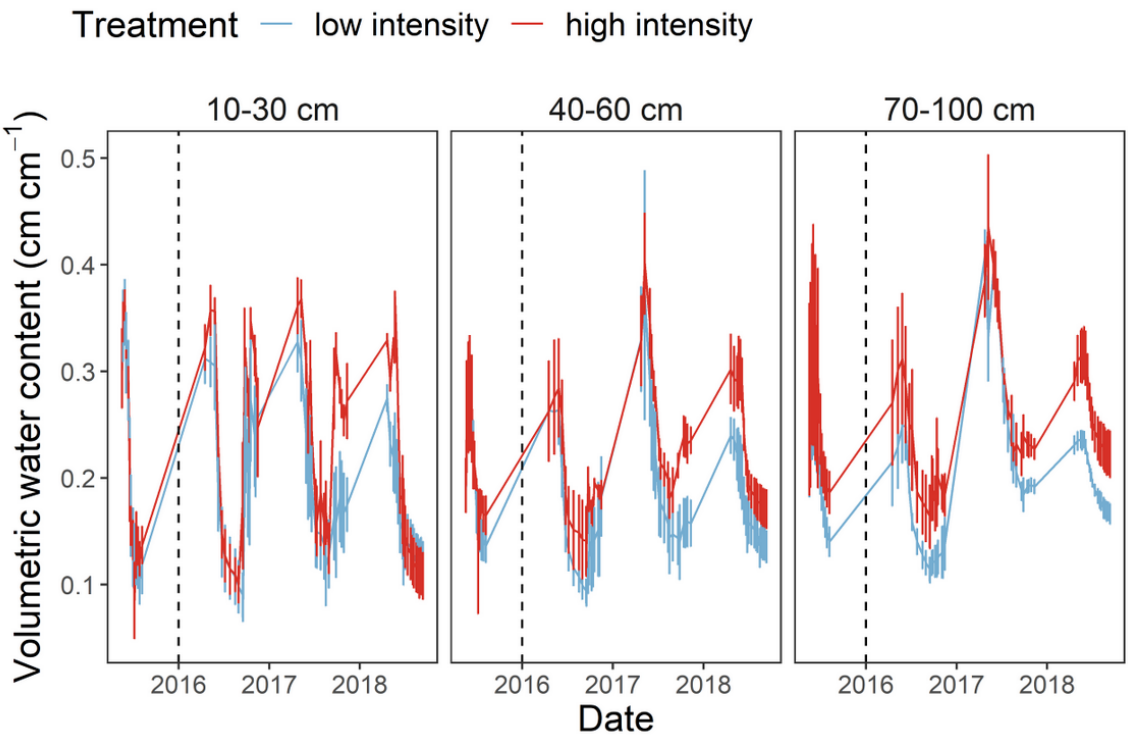

Figure 2.3 Volumetric water content (mean ± standard error) at three soil depths (10-30 cm, 40-60 cm and 70-100 cm) in experimental plots receiving either low intensity or high intensity precipitation events. Low intensity (n = 6) and high intensity (n = 5) precipitation plots received minimum precipitation events of 1, control, 2 or 3 mm or 4, 8, and 18 mm events, respectively. Plots receiving larger precipitation events (but the same total annual precipitation) demonstrated greater volumetric water content than plots receiving smaller precipitation events (Appendix S2.3). Dashed line denotes start date of precipitation treatments.

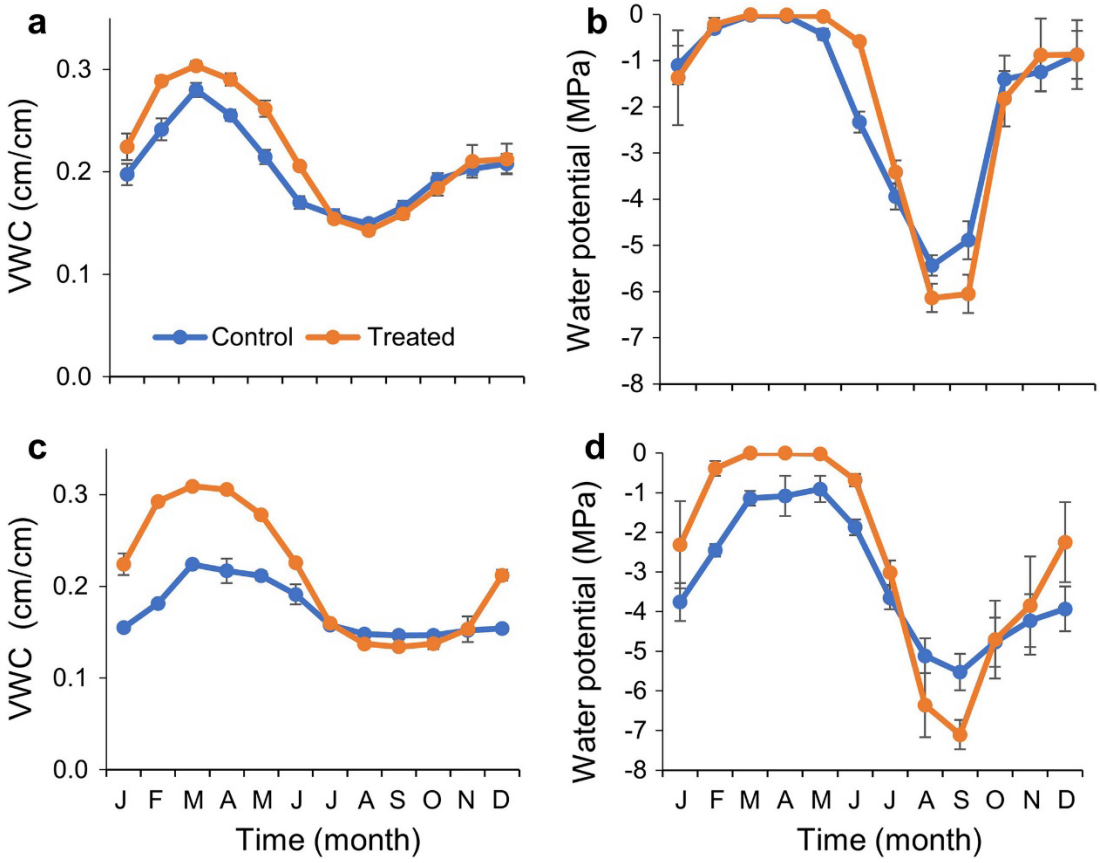

Figure 2.4 Shallow (10-30 cm; a and b) and deep (60-100 cm; c and d) soil moisture over time in a treated and control plot. Volumetric water content (a and c) and soil water potential (b and d) were measured separately with three sensors for each depth in one control plot and one treated plot in which all precipitation events were 4 mm or greater. Total annual precipitation was the same in both treated and control plots. Monthly values represent averages from hourly measurements across 2016, 2017 and 2018.

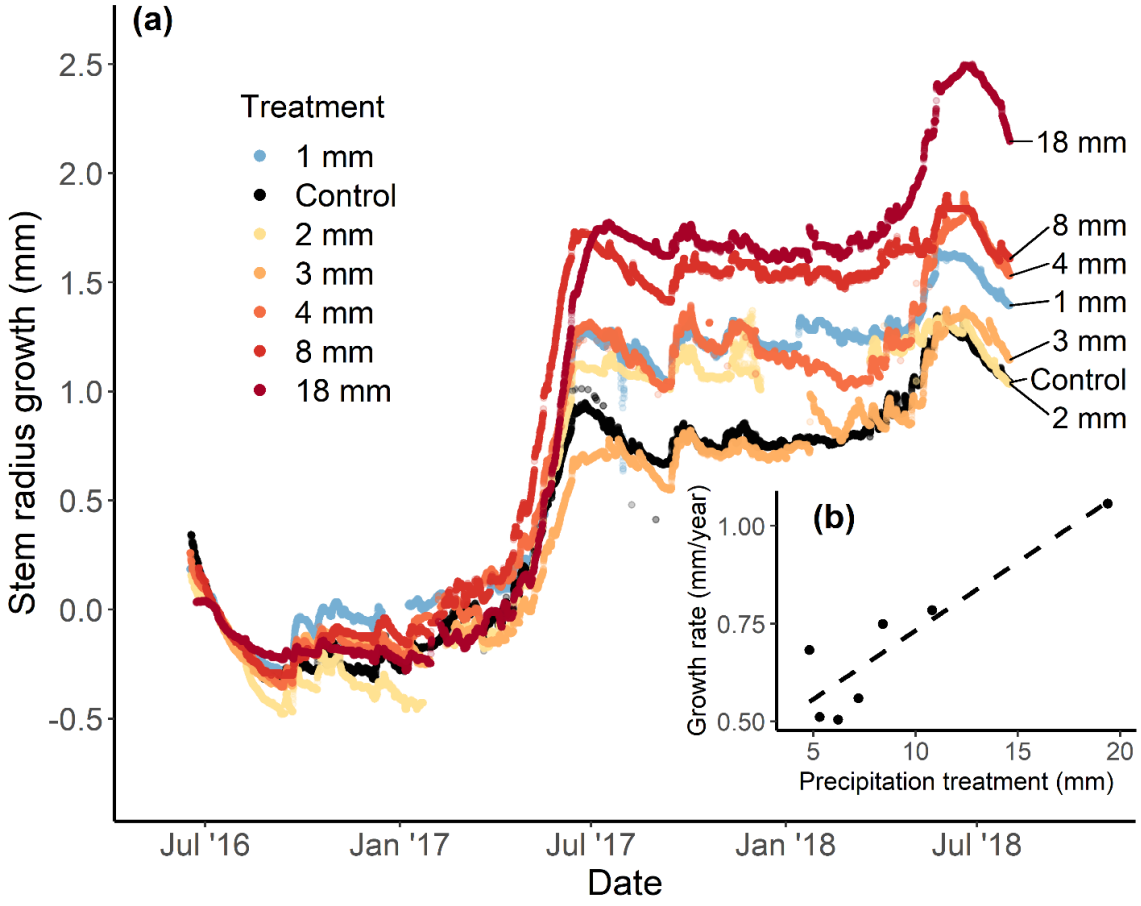

Figure 2.5 Sagebrush stem radius growth in plots receiving different sized precipitation events (i.e., 1-18 mm). All plots received the same annual precipitation, but differed in the size of individual precipitation events. (a) Values on the y-axis represent change in the stem radius (mm) relative to 12 July 2016. (b) Total change in stem radius versus mean precipitation on days with precipitation, showing ordinary least squares regression line ($F_{1,5} = 22.9$, $P = 0.005$, $R^2 = 0.77$; growth rate = 0.38 + 0.035*treatment).

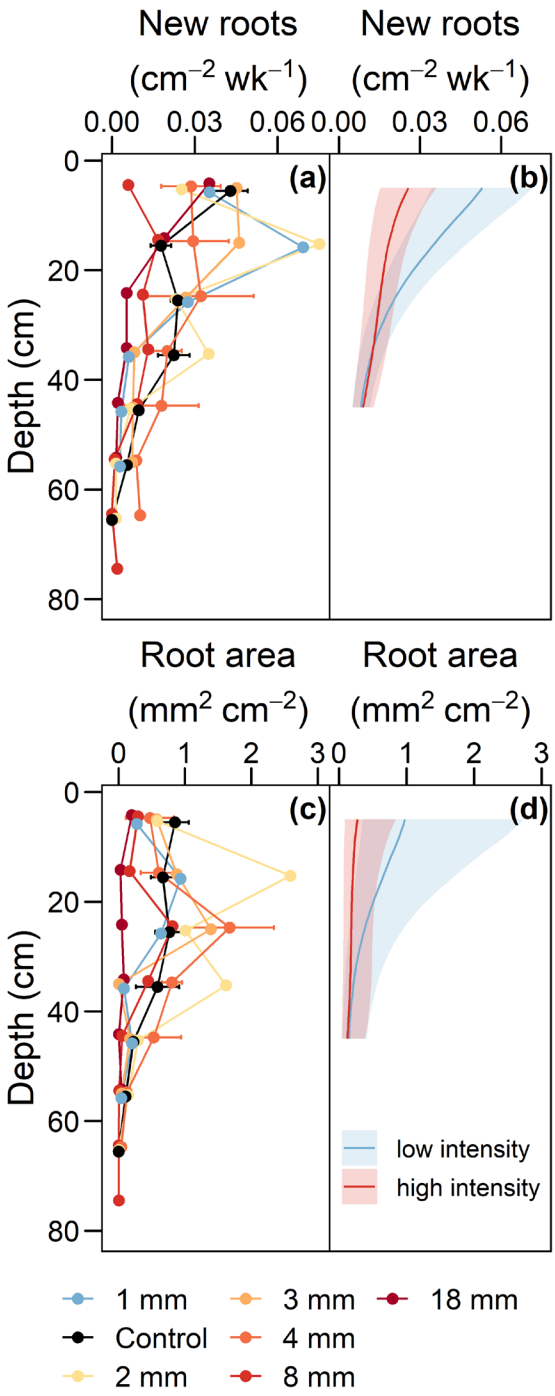

Figure 2.6 Root growth with depth in different precipitation intensity treatments. (a) Mean new root growth rate and (c) mean root area, across depth by precipitation intensity treatment. Error bars (± 1 SE) are shown on replicated treatments (control and 4 mm treatment). (b) Model predictions for low (3, 2, 1 mm and control) and high (18, 8, 4 mm) precipitation intensity treatments for new root growth rate and (d) root area. Shading shows 95% confidence intervals.

CHAPTER 3

WINTER WHEAT RESISTANT TO INCREASES IN RAIN AND SNOW INTENSITY IN A SEMI-ARID SYSTEM[2]

Abstract

As the atmosphere warms, precipitation events have been predicted and observed to become fewer and larger. Changes in precipitation patterns can have large effects on dryland agricultural production, but experimental tests on the effects of changing precipitation intensity are limited. Over 3 years, we tested the effects of increased precipitation intensity on winter wheat (*Triticum aestivum* L.; Promontory variety) in a temperate dryland agricultural system that was on a rotation of crop and fallow years. We used 11 (2.1 × 2.5 m) shelters to collect and redeposit rain and snow as larger, more intense events. Total precipitation was the same in all plots, but event sizes in each plot varied from 1 to 18 mm. Treatments increased soil water availability, but winter wheat biomass and grain yield did not differ among treatments. Similarly, other measured plant growth responses, including vegetation greenness, leaf area index, canopy temperature, photochemical efficiency, root area, and new root growth, did not differ among treatments. Results indicate that at least in the semiarid climate and silt loam soils studied here, anticipated increases in precipitation intensity are unlikely to affect winter wheat production negatively. Further, increased precipitation intensity may mitigate water stress caused by increasing temperatures and encourage the use of wheat varieties that utilize deeper, later season soil water.

---

[2]Holdrege, M. C.; Beard, K. H.; Kulmatiski, A. Winter wheat resistant to increases in rain and snow intensity in a semi-arid system. Agronomy 2021, 11, 751. https://doi.org/10.3390/agronomy11040751

Introduction

Globally, rainfed agriculture accounts for 80% of cultivated land and 60% of food production [1]. Because this type of agriculture is not subsidized by irrigation, it is sensitive to climate change, particularly in arid and semi-arid climates [2,3]. While the effects of warming and changes in the amount of precipitation have been widely studied, a less well-understood aspect of climate change is increasing precipitation intensity. As the atmosphere warms, precipitation events are predicted and have been observed to become fewer and larger [4,5]. Fewer, larger precipitation events are likely to change how water moves through the soils and, therefore, are likely to affect plant growth in agricultural, and particularly rainfed, systems [6–8].

How larger precipitation events impact plant growth depends on what happens to the rainfall, which is a function of the biotic and abiotic conditions of the system. For example, larger precipitation events may decrease interception and increase percolation [9,10]. Deeper water percolation may especially benefit deep-rooted plants [11]. In natural grasslands, increased precipitation intensity has tended to increase plant growth in arid, semi-arid, and sandy systems and decrease plant growth in mesic systems [6,12–15]. Agricultural systems may be more likely to respond negatively to increased precipitation intensity due to increased overland flow or percolation below the often shallow rooting zones.

To limit vulnerability, dryland crop producers select crops and varieties for climate-resistant traits, such as optimized water uptake, high water-use efficiency through conservative water use, and drought escape (e.g., early maturity) [3,16]. However, both observational and modeling studies have reported a wide range of crop responses to

precipitation intensity, from positive to negative [8,17–19]. Thus, uncertainty remains regarding how crops, especially those dependent on natural rainfall, will respond to altered precipitation regimes [20,21]. Because it is reasonable to expect both positive and negative responses, there is a need for experimentation to better constrain the conditions under which increasing precipitation intensity will increase or decrease crop productivity.

Wheat is the third most produced crop in the world, after maize and rice [22]. In the United States, wheat is the most widely grown cereal crop, a large proportion (70%–80%) of which is winter wheat (*Triticum aestivum* L.), and winter wheat is primarily grown under rainfed conditions [23,24]. Winter wheat is well suited for water-limited systems because it is planted in the fall, allowing it to develop earlier in the growing season and avoid midsummer droughts [25]. Observational studies suggest that winter wheat tends to be more resistant to changes in climate than other crops, including being resistant to increases in precipitation intensity [18,26]. Rezaei et al. [27] reported that winter wheat growth shifted 2 weeks earlier over the past half century, allowing yields to be unaffected by increasing summer temperatures. However, winter wheat can be sensitive to water stress that occurs early in the growing season, for example, during flowering [28].

While valuable, observational studies that link climate to crop yield often suffer from strong correlations between climate variables, which makes evaluating the impacts of individual variables difficult [29,30]. Experiments measuring the effects of increased precipitation intensity on winter wheat have found neutral [31] and negative [32] responses. Studies of other crops, using experimental manipulations of precipitation intensity, have also found limited crop responses [33–35]. However, these experiments

were conducted in relatively mesic sites in Europe, making it unclear whether the results generalize to winter wheat grown in more arid climates.

Experiments can help provide estimates of the effects of individual climate variables and improve our mechanistic understanding of the impacts of climate change on crops. Our objective was to measure winter wheat responses to increasing precipitation intensity in a semi-arid dryland system in northern Utah, USA, to isolate the effect of one aspect of climate change on a dryland crop. We established plots of winter wheat that received fewer, larger precipitation events while maintaining the same total precipitation. We measured soil moisture and above- and belowground winter wheat growth responses to treatments during 2 years separated by a fallow year.

Materials and Methods

Site description

The experiment was conducted at the Emily Godfrey Fonnesbeck Research Farm in Clarkston, Utah, USA (41°53′44” N; 112°2′39” W; elevation: 1485 m) in an area that was naturally a shrub-steppe ecosystem. The mean annual precipitation in the area is 461 mm, with 36% falling as snow [36]. Winter wheat was grown in plots in 2017 and 2019, and both years were wetter than average (636 and 586 mm, respectively; Figure 3.1). The mean temperatures in 2017 (9.6 °C) and 2019 (8.9 °C) were near the historical mean annual temperature of 9.2 °C (Figure 3.1). The soils are deep, well-drained silt loams in the Mendon series [37], and contain 23% sand, 62% silt, and 15% clay. In shallow (0−30 cm) soils, the organic matter is 20 g kg^{-1}, pH is 7.2, the phosphorous concentrations are 0.5–3.9 mg kg^{-1}, and the potassium concentrations are 311–431 mg kg^{-1} [38]. The area in

which the plots were located was in a crop rotation consisting of alternating years of winter wheat and fallow during the experiment. We planted the Promontory variety, a high-yielding hard red winter wheat [39]. This early-maturing variety was developed for dryland crop production in a crop fallow system in low-rainfall areas of Utah and southern Idaho, USA; it maintains good test weight under lower-than-average moisture conditions and has resistance to dwarf bunt ([39,40]; D. Hole, pers. comm.).

Experimental design

The experimental design generally followed that of Holdrege et al. [10]. Broadly, precipitation was collected and redeposited as larger events of fixed sizes (i.e., 1 to 18 mm) so that all plots received the same total amount of precipitation, but that precipitation was deposited as either many small or few large events.

In May 2015, 14 plots were established 6 m apart in three rows in a 50 × 90 m area on a low-angle slope (1° slope). Three plots were shelter-free controls and used to determine shelter effects (Appendix S3.1: Figures S3.1 and S3.2, Table S3.1). The remaining 11 plots were covered with 2.1 × 2.5 × 1.9 m (w × l × h) rainout shelters beginning April 2016 (Figure 3.2). A clear acrylic (5.1 mm thick, 92% light transmittance) roof covered each plot. Rainwater from each roof was collected in a water tank adjacent to the shelter. The tanks ranged from 75 to 380 L depending on the treatment size. Tethered floating outlets were installed in the water tanks so that once water accumulated to the desired level for the treatment, the outlet sank, causing the tank to drain [41]. The tanks drained into 12 drip nozzles via drip irrigation tubing that was fixed to the ground.

To allow regression analyses, seven plots were assigned to different treatment

levels (representing precipitation event sizes ranging from 1 to 18 mm [9]; Table 3.1). Two additional replicate plots (for a total of three plots) were assigned to each of two treatment levels (sheltered-control plots, in which precipitation was immediately redeposited onto plots, and "4 mm" plots, which had 4 mm minimum precipitation event sizes; described below). To increase the sample size, analyses were also performed on data split into high- and low-precipitation intensity categories (Table 3.1).

Precipitation event sizes (i.e., treatments) were selected to reflect changes in precipitation intensity anticipated with temperature changes from −1 to +10 °C relative to current temperatures. Consistent with the Clausius–Clapeyron relation, precipitation event sizes were designed to increase by 7% per 1 °C of warming [10,42]. This method resulted in rain event sizes of 2, 3, 4, 8, and 18 mm for hypothetical temperature increases of 1, 2, 3, 5, and 10 °C (Table 3.1; Figure S3.3; see Appendix S3.2 for additional details). Rainfall intensity was manipulated from April to November in 2016–2018 and April to August in 2019. To further expand our inference, one treatment designed to reflect precipitation intensity associated with a −1 °C temperature change was added. In this treatment, irrigation was triggered manually approximately monthly during the growing season, depositing additional 1 mm events (hereafter referred to as the 1 mm treatment). All treatments received the same total precipitation and only differed in event size and frequency. The seasonality of precipitation was not manipulated.

To provide an example of how precipitation treatments functioned, assume that there was a natural 2 mm rain event one day, followed by a 6 mm event on a day the next week, and that the tanks all started empty, as was the case at the beginning of the experiment. The 2 mm of rain would be diverted from the shelter roofs into the tanks and

be redeposited onto the 1 mm, control, and 2 mm treatment plots. In the other treatments, the water would be stored in the tank and not redeposited. When the following 6 mm precipitation event occurred, the 1 mm, control, 2 mm, and 3 mm treatments would all receive 6 mm of water. The 8 mm treatment plot would receive 8 mm of water (6 mm from this storm plus 2 mm from the previous storm). The 18 mm treatment would still receive no precipitation (it would require another 10 mm of rainfall to occur for water to be redeposited).

As with rainfall, snowfall manipulations were used to create fewer, larger snowfall events while holding the total snowfall on the plots constant. Snow treatments were applied from late December to early March such that the plots received the historical mean snow water equivalent for that period. Snow addition frequencies were calculated using historical data (1928–2014) of snow events >4 cm from those winter months [36]. A 7% change in event size for each 1 °C was estimated to result in a median of 9, 8, 7, 6, 5, 4, and 2 snow events per season for the 1 mm, control, 2 mm, 3 mm, 4 mm, 8 mm, and 18 mm treatments. Therefore, during the 2016/17 and 2018/19 winters, snow that was collected off of the shelters was added back to the plots across nine, eight, seven, six, five, four, and two shoveling events for the respective treatments.

The plots were seeded with winter wheat on 30 September 2016 and 15 October 2018 and were hand-harvested on 28 July 2017 and 3 August 2019, respectively. The plots were tilled to a depth of 13 cm before planting and seeded at a rate of 12.5 g m^{-2} with a row spacing of 15 cm. On the same schedule, the area between the plots was also tilled and planted at that rate to maintain similar environmental conditions around the plots. The fallow periods were from August 2015 to September 2016 and August 2017 to

October 2018. Reflecting weed-suppression practices, Roundup PowerMAX (48.7% glyphosate; Bayer, Research Triangle Park, USA) was applied in the spring of 2016 and 2018 (1.2 L ha^{-1} application rate). No fertilizer was applied to the plots during the experiment.

Treatment responses

Volumetric water content was measured twice each month during the growing season using a capacitance sensor in an access tube in each plot (Diviner 2000, Sentek Pty Inc., Stepney, Australia). Additionally, hourly measurements of soil water potential were taken at six depths in one sheltered-control plot and one 4 mm treatment plot beginning in October 2015 (229L heat dissipation sensors, Campbell Scientific, Logan, UT, USA).

Several nondestructive measurements were made roughly two times per month during the growing season to assess plant growth over time. Vegetation "greenness" was measured using the normalized difference vegetation index (NDVI; SRS-NDVI Sensor, Meter Group, Inc., Pullman, WA, USA). Plant leaf area was estimated using the leaf area index (LAI; ACCUPAR LP−80, Meter Group, Inc., Pullman, WA, USA). Plant carotenoid content was used as an indicator of photosynthetic efficiency and measured using the photochemical reflectance index (PRI; SRS-PRI Sensor, Meter Group, Inc., Pullman, WA, USA; [43]). Canopy temperature was measured as an indicator of water stress (SI-111 infrared radiometer, Apogee Instruments, Logan, UT, USA). The infrared radiometer (which also contained an air temperature sensor) was mounted at a height of 1 m and faced downward at a 45° angle so that vegetation limited the sensor's view of bare ground. The difference between the canopy temperature and the air temperature ($T_c - T_a$)

was used as a relative index of plant water stress. This value increases when crops experience water stress because leaves become warmer when transpiration is reduced [44]. Measurements of the NDVI (sensor field of view, 1.75 m^2), PRI (field of view, 1.75 m^2), and canopy temperature (field of view, 1.1 m^2) were made from two fixed locations in each plot, and the LAI was measured in eight fixed locations. The plot-level averages of these values were used in the analyses.

At the end of the growing season, mean canopy height was measured in four 30 cm radius circles in each plot. Then, all aboveground vegetation (both wheat and weeds) from the plots was harvested. Wheat from a 1 × 1 m subplot in the plot center was weighed wet and then threshed to measure grain yield. The dry weight of the wheat plants from this center subplot was not measured because the plants could not be oven-dried before threshing; however, it was estimated using a wet-to-dry weight conversion from wheat in the remainder of the plot. To derive biomass measurements, collected plant material was oven-dried at 60 °C to constant weight and weighed.

To measure root responses, one 2 m long by 5 cm wide acrylic plastic tube was installed at a 30° angle in each plot. A video microscope camera was used to capture images every 5.2 cm down one side of the tube (Bartz Technology Co., Carpinteria, CA, USA). Images were collected twice monthly from May to July in 2016 and 2018. Rootfly software (version 2.0.2, Wells and Birchfield, Clemson University, SC, USA) was used to measure root length and width and the number of new roots in the images. Root data were binned into 10 cm vertical increments (0–10, 10–20, 20–30, 30–40, 40–50, 50–60).

Analysis

Linear mixed-effects models were used to analyze aboveground biomass, grain yield, and wheat height data ("lme4" package [45]). The predictor variables were treatment (i.e., mean precipitation event size, a continuous variable), year (discrete variable), and treatment × year interaction. The plot was treated as a random effect. In cases where no significant treatment × year interaction was detected, models were rerun without the interaction term, and those results were reported.

Soil water potential, NDVI, LAI, PRI, radiometer, root area, and new root growth were analyzed using generalized additive mixed models (GAMMs) so nonlinear responses to date (soil water potential, NDVI, PRI, LAI, $T_c - T_a$) or depth (root data) could be modeled ("mgcv" package [46]). For each dataset and year, three GAMMs were fit that contained the fixed effect of either time or depth: (1) a null model where a single spline was fit to depth or time (no treatments distinguished), (2) a model that grouped treatments into two levels: low intensity (1 mm, control, 2 mm, and 3 mm treatments: six plots in total) and high intensity (4 mm, 8 mm, and 18 mm treatments: five plots in total), and (3) a model that separated all treatments. All GAMMs treated the plot as a random effect, and covariance among repeated measurements within plots was modeled using a first-order autoregressive structure.

For regression models, variables were considered significant if $p < 0.05$, and for GAMMs, top models were those with the lowest Akaike's information criterion (AIC), and models were considered similar if $\Delta AIC < 2$ [47]. All analyses were conducted using R version 3.6.2 [48].

Results

Soil moisture effects

During the summer, the mean monthly soil water potential was lower in the control plot than the 4 mm plot (Figures 3.3 and S3.4; Table S3.2). These differences in water potential were greatest from July through September and translate to 0.020 and 0.019 cm cm^{-1} more volumetric soil water in treated than in control plots during those months in shallow and deep soils, respectively. However, volumetric water content, which was measured less-frequently, but in every plot, did not show a treatment effect (Figure S3.5; Table S3.3).

Biotic effects

The null models best described the twice-monthly NDVI and LAI measurements in both 2017 and 2019 (Table S3.4), indicating that treatments did not affect the seasonal trend in vegetation growth (Figure 3.4). Similarly, null models best described PRI and infrared radiometer ($T_c - T_a$) measurements (Figure 3.4; Table S3.4), suggesting that treatments did not affect the seasonal trend in photochemical efficiency (assessed using PRI) and water stress (assessed using $T_c - T_a$).

End-of-growing-season measurements of wheat growth did not change significantly with treatment (aboveground biomass, $\beta = 4.24$, $F_{1,9} = 1.28$, $p = 0.29$; grain yield, $\beta = 1.68$, $F_{1,9} = 0.23$, $p = 0.64$; wheat height, $\beta = 0.08$, $F_{1,9} = 0.15$, $p = 0.71$) (Figure 3.5). Aboveground wheat biomass, grain yield, and wheat height were higher in 2019 than 2017 (Figure 3.5; $p < 0.05$). In all three models, there was no treatment × year interaction ($p > 0.05$). Similarly, the total aboveground biomass of weeds (here defined as

any nontarget plant species) did not respond to treatment (Figure 3.5; $\beta = -3.15$, $F_{1,9} = 2.69$, $p = 0.14$) and was higher in 2019 than 2017 (Figure 3.5; $p = 0.02$), with no treatment × year interaction ($p = 0.18$). Wheat and weed biomass from the center 1 × 1 m subplot (as opposed to biomass from the entire plot) also did not have a significant treatment response ($p > 0.05$), suggesting that edge effects did not have undue influence on biomass responses. In 2019, 98% of weed biomass was composed of four species: *Polygonum douglasii* Green (34%), *Lactuca serriola* L. (22%), *Ranunculus testiculatus* (Crantz) Roth (21%), and *Agropyron cristatum* (L.) Gaertn. (21%); weeds were not separated by species in 2017. When analyzed separately, none of these four species responded to treatment ($p > 0.05$).

Mean root area and new root growth were higher in 2017 than in 2019 (Figure 3.6). In both 2017 and 2019, null models best described root area and new root growth (Figure 3.6; Table S3.5), suggesting that in both years, treatments did not impact root area or new root growth.

Discussion

Because climate variation includes changes in the amount, timing, and intensity of precipitation among other factors (e.g., temperature, relative humidity, and wind speed), it can be difficult to predict how anticipated future climates will affect crop production [49–51]. By manipulating only precipitation intensity over 3 years, our experiment isolated the effect of one aspect of climate change in a dryland crop system. Consistent with previous observational studies that found winter wheat to be resistant to changes in precipitation intensity [18,26], we found no response of winter wheat to a wide range of precipitation intensity treatments. This is in contrast to the findings of a paired study in a

nearby rangeland site that used the same methods and experimental design, and that documented increased shrub growth in response to these same increased precipitation intensity treatments [10]. Our result that winter wheat was not responsive to treatments was consistent across all above- and belowground physiological and biomass measurements, including grain yield. Though convincing, it was somewhat surprising that wheat growth did not respond positively to the observed increases in soil water potential created by treatments. Results suggest that anticipated increases in precipitation intensity are unlikely to affect winter wheat production at our site in the foreseeable future.

Increased precipitation intensity has the potential to either increase or decrease soil moisture, depending on site conditions (i.e., soil texture, slope, and climate [52,53]). While our twice-monthly soil moisture measurements did not detect treatment effects, our hourly measurements revealed greater soil moisture in a treated than a control plot, particularly in the summer. This was consistent with observations from other studies using similar treatments in arid and semi-arid grasslands and savannas [12,41,54]. Given that all treatments received the same amount of precipitation, we assume that more water moved into the soil with larger precipitation events because a smaller proportion of water was lost to evaporation. The fact that deep-rooted plants have been observed to respond positively to increased precipitation intensity in other studies [41,54] suggests that it may be possible to select wheat varieties (i.e., with deeper roots) that can more fully exploit soil water resources made available by increasing precipitation intensity. Future experiments that measure responses of multiple wheat varieties to precipitation intensity could test this hypothesis.

Treatment effects on soil water potential were greatest from July through September, when plants were not growing [25]. Under hot and dry summer conditions, winter wheat genotypes that have earlier phenology have higher yields [55]. However, the optimal phenological strategy will vary with climate because maximizing yield in water-limited systems often relies on synchronizing phenology with soil moisture [56]. Therefore, other dryland crops or varieties of wheat that continue their growth late season may be more likely to respond positively to the increased soil water availability associated with increased precipitation intensity.

Winter wheat root depth and deep-root densities have been observed to increase in response to drought [57–60]. Additionally, positive relationships between winter wheat yield and maximum rooting depth and deep-root density have been observed under water-limited conditions, but not wet conditions [57,59]. We did not observe changes in root area or new growth of deep roots in response to changes in precipitation intensity. Results suggest that the Promontory wheat variety used in this study is well adapted to the typically dry conditions at the site, but less well adapted to take advantage of the increased soil water availability associated with our increased precipitation intensity treatments.

Aboveground biomass of weeds, 79% of which were annual forbs, also did not respond to treatments. In contrast, in a greenhouse study, annual weed emergence increased with precipitation intensity under dry conditions, but with variable effects under wetter conditions [7]. In natural grasslands, forb productivity has been documented to have both positive [61,62] and neutral [63,64] responses to increased precipitation intensity. The lack of weed response in this experiment and the variety of responses seen

in other studies suggest that the weed growth response to increased precipitation intensity likely depends on the weed species and the environmental conditions.

Our study isolated the effects of altered precipitation intensity from other climate change effects, such as mean annual precipitation, temperature, and CO_2 fertilization. Therefore, we cannot assess the net effects of climate change on this cropping system. Warming has been forecasted to decrease wheat yield in North America [65], while research in Europe suggests that winter wheat yields may increase due to increased radiation use efficiency caused by higher CO_2 concentrations, despite increases in summertime drought [66]. A meta-analysis of 90 modeling studies helps explain these disparate findings and indicates that both positive and negative effects of climate change on wheat are possible, and the outcome largely depends on which of the counteracting effects of CO_2 fertilization or warming are stronger [51]. Our results suggest that in this system, increased precipitation intensity is unlikely to exacerbate increased water stress that could be caused by warming. However, positive, neutral, and negative responses to increased precipitation intensity have been observed in other crops [8,17,18], underscoring the need for experiments such as ours to help estimate likely growth responses of specific crops.

Experiments manipulating precipitation intensity in agricultural settings are limited (but see [31,32,34]). Experiments in grasslands suggest that increased precipitation intensity will increase plant productivity in arid sites and decrease productivity in mesic sites [12,13,67]. The semi-arid cropland studied here may fall into a climatic window in which the advantages of decreased interception and evaporation are balanced by the disadvantages of overland flow and percolation below the rooting zone

that are more likely in mesic systems. It is important to note that dryland agricultural systems are less likely to benefit from increased precipitation intensity relative to diverse grasslands and shrublands because these natural systems have deeper, more extensive, and more diverse rooting systems that can better exploit soil water resources [68]. Additionally, the two growing seasons studied were wetter than average for the site. Treatments may have had neutral to slightly positive effects on wheat growth in drier years because treatments increased soil water availability.

Conclusions

While we detected differences in above- and belowground wheat growth among growing seasons, winter wheat was highly resistant to a wide range of precipitation intensity treatments at our site. Winter wheat is often planted in dryland systems because it is resistant to climate variability, especially summer droughts. Our results demonstrate that this variety of winter wheat is resistant to changes in precipitation intensity, including increased soil water availability, in this dryland system. While other climate effects must be considered (i.e., temperature), our results indicate that under the climatic and edaphic conditions studied, increased precipitation intensity is unlikely to exacerbate potential negative impacts of climate change on winter wheat, which is important given that increases in precipitation intensity are expected regardless of changes in total annual precipitation.

Data availability

Data and code used in this manuscript are available in Holdrege, Beard, and Kulmatiski. (2021). Winter wheat responses to increased precipitation intensity, Utah,

USA (2016-2019). Knowledge Network for Biocomplexity. doi:10.5063/0000GQ.

References

1. UNESCO United Nations World Water Development Report 2020: Water and Climate Change; Paris, 2020;
2. Venkateswarlu, B.; Shanker, A.K. Dryland agriculture: Bringing resilience to crop production under changing climate. In Crop Stress and its Management: Perspectives and Strategies; Springer Netherlands: Dordrecht, 2012; pp. 19–44 ISBN 9789400722200.
3. Stewart, B.A. Dryland Farming. In Reference Module in Food Science; Elsevier B.V.: Amsterdam, The Netherlands, 2016.
4. Donat, M.G.; Lowry, A.L.; Alexander, L.V.; O'Gorman, P.A.; Maher, N. More extreme precipitation in the world's dry and wet regions. Nat. Clim. Chang. **2016**, 6, 508–513, doi:10.1038/nclimate2941.
5. Fischer, E.M.; Knutti, R. Observed heavy precipitation increase confirms theory and early models. Nat. Clim. Chang. **2016**, 6, 986–991, doi:10.1038/nclimate3110.
6. Wilcox, K.R.; von Fischer, J.C.; Muscha, J.M.; Petersen, M.K.; Knapp, A.K. Contrasting above- and belowground sensitivity of three Great Plains grasslands to altered rainfall regimes. Glob. Chang. Biol. **2015**, 21, 335–344, doi:10.1111/gcb.12673.
7. Robinson, T.M.P.; Gross, K.L. The impact of altered precipitation variability on annual weed species. Am. J. Bot. **2010**, 97, 1625–1629, doi:10.3732/ajb.1000125.
8. Fishman, R. More uneven distributions overturn benefits of higher precipitation

for crop yields. Environ. Res. Lett. **2016**, 11, doi:10.1088/1748-9326/11/2/024004.

9. Smith, N.G.; Rodgers, V.L.; Brzostek, E.R.; Kulmatiski, A.; Avolio, M.L.; Hoover, D.L.; Koerner, S.E.; Grant, K.; Jentsch, A.; Fatichi, S.; et al. Toward a better integration of biological data from precipitation manipulation experiments into Earth system models. Rev. Geophys. **2014**, 52, 412–434, doi:10.1002/2014RG000458.
10. Holdrege, M.C.; Beard, K.H.; Kulmatiski, A. Woody plant growth increases with precipitation intensity in a cold semi-arid system. Ecology **2020**, 0, 1–11, doi:10.1002/ecy.3212.
11. Gherardi, L.A.; Sala, O.E. Enhanced precipitation variability decreases grass- and increases shrub-productivity. Proc. Natl. Acad. Sci. **2015**, 112, 12735–12740, doi:10.1073/pnas.1506433112.
12. Heisler-White, J.L.; Blair, J.M.; Kelly, E.F.; Harmoney, K.; Knapp, A.K. Contingent productivity responses to more extreme rainfall regimes across a grassland biome. Glob. Chang. Biol. **2009**, 15, 2894–2904, doi:10.1111/j.1365-2486.2009.01961.x.
13. Heisler-White, J.L.; Knapp, A.K.; Kelly, E.F. Increasing precipitation event size increases aboveground net primary productivity in a semi-arid grassland. Oecologia **2008**, 158, 129–140, doi:10.1007/s00442-008-1116-9.
14. Good, S.P.; Caylor, K.K. Climatological determinants of woody cover in Africa. Proc. Natl. Acad. Sci. **2011**, 108, 4902–4907, doi:10.1073/pnas.1013100108.
15. Case, M.F.; Staver, A.C. Soil texture mediates tree responses to rainfall intensity

in African savannas. New Phytol. **2018**, 219, 1363–1372, doi:10.1111/nph.15254.

16. Bodner, G.; Nakhforoosh, A.; Kaul, H.P. Management of crop water under drought: a review. Agron. Sustain. Dev. **2015**, 35, 401–442, doi:10.1007/s13593-015-0283-4.
17. Shortridge, J. Observed trends in daily rainfall variability result in more severe climate change impacts to agriculture. Clim. Change **2019**, 157, 429–444, doi:10.1007/s10584-019-02555-x.
18. Troy, T.J.; Kipgen, C.; Pal, I. The impact of climate extremes and irrigation on US crop yields. Environ. Res. Lett. **2015**, 10, doi:10.1088/1748-9326/10/5/054013.
19. Mearns, L.O.; Rosenzweig, C.; Goldberg, R. The effect of changes in daily and interannual climatic variability on CERES-Wheat: A sensitivity study. Clim. Change **1996**, 32, 257–292, doi:10.1007/BF00142465.
20. Butler, E.E. Heavy rain, come today. Nat. Clim. Chang. **2020**, 10, 805–806, doi:10.1038/s41558-020-0834-9.
21. Rockström, J.; Karlberg, L.; Wani, S.P.; Barron, J.; Hatibu, N.; Oweis, T.; Bruggeman, A.; Farahani, J.; Qiang, Z. Managing water in rainfed agriculture-The need for a paradigm shift. Agric. Water Manag. **2010**, 97, 543–550, doi:10.1016/j.agwat.2009.09.009.
22. FAO World Food and Agriculture - Statistical Yearbook 2020; FAO, 2020; ISBN 978-92-5-133394-5.
23. Vocke, G.; Ali, M. US wheat production practices, costs, and yields: variations across regions. USDA-ERS **2013**, EIB-116, 30pp.

24. Jensen, K.J.S.; Hansen, S.; Styczen, M.E.; Holbak, M.; Jensen, S.M.; Petersen, C.T. Yield and development of winter wheat (Triticum aestivum L.) and spring barley (Hordeum vulgare) in field experiments with variable weather and drainage conditions. Eur. J. Agron. **2021**, 122, 126075, doi:10.1016/j.eja.2020.126075.

25. Webber, H.; Ewert, F.; Olesen, J.E.; Müller, C.; Fronzek, S.; Ruane, A.C.; Bourgault, M.; Martre, P.; Ababaei, B.; Bindi, M.; et al. Diverging importance of drought stress for maize and winter wheat in Europe. Nat. Commun. **2018**, 9, 1–10, doi:10.1038/s41467-018-06525-2.

26. Li, X.; Troy, T.J. Changes in rainfed and irrigated crop yield response to climate in the western US. Environ. Res. Lett. **2018**, 13, 064031, doi:10.1088/1748-9326/aac4b1.

27. Rezaei, E.E.; Siebert, S.; Ewert, F. Intensity of heat stress in winter wheat - Phenology compensates for the adverse effect of global warming. Environ. Res. Lett. **2015**, 10, doi:10.1088/1748-9326/10/2/024012.

28. Gooding, M.J.; Ellis, R.H.; Shewry, P.R.; Schofield, J.D. Effects of restricted water availability and increased temperature on the grain filling, drying and quality of winter wheat. J. Cereal Sci. **2003**, 37, 295–309, doi:10.1006/jcrs.2002.0501.

29. White, J.W. Comments on a report of regression-based evidence for impact of recent climate change on winter wheat yields. Agric. Ecosyst. Environ. **2009**, 129, 547–548, doi:10.1016/j.agee.2008.10.025.

30. Sheehy, J.E.; Mitchell, P.L.; Ferrer, A.B. Decline in rice grain yields with temperature: Models and correlations can give different estimates. F. Crop. Res.

2006, 98, 151–156, doi:10.1016/j.fcr.2006.01.001.

31. Patil, R.H.; Laegdsmand, M.; Olesen, J.E.; Porter, J.R. Growth and yield response of winter wheat to soil warming and rainfall patterns. J. Agric. Sci. **2010**, 148, 553–566, doi:10.1017/S0021859610000419.

32. Tataw, J.T.; Baier, F.; Krottenthaler, F.; Pachler, B.; Schwaiger, E.; Wyhlidal, S.; Formayer, H.; Hösch, J.; Baumgarten, A.; Zaller, J.G. Climate change induced rainfall patterns affect wheat productivity and agroecosystem functioning dependent on soil types. Ecol. Res. **2016**, 31, 203–212, doi:10.1007/s11284-015-1328-5.

33. Drebenstedt, I.; Schmid, I.; Poll, C.; Marhan, S.; Kahle, R.; Kandeler, E.; Högy, P. Effects of soil warming and altered precipitation patterns on photosynthesis, biomass production and yield of barley. J. Appl. Bot. Food Qual. **2020**, 93, 44–53, doi:10.5073/JABFQ.2020.093.006.

34. Poll, C.; Marhan, S.; Back, F.; Niklaus, P.A.; Kandeler, E. Field-scale manipulation of soil temperature and precipitation change soil CO2 flux in a temperate agricultural ecosystem. Agric. Ecosyst. Environ. **2013**, 165, 88–97, doi:10.1016/j.agee.2012.12.012.

35. Drebenstedt, I.; Hart, L.; Poll, C.; Marhan, S.; Kandeler, E.; Böttcher, C.; Meiners, T.; Hartung, J.; Högy, P. Do soil warming and changes in precipitation patterns affect seed yield and seed quality of field-grown winter oilseed rape? Agronomy **2020**, 10, doi:10.3390/agronomy10040520.

36. Menne, M.J.; Durre, I.; Vose, R.S.; Gleason, B.E.; Houston, T.G. An overview of the Global Historical Climatology Network-Daily Database. J. Atmos. Ocean.

Technol. **2012**, 29, 897–910, doi:10.1175/JTECH-D-11-00103.1.

37. Soil Survey Staff Natural Resrouces Conservation Service, United States Department of Agriculture: Web Soil Survey Available online: https://websoilsurvey.sc.egov.usda.gov/ (accessed on Oct 7, 2018).

38. Hodges, R.; Clawson, R.; Cardon, G.E. Soil Series: Elevation and Agricultural Soil Test Survey of the Godfrey Dryland Experimental Farm, Clarkston, Utah. All Curr. Publ. 2017, Paper 1797.

39. Hole, D.J.; Dewey, W.; Albrechtsen, R.S. Registration of 'Promontory' Wheat. Crop Sci. **1995**, 35, 1206–1207, doi:10.2135/cropsci1995.0011183X003500040055x.

40. Robertson, D.L.; Guy, S.O.; Brown, B.D. Southern Idaho dryland winter wheat production guide; University of Idaho, College of Agricultural and Life Sciencies Extension Bulletin 827; 2004;

41. Kulmatiski, A.; Beard, K.H. Woody plant encroachment facilitated by increased precipitation intensity. Nat. Clim. Chang. **2013**, 3, 833–837, doi:10.1038/nclimate1904.

42. O'Gorman, P.A.; Muller, C.J. How closely do changes in surface and column water vapor follow Clausius-Clapeyron scaling in climate change simulations? Environ. Res. Lett. **2010**, 5, doi:10.1088/1748-9326/5/2/025207.

43. Garbulsky, M.F.M.F.; Peñuelas, J.; Gamon, J.; Inoue, Y.; Filella, I.; Penuelas, J.; Gamon, J.; Inoue, Y.; Filella, I. The photochemical reflectance index (PRI) and the remote sensing of leaf, canopy and ecosystem radiation use efficiencies. A review and meta-analysis. Remote Sens. Environ. **2011**, 115, 281–297,

doi:10.1016/j.rse.2010.08.023.

44. Payero, J.O.; Irmak, S. Variable upper and lower crop water stress index baselines for corn and soybean. Irrig. Sci. **2006**, 25, 21–32, doi:10.1007/s00271-006-0031-2.

45. Bates, D.; Mächler, M.; Bolker, B.; Walker, S. Fitting linear mixed-effects models using lme4. J. Stat. Softw. **2015**, 67, 1–48, doi:10.18637/jss.v067.i01.

46. Wood, S.N. Fast stable restricted maximum likelihood and marginal likelihood estimation of semiparametric generalized linear models. J. R. Stat. Soc. Ser. B **2011**, 73, 3–36, doi:10.1111/j.1467-9868.2010.00749.x.

47. Burnham, K.P.; Anderson, D.R. Model selection and inference: A practical information-theoretic approach; 2nd ed.; Springer: New York, 2002; ISBN 978-0-387-22456-5.

48. R Core Team R: A Language and Environment for Statistical Computing 2019.

49. Iizumi, T.; Ramankutty, N. Changes in yield variability of major crops for 1981-2010 explained by climate change. Environ. Res. Lett. **2016**, 11, doi:10.1088/1748-9326/11/3/034003.

50. Ray, D.K.; Gerber, J.S.; Macdonald, G.K.; West, P.C. Climate variation explains a third of global crop yield variability. Nat. Commun. **2015**, 6, 1–9, doi:10.1038/ncomms6989.

51. Wilcox, J.; Makowski, D. A meta-analysis of the predicted effects of climate change on wheat yields using simulation studies. F. Crop. Res. **2014**, 156, 180–190, doi:10.1016/j.fcr.2013.11.008.

52. Knapp, A.K.; Beier, C.; Briske, D.D.; Classen, A.T.; Luo, Y.; Reichstein, M.;

Smith, M.D.; Smith, S.D.; Bell, J.E.; Fay, P. a.; et al. Consequences of more extreme precipitation regimes for terrestrial ecosystems. Bioscience **2008**, 58, 811–821, doi:10.1641/B580908.

53. Kulmatiski, A.; Adler, P.B.; Foley, K.M. Hydrologic niches explain species coexistence and abundance in a shrub-steppe system. J. Ecol. **2020**, 108, 998–1008, doi:10.1111/1365-2745.13324.

54. Berry, R.S.; Kulmatiski, A. A savanna response to precipitation intensity. PLoS One **2017**, 12, 1–18, doi:10.1371/journal.pone.0175402.

55. Lopes, M.S.; Royo, C.; Alvaro, F.; Sanchez-Garcia, M.; Ozer, E.; Ozdemir, F.; Karaman, M.; Roustaii, M.; Jalal-Kamali, M.R.; Pequeno, D. Optimizing winter wheat resilience to climate change in rain fed crop systems of Turkey and Iran. Front. Plant Sci. **2018**, 9, 1–14, doi:10.3389/fpls.2018.00563.

56. Blum, A. Effective use of water (EUW) and not water-use efficiency (WUE) is the target of crop yield improvement under drought stress. F. Crop. Res. **2009**, 112, 119–123, doi:10.1016/j.fcr.2009.03.009.

57. Fang, Y.; Du, Y.; Wang, J.; Wu, A.; Qiao, S.; Xu, B.; Zhang, S.; Siddique, K.H.M.; Chen, Y. Moderate drought stress affected root growth and grain yield in old, modern and newly released cultivars of winter wheat. Front. Plant Sci. **2017**, 8, 1–14, doi:10.3389/fpls.2017.00672.

58. Barraclough, P.B.; Weir, A.H.; Kulhmann, H. Factors affecting the growth and distribution of winter wheat roots under UK field conditions. In Plant roots and their environment; Elsevier Science Publishers B.V., 1991; Vol. 24, pp. 410–417.

59. Itoh, H.; Hayashi, S.; Nakajima, T.; Hayashi, T.; Yoshida, H.; Yamazaki, K.;

Komatsu, T. Effects of soil type, vertical root distribution and precipitation on grain yield of winter wheat. Plant Prod. Sci. **2009**, 12, 503–513, doi:10.1626/pps.12.503.

60. Hodgkinson, L.; Dodd, I.C.; Binley, A.; Ashton, R.W.; White, R.P.; Watts, C.W.; Whalley, W.R. Root growth in field-grown winter wheat: Some effects of soil conditions, season and genotype. Eur. J. Agron. **2017**, 91, 74–83, doi:10.1016/j.eja.2017.09.014.

61. Grant, K.; Kreyling, J.; Dienstbach, L.F.H.; Beierkuhnlein, C.; Jentsch, A. Water stress due to increased intra-annual precipitation variability reduced forage yield but raised forage quality of a temperate grassland. Agric. Ecosyst. Environ. **2014**, 186, 11–22, doi:10.1016/j.agee.2014.01.013.

62. Grant, K.; Kreyling, J.; Beierkuhnlein, C.; Jentsch, A. Importance of seasonality for the response of a mesic temperate grassland to increased precipitation variability and warming. Ecosystems **2017**, 20, 1454–1467, doi:10.1007/s10021-017-0122-3.

63. Fay, P.A.; Blair, J.M.; Smith, M.D.; Nippert, J.B.; Carlisle, J.D.; Knapp, A.K. Relative effects of precipitation variability and warming on tallgrass prairie ecosystem function. Biogeosciences **2011**, 8, 3053–3068, doi:10.5194/bg-8-3053-2011.

64. Nippert, J.B.; Knapp, A.K.; Briggs, J.M. Intra-annual rainfall variability and grassland productivity: Can the past predict the future? Plant Ecol. **2006**, 184, 65–74, doi:10.1007/s11258-005-9052-9.

65. Asseng, S.; Ewert, F.; Rosenzweig, C.; Jones, J.W.; Hatfield, J.L.; Ruane, A.C.;

Boote, K.J.; Thorburn, P.J.; Rötter, R.P.; Cammarano, D.; et al. Uncertainty in simulating wheat yields under climate change. Nat. Clim. Chang. **2013**, 3, 827–832, doi:10.1038/nclimate1916.

66. Richter, G.M.; Semenov, M.A. Modelling impacts of climate change on wheat yields in England and Wales: Assessing drought risks. Agric. Syst. **2005**, 84, 77–97, doi:10.1016/j.agsy.2004.06.011.

67. Walter, J.; Grant, K.; Beierkuhnlein, C.; Kreyling, J.; Weber, M.; Jentsch, A. Increased rainfall variability reduces biomass and forage quality of temperate grassland largely independent of mowing frequency. Agric. Ecosyst. Environ. **2012**, 148, 1–10, doi:10.1016/j.agee.2011.11.015.

68. DuPont, S.T.; Beniston, J.; Glover, J.D.; Hodson, A.; Culman, S.W.; Lal, R.; Ferris, H. Root traits and soil properties in harvested perennial grassland, annual wheat, and never-tilled annual wheat. Plant Soil **2014**, 381, 405–420, doi:10.1007/s11104-014-2145-2.

Tables

Table 3.1 Treatment descriptions, number of replicate plots (N), and the mean daily rain on days with rainfall. All treatments received the same total water and only differed in event size and frequency. Treatment names were based on event sizes, that is, the amount of water that would be collected from shelter roofs and accumulate in the tanks before being redeposited. Mean daily rain on days with >0 mm of rain was calculated using observed rainfall during the experiment (Appendix S3.2; Figure S3.3). These values are larger than the event sizes because when large natural rain events occurred, water would be redeposited onto the plot multiple times in one day (i.e., multiple "events" in 1 day). The "intensity category" grouped treatments into low- and high-precipitation-intensity categories that were used in the analyses. Shelterless control plots were not included in the analyses of treatment effects but were used to assess shelter effects.

Treatments	Description	N	Mean Daily Rainfall (mm)	Intensity Category
Shelterless control	Ambient plot (no rainout shelter)	3	5.6	
1 mm	Received more frequent, small events than control plots.	1	4.9	Low intensity
Control	Sheltered-control plot, water was redeposited immediately after being collected from the shelter roof.	3	5.6	Low intensity
2 mm	Water was redeposited once enough rainwater was collected in the tank to create a 2 mm event.	1	6.9	Low intensity
3 mm	Water was redeposited once enough rainwater was collected in the tank to create a 3 mm event.	1	8.3	Low intensity
4 mm	Water was redeposited once enough rainwater was collected in the tank to create a 4 mm event.	3	9.1	High intensity
8 mm	Water was redeposited once enough rainwater was collected in the tank to create an 8 mm event.	1	11.5	High intensity
18 mm	Water was redeposited once enough rainwater was collected in the tank to create an 18 mm event.	1	20.5	High intensity

Figures

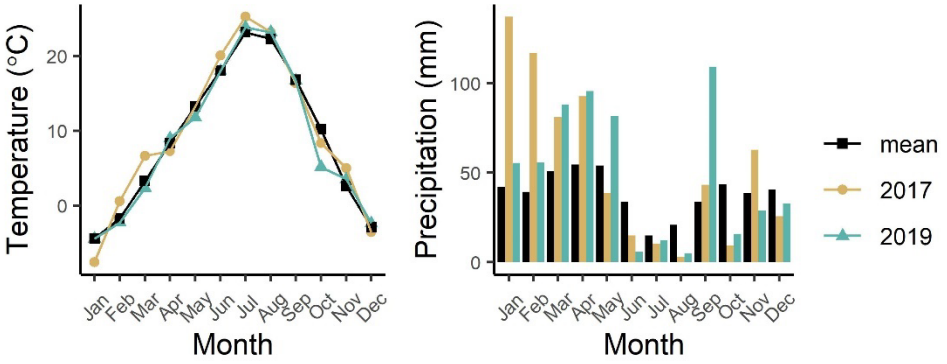

Figure 3.1 Monthly temperature and precipitation in 2017 and 2019, the years during which winter wheat was grown in plots. Historical mean monthly values of records from 1928–2019 are also shown.

Figure 3.2 Shelters (2.1 × 2.5 m) were used to redistribute rain and snow as fewer, larger events at a dryland agriculture site, Utah, USA. Two of three rows of plots are visible in the photograph.

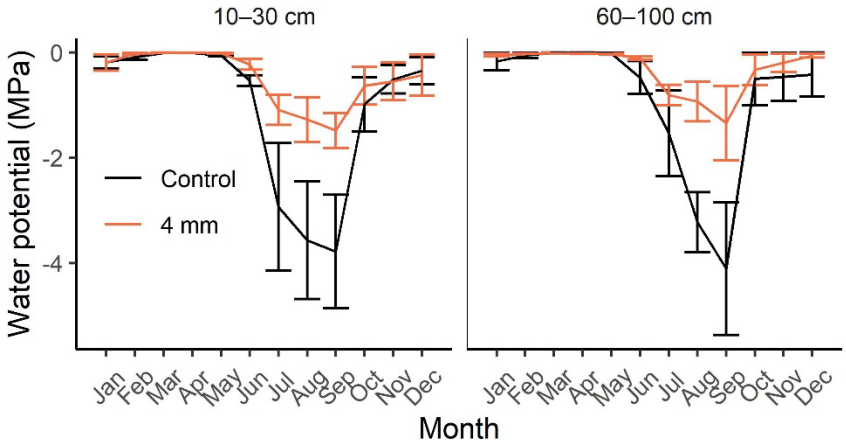

Figure 3.3 Shallow (10–30 cm; left panel) and deep (60–100 cm; right panel) soil water potential over time in a 4 mm event size treated plot and control plot. Water potential was measured separately with three sensors for each depth in each plot. Total annual precipitation was the same in both plots. Monthly values represent averages from hourly measurements from April 2016 to August 2019, the period during which precipitation treatments occurred. Error bars are standard errors based on the three sensors at each depth.

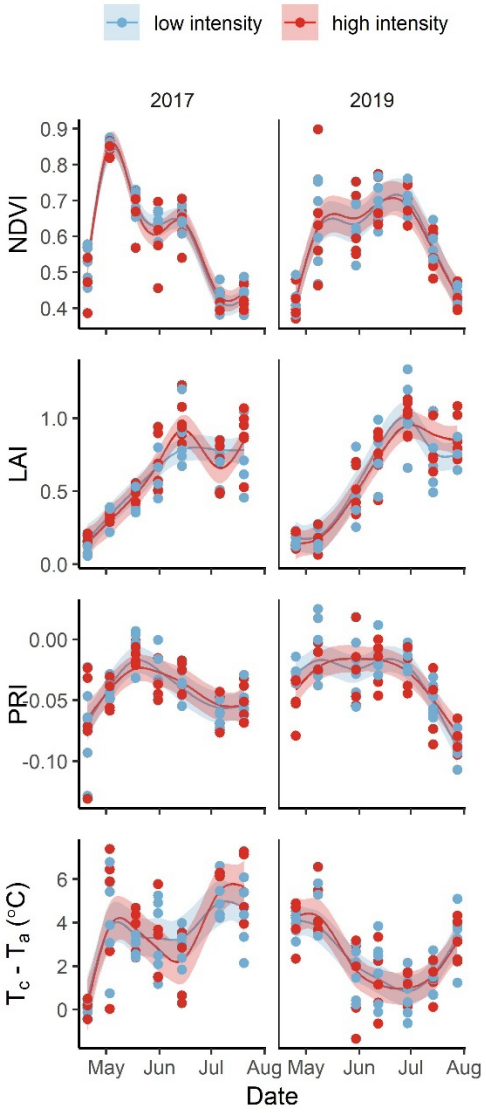

Figure 3.4 Normalized difference vegetation index (NDVI), leaf area index (LAI), photochemical reflectance index (PRI), and the difference between canopy and air temperature ($T_c - T_a$) in low- versus high-precipitation-intensity plots. Data from 2017 (left panels) and 2019 (right panels) are shown. The lines show the predicted values from the generalized additive mixed models (GAMMs), and the shaded regions are 95% confidence intervals. Treatments were grouped into two precipitation intensity categories: low intensity (1 mm, control, 2 mm, and 3 mm treatments) and high intensity (4 mm, 8 mm, and 18 mm treatments). While the null models outperformed the GAMMs presented here (indicating no significant treatment responses; Table S3.4), they are shown to illustrate our data.

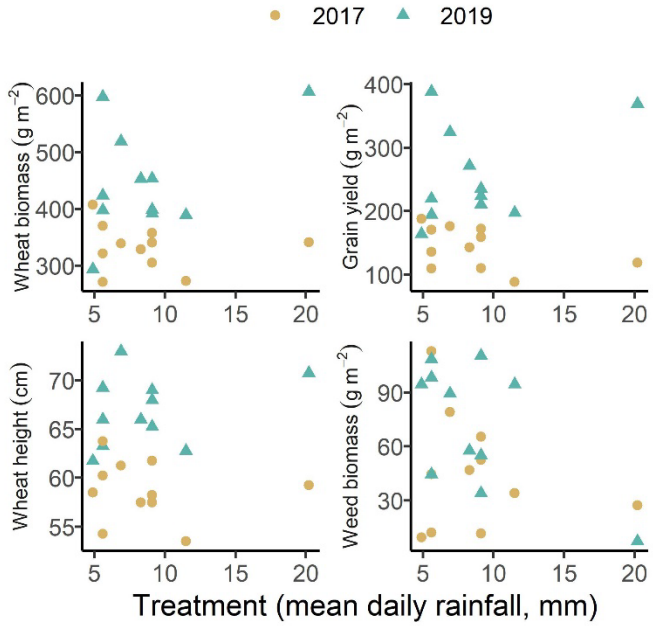

Figure 3.5 Aboveground wheat biomass, grain yield, wheat height, and aboveground weed biomass vs. mean daily rainfall (mean rainfall on days that received >0 mm rain; Table 3.1). Mean daily rainfall was not a significant predictor of the response variables shown here.

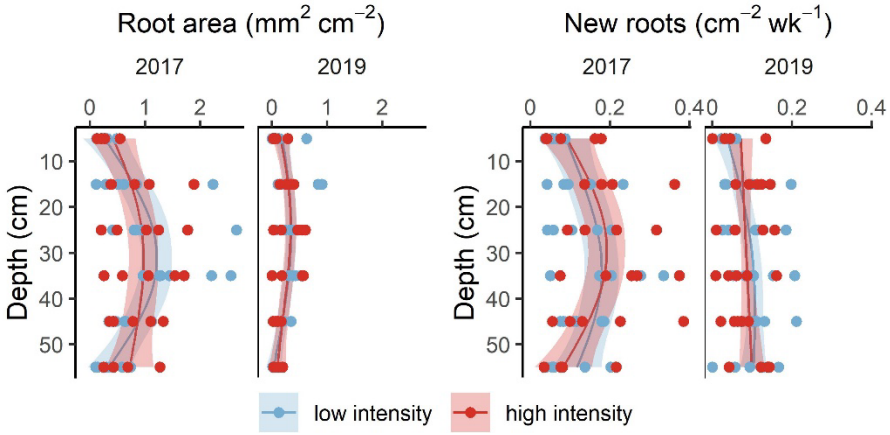

Figure 3.6 Root area (left panels) and new root growth rate (right panels) in low- versus high-precipitation-intensity treatment plots. Values are means of twice-monthly measurements during the growing seasons of 2017 and 2019. Lines show the predicted values from the GAMMs, and the shaded regions are 95% confidence intervals. Treatments were grouped into two precipitation intensity categories: low intensity (1 mm, control, 2 mm, and 3 mm treatments) and high intensity (4 mm, 8 mm, and 18 mm treatments). While the null models outperformed the models presented here (indicating no significant treatment responses; Table S3.5), they are shown to illustrate our data.

CHAPTER 4

PRECIPITATION INTENSIFICATION INCREASES SHRUB DOMINANCE IN ARID, NOT MESIC, ECOSYSTEMS[3]

Abstract

Precipitation events have been predicted and observed to become fewer, but larger, as the atmosphere warms. This precipitation intensification is likely to have large ecohydrological effects in arid and semi-arid ecosystems, where soil water availability often limits plant growth. Yet, conflicting evidence suggests that larger precipitation events may either increase or decrease productivity in these ecosystems, due to differential effects on soil water availability mediated by aridity, soil properties, or vegetation type. Therefore, additional studies are needed to quantify how precipitation intensity will affect plant growth over large spatial scales, especially in ecosystems where woody plants are dominant. Here, we use an individual plant-based ecohydrological model (STEPWAT2) to simulate the effects of 25%, 50%, and 100% increases in precipitation event sizes on water cycling and shrub, grass, and forb biomass in 200 shrub-steppe sites across the western United States. Simulations did not change annual precipitation amounts and were performed for 0 °C, 3 °C, and 5 °C warming. Larger precipitation events decreased evaporation and 'pushed' water into shrub root zones in arid and semi-arid sites, but 'pushed' water below shrub root zones in mesic sites. This resulted in increased shrub biomass in arid and semi-arid sites, but not in mesic sites. The positive effect of precipitation intensification on shrubs partially counteracted the mostly

[3] Holdrege M. C, A. Kulmatiski, K. H. Beard, & K. A. Palmquist. Precipitation intensification increases shrub dominance in arid, not mesic, ecosystems. In preparation.

negative effects of warming. In contrast to shrubs, grasses and forbs showed no consistent response to precipitation intensification resulting in a competitive advantage for shrubs in arid and semi-arid sites under a wide range of warming and soil texture conditions. Results suggest that precipitation intensification may contribute to ongoing woody plant encroachment observed in arid and semi-arid ecosystems around the world.

Introduction

As the atmosphere warms, precipitation events become fewer and larger (i.e., increased precipitation intensity; Du et al., 2019; Pendergrass & Knutti, 2018; Trenberth, 2011). Increases in precipitation intensity may decrease interception and evaporation but increase run-off or percolation depth (Guan et al., 2014; Hou et al., 2021; Knapp et al., 2008). Consequently, the net effect on water availability for plants depends on whether reductions in evaporation are smaller or larger than increases in water loss via run-off or drainage. However, the effects of precipitation intensity on soil water fluxes are rarely tested directly, and there is a lack of consensus regarding how plant productivity and composition will respond (Case & Staver, 2018; Good & Caylor, 2011; Kulmatiski & Beard, 2013). Some evidence suggests that plant productivity and woody plant growth decreases with increasing precipitation intensity (Good & Caylor, 2011; Xu et al., 2015, 2018). Other studies have documented increases in woody plant growth as water is 'pushed' below shallow grass root zones and into slightly-deeper woody plant root zones (Berry & Kulmatiski, 2017; Kulmatiski & Beard, 2013). Others have highlighted the importance and context-dependence of aridity, seasonality, soil type, soil texture, vegetation type, and slope (Bates et al., 2006; Case & Staver, 2018; Knapp et al., 2008; Liu et al., 2020; Ritter et al., 2020; Zeppel et al., 2014).

The impacts of increased precipitation intensity are likely to depend on climate, particularly aridity. Arid and semi-arid ecosystems, defined by annual precipitation being less than half of potential evapotranspiration (Middleton & Thomas, 1997), represent over 40% of terrestrial land area (Prăvălie, 2016), and are especially sensitive to changes in water cycling (Noy-Meir, 1973). Previous work, primarily from grasslands, suggests that increased precipitation intensity tends to increase plant productivity in arid sites but decrease productivity in mesic sites (Liu et al., 2020; Wilcox et al., 2015; Zeppel et al., 2014). While it remains difficult to distinguish changes in evaporation from changes in transpiration, it is likely that interception and evaporation decrease as precipitation event size increases. This decline in evaporation can be expected to increase soil water availability unless more water is lost to runoff or percolation below the rooting zone (Knapp et al., 2008). Therefore, increases in soil water availability that result from precipitation intensification may be larger in arid sites where little deep drainage occurs. Most insight into the effects of precipitation intensity is derived from studies in temperate grasslands, or in subtropical savannas; less is known about how temperate shrub-steppe ecosystems, which are widespread in North America, South America, and Asia will respond (West, 1983).

Differences in soil texture and associated differences in plant-available water holding capacity and percolation rates may also influence water cycling and plant responses to increased precipitation intensity (i.e., the inverse texture effect; Knapp et al., 2008; Noy-Meir, 1973). For example, in mesic sites, the greater water holding capacity of fine-textured soils may reduce water losses to drainage (Knapp et al., 2008; Noy-Meir, 1973). However, in arid sites, slow percolation rates in fine-textured soils may increase

evaporation while coarse-textured soils may allow precipitation to percolate deeper into the soil where it is more protected (Case & Staver, 2018). Therefore, increased precipitation intensity may increase plant growth on coarse-textured in arid sites and fine-textured in mesic sites (Knapp et al., 2008).

Woody and herbaceous plant functional types may respond differently to changes in precipitation intensity (Liu et al., 2020). The two-layer hypothesis suggests that woody plants may benefit from increased precipitation intensity due to deeper percolation of water where woody plants have a competitive advantage over more shallowly-rooted herbaceous plants (Berry & Kulmatiski, 2017; Walter, 1971; Ward et al., 2013). Manipulative field experiments, one in a sub-tropical savanna (Kulmatiski & Beard, 2013) and one in a temperate shrub-steppe (Holdrege et al., 2021), provide evidence that more deeply-rooted woody plants preferentially benefit from larger precipitation events. However, some observational studies have found negative woody plant responses to increased intensity, potentially due to competition with grasses that have faster water uptake (Good & Caylor, 2011; Xu et al., 2018). This lack of consensus underscores the need for additional studies that evaluate woody and herbaceous plant responses to precipitation intensity across large spatial scales.

Manipulative field experiments cannot feasibly test a complete range of aridity, soil texture, climate, and plant-community type conditions. Observational studies allow for the assessment of ecosystem responses across broad spatial scales that represent many site-specific conditions, but assessing causal effects is challenging in part because of the strong correlation among climatic variables (Dolby, 2021). Process-based simulation models represent complex processes that are difficult to measure directly, can be applied

across broad spatial and temporal scales, and can be used to evaluate the causes and effects of multiple treatments, which makes them useful for addressing questions that cannot otherwise be answered (Smith & Huston, 1989). Therefore, simulation modeling can complement and expand on knowledge generated by empirical studies.

Here we used an individual-based plant simulation model (STEPWAT2) to evaluate the response of big sagebrush-dominated ecosystems to increased precipitation intensity at 200 sites covering a wide range of conditions in the western United States. Simulations increased mean precipitation event sizes (1.25x, 1.5x and 2x) and decreased frequency, without changing total annual precipitation. Our goals were to understand how increased precipitation intensity influences soil moisture, soil water fluxes (e.g., transpiration, evaporation, and drainage), and aboveground biomass of woody and herbaceous plant functional types across a range of climatic and soil texture conditions. To put our results in context, we compared the effects of increased precipitation intensity to the effects of two warming scenarios (3 °C and 5 °C increases) on plant functional type biomass.

Methods

Study area

We conducted simulations using climate data from 200 sites in the western United States representative of big sagebrush (*Artemisia tridentata* Nutt.) ecosystems (Figure 4.1; Palmquist et al., 2021). Sagebrush ecosystems currently cover an estimated 651,000 km^2 in the western United States, which is roughly half of their historical extent (Remington et al., 2021). The sites chosen cover a wide range of climate conditions

currently found in the region (Palmquist et al., 2021), with mean annual precipitation ranging from 178 mm to 1028 mm and mean annual temperature ranging from 1 °C to 13 °C.

Modeling approach

We used the STEPWAT2 model to simulate big sagebrush ecosystem responses to precipitation intensification. STEPWAT2 couples a process-based soil-water model (SOILWAT2) that operates on a daily time-step with an individual-based plant simulation model (STEPPE) that operates on a yearly time-step (Palmquist et al., 2018; Schlaepfer et al., 2012). STEPWAT2 is designed for use in water-limited systems and has been validated in big sagebrush ecosystems (Palmquist et al., 2018). Ecohydrological variables are simulated within SOILWAT2 based on daily minimum and maximum temperature, and precipitation, monthly cloud cover, humidity, wind speed, plant biomass, rooting distributions, and soil texture (Schlaepfer et al., 2012). Key ecohydrological output variables from SOILWAT2 used in this study include the amount of water transpired by shrubs, grasses, and forbs from each of eight soil depths (0 – 10, 10 – 20, 20 – 30, 30 – 40, 40 – 60, 60 – 80, 80 – 100, 100 – 150 cm), evaporation (total evaporation of water intercepted by vegetation and litter, and from bare soil), water drainage (here defined as deep drainage past 150 cm), and the number of 'wet days' per year (number of days water potential is above wilting point, here defined as -1.5 MPa; Savage et al., 1996). Net run-off was not simulated because plots were treated as being on level ground (i.e., zero slope).

Within STEPWAT2, individual plants are simulated in 1 m x 1 m plots, which is roughly the area that a big sagebrush plant occupies (Palmquist et al., 2021; Sturges,

1977). Species-specific plant traits (i.e. growth rate, probability of establishment, minimum and maximum biomass, maximum age) and soil water availability are used to simulate establishment, competition, growth, and death of individual plants (described in detail in Palmquist et al., 2018). Competition between plant individuals occurs through multiple mechanisms: greater allocation of resources to larger individuals (representing intraspecific competition) and differential allocation of resources based on functional type-specific relative rooting depth distributions and phenology in relation to temporal and spatial patterns of soil water availability (interspecific competition). Plant mortality occurs due to resource limitation, when plants are growing slowly, and to represent plant survivorship patterns in which only a small proportion of individuals reach their maximum age (Palmquist et al., 2018). Simulations start with a seedbank and no vegetation established.

We simulated aboveground annual biomass (hereafter, biomass) for individuals for one representative species belonging to each of 10 plant functional types: big sagebrush, non-big sagebrush shrubs, C_3 perennial grasses, C_3 annual grasses, C_4 perennial grasses, C_3 perennial warm-season forbs, C_3 perennial cool-season forbs, C_3 annual warm-season forbs, C_3 annual cool-season forbs, and succulents (species-specific parameters used are provided in Palmquist et al., 2021; see Appendix S4.1 for species list). To represent that the optimum temperature for photosynthesis is higher for C_4 than C_3 plants (Sage, 2004; Yamori et al., 2014), growth rates are modified based on mean annual temperature, which influences biomass responses to warming. Above a mean annual temperature of 9.5 °C, growth rates of C_3 plants are reduced by 33%, and those of C_4 plants are increased by 50% (Palmquist et al., 2018; Epstein et al., 1997). When this

growth rate modifier is used in shrublands, it decreases C_3 shrub growth rates with warming when the annual temperature crosses the 9.5 °C threshold (i.e., a site transitions from 'cool' to 'warm'). This general response is supported by observational data that suggests big sagebrush growth increases with warming at temperatures below 9 °C and decreases above 9 °C (Kleinhesselink & Adler, 2018). While STEPWAT2 output included biomass for each of 10 functional types, we focused on aggregated biomass data of four main groups: shrubs, C_3 perennial grasses, C_4 perennial grasses, and forbs, which are dominant plant functional types in these ecosystems.

SOILWAT2 simulates transpiration by month and soil layer for three more coarsely defined functional types (shrubs, grasses, and forbs), and this transpired water is then apportioned to the 10 functional types within STEPPE. Our analyses of transpiration responses focused on total transpiration (i.e., total of all plants), and transpiration of the three functional types for which it was directly simulated (shrubs, grasses, and forbs). Resource partitioning depends on the rooting profile, phenology, and biomass of each of the 10 functional types, along with the distribution of soil water with depth. Individual plants are resource-limited when the total annual transpiration apportioned to them is insufficient, causing decreased growth rates and increased mortality (Palmquist et al., 2018).

STEPWAT2 was run in a fully factorial design including four precipitation intensity treatments, three levels of warming, and four soil textures (described below) for 200 iterations at each of the 200 sites to determine soil water and biomass responses. Running the model for 200 iterations is roughly analogous to having 200 separate, 1 m x 1 m plots at each site; the plant community is independently simulated in every iteration.

We ran each simulation for 150 years; the first 100 years of the simulation are needed for plant communities to reach a stable state and were excluded from analyses. Ambient intensity and ambient warming treatments served as controls and were based on current precipitation intensity and temperature at each site. The R program rSFSTEP2 (Palmquist et al., 2018) was used to concurrently run STEPWAT2 for all 200 sites (Appendix S4.2). All simulations included light grazing (24% removal of the current year's grass and forb biomass growth; Milchunas & Lauenroth, 1993), and no fire.

Precipitation intensity and warming treatments

Thirty years (1981-2010) of daily precipitation and temperature data from the Daymet data product (1 km^2 resolution; Thornton et al., 2016) were used as the basis for precipitation intensity and warming treatments. Precipitation manipulations increased mean daily precipitation event size (i.e., mean precipitation on days with > 0 precipitation) by 0% ('ambient intensity' treatment), 25% ('1.25x intensity'), 50% ('1.5x intensity'), and 100% ('2x intensity'). Manipulations decreased the total number of precipitation events by 0%, 20%, 33%, and 50% for the ambient (control), 1.25x, 1.5x and 2x intensity treatments, respectively. The mean length of multiday precipitation events and mean total precipitation (monthly and yearly) remained unchanged. Uncertainty exists in the magnitudes of expected increases in precipitation intensity under future conditions (Du et al., 2019; Myhre et al., 2019; Pendergrass & Knutti, 2018). These treatment levels were not meant to serve as projections but rather were applied to determine ecosystem sensitivity to relatively moderate to extreme increases in intensity. For context, Clausius-Clapeyron scaling (i.e., 7%/°C increase in saturation vapor pressure) can been used as a first approximation of expected increases in precipitation

intensity (O'Gorman & Muller, 2010; Pendergrass, 2018), and it suggests that 1.25x, 1.5x, and 2x increases in precipitation intensity would require roughly 3 °C, 6 °C, and 10 °C warming, respectively.

STEPWAT2 contains a first-order Markov weather generator that was used to generate 150 year-long sequences of daily precipitation and temperature that in the case of the ambient treatment had similar statistical properties to the original 30-year weather data sequence from a site (see Palmquist et al., 2018 for details). Precipitation intensity manipulations were achieved by adjusting the probability of precipitation and expected event size on days that receive precipitation, which are inputs to the weather generator (Appendix S4.2). For example, with the 2x intensity manipulation, for each day of the year, the probability of precipitation was halved and the mean and standard deviation of precipitation event size was doubled.

In addition to no warming (ambient), two warming levels were chosen to evaluate the effects of precipitation intensification relative to warming, which has received considerably more attention. These warming levels were calculated as the median increase in mean annual temperature across 13 GCMs and the 200 sites under end-of-century (2071 – 2100) conditions for a moderate and more severe emissions scenarios (representative concentration pathway [RCP]4.5 and RCP8.5). This resulted in a 3.07 °C and 5.40 °C increase in temperature ('3 °C' and '5 °C' warming treatments, hereafter) for RCP4.5 and RCP8.5, respectively. Temperature manipulations for each site were achieved by increasing minimum and maximum temperatures simulated by the weather generator for each day of the year by a mean of 3.07 °C and 5.40 °C, respectively.

Aridity and soil texture

To compare responses across an aridity index (mean annual precipitation/potential evapotranspiration; Cherlet et al., 2018), potential evapotranspiration (estimated within SOILWAT2) and mean annual precipitation were calculated for each site. Lower values of aridity indicate drier conditions, and values less than one indicate there is an annual moisture deficit because precipitation inputs are less than evaporative demand. We focus on aridity instead of mean annual precipitation because it can, for example, separate hot dry and cool dry sites that have the same mean annual precipitation. Though, similar conclusions were drawn when mean annual precipitation was used (Appendix S4.3).

Four fixed soil texture levels were used in model simulations at each site, so that the effects of differences in climate among sites could be isolated from the effects of soil texture. Soil textures were calculated using data from NRCS STATSGO 1 km^2 grid cells (Soil Survey Staff, 2012) that contained > 66% sagebrush (Bradford et al., 2019; U.S. Geological Survey Gap Analysis Program, 2016). The model was run using a median soil as well as three different soils high in sand, silt, and clay content, respectively (Appendix S4.4). The 'median' soil texture was determined by calculating median sand and clay content across grid cells, which resulted in a silt loam containing 31% sand, 52% silt, and 17% clay (hereafter 'loam'). The sandy soil was chosen by calculating the 95^{th} percentile of sand content across grid cells (63% sand, 24 % silt, and 13% clay; a sandy loam, hereafter 'sand'). Soils high in silt and clay content were similarly calculated using 95^{th} percentiles (16% sand, 77% silt, 7% clay, a silt loam, hereafter 'silt'; and 32% sand, 34% silt, 34% clay, a clay loam, hereafter 'clay').

Analyses

Soil water and biomass variables were summarized by averaging the last 50 years of simulations for each site, precipitation intensity, warming, and soil texture combination. Data presented are averages across years and the 200 model iterations for a site. Treatment responses were calculated as the absolute and percent difference between treatment and ambient (control) conditions at each site.

To address how increased precipitation intensity influenced soil water, for each site we calculated the change in total transpiration (across all plant functional types) and the amount of water transpired annually from each soil depth. Additionally, for each site, we calculated transpiration and the proportion of wet days in surface (0 – 10 cm) and sub-surface (10 – 150 cm) soils for each day of the year. The proportion of wet days at a site for a specific day and soil depth was calculated as the proportion of times that day of the year had wet soil (> -1.5 MPa) across years and model iterations. Additionally, we calculated changes in the total amount of water lost to evaporation and drainage.

Next, we examined how soil water responses to increased precipitation intensity differed with aridity and soil texture. The relationships between soil water fluxes (i.e., total transpiration, evaporation and drainage) and aridity were examined for each of the four soil textures. To estimate the non-linear relationships between these soil water fluxes and aridity, locally estimated scatterplot smoothing (LOESS) curves were fit ('loess' function in R). We extracted the maxima and minima from these curves as well as the point at which the curve crossed zero (i.e., the aridity index value at which a response transitioned between negative and positive). Post-hoc analyses revealed small soil texture effects (see Results and Appendix S4.4), and so values for the median soil texture (loam)

are presented for clarity.

To assess how precipitation intensification impacted individual plant functional types, we determined how both transpiration and biomass of key plant functional types responded to treatments and how responses differed with aridity and soil texture. LOESS curves were fit to describe how responses varied with aridity.

To put the impacts of increases in precipitation intensity in context, we calculated biomass responses of each plant functional type to increased intensity only, warming only, and increased intensity plus warming. We focus on whether the effects of an extreme increase in precipitation intensity (2x intensity) approaches the magnitude of response of a moderate level of warming (3° C). Analyses were conducted using R version 4.0.1 (R Core Team, 2020).

Results

Mean changes in soil water fluxes

Increases in precipitation intensity led to small mean increases in total transpiration, primarily because, on average across the 200 sites, plants extracted less water from surface (0 – 10 cm) soils, and more from sub-surface soils (10 – 150 cm; Figure 4.2, Appendix S4.5). Transpiration increased by 0.4 (-0.6 – 1.3) cm $year^{-1}$ (mean, 5^{th} – 95^{th} percentiles), 0.6 (-0.8 – 1.7) cm $year^{-1}$, and 0.8 (-1.4 – 2.6) cm $year^{-1}$ in response to the 1.25x, 1.5x, and 2x treatments, respectively. This translates to changes in transpiration of 2.2% (-2.3 – 6.4%; 1.25x intensity), 3.5% (-2.5 – 8.5%; 1.5x intensity), and 5.1% (-5.4 – 14.2%; 2x intensity). Increases in water uptake from sub-surface soils occurred mostly in the mid- to late-growing season (Figure 4.3). In contrast to surface

soils, the proportion of wet days in sub-surface soils increased with precipitation intensity, especially later in the season (July-October; Figure 4.3), indicating that mean increases in transpiration were due to more late-season deep-water storage.

Mean annual water losses at a given site due to transpiration, evaporation, and deep drainage accounted for all the mean annual precipitation. Therefore, because treatments did not alter total precipitation, changes in transpiration necessarily coincided with changes in the amount of water lost to evaporation and drainage (Appendix S4.6). The 2x intensity treatment decreased evaporation by -16% (-23.1 – -8.7%), while the 1.25x and 1.5x treatments caused smaller reductions (Figure 4.4). The 2x intensity treatment increased drainage by 54.8% (12.5 – 106.7%). Because drainage under ambient conditions tended to be small in most sites, these large percent increases in drainage represent absolute increases of only 1.4 cm (0.1 – 3.3 cm) per year (Figure 4.4c).

Changes in soil water fluxes with varying aridity and soil texture

Total transpiration responses varied substantially among sites. In more arid sites, transpiration generally increased in response to precipitation intensification, while in more mesic sites, transpiration decreased or remained unchanged (Figure 4.4a). Across precipitation intensity treatments, on average transpiration increased the most (i.e., maxima of the curve) at an aridity index value of 0.33, decreased the most (i.e., minima of the curve) at 0.84 aridity, and the transition point between positive and negative responses occurred at 0.54 aridity (Figure 4.4a). Evaporation decreased the most at an aridity of 0.40 (Figure 4.4b). The greatest increase in drainage occurred at 0.75 aridity (Figure 4.4c). In arid and semi-arid sites (aridity < 0.54), decreases in evaporation tended to be larger than increases in drainage (Figure 4.4). In more mesic sites (aridity > 0.54)

decreases in evaporation were smaller than increases in drainage (Figure 4.4).

Compared to aridity, differences in soil texture had only limited impact on soil water responses to treatments (Appendix S4.4). In response to the 2x intensity treatment, total transpiration increased the most on the silt soil (6.1% mean increase), while increases were smaller on the loam (5.1%), clay (4.4%), and sand (3.9%) soils. Additionally, the relationships between changes in transpiration and aridity were similar among soil textures (Appendix S4.4). Decreases in evaporation were also similar across textures, ranging from -15.5% (silt) to -17.4% (sand) in response to 2x intensity, representing differences of only 0.2 cm annually. The increase in water lost to drainage as a result of 2x intensity was smallest for the silt soil (1.0 cm/year) and largest for the sand (1.8 cm/year).

Responses of individual plant functional types

Shrub transpiration (i.e., the sum of water transpired from all depths by shrubs), which on average made up 73% of total transpiration, exhibited the largest response to precipitation intensity, increasing in arid sites, and decreasing in more mesic sites (Figure 4.5a; Appendix S4.5). In response to increasing precipitation intensity, shrubs decreased surface soil (0 – 10 cm) water uptake and increased water uptake from all sub-surface soil layers (10 – 150 cm) (Figure 4.2). For example, the percent of shrub transpiration that originated from sub-surface soils increased from 66.6% to 76.1% in response to the 2x intensity treatment (Figure 4.2).

Grasses and forbs also had less water uptake from surface soils in response to increased precipitation intensity (Figure 4.2, Appendix S4.5). But these more shallow-rooted plants only exhibited substantial increases in water uptake from moderate depths

(10 – 40 cm), not from the deepest soils (40 – 150 cm) (Figure 4.2, Appendix S4.5). The percent of transpired water originating from moderate depths (10 – 40 cm) increased from 43.4% to 50.5% in grasses, and 44.8% to 55.1% in forbs, in response to 2x intensity. The percent of transpired water originating from the deepest soils (40 – 150 cm) only increased from 19.4% to 22.6% and 12.2% to 14.6%, respectively. Total grass and forb transpiration exhibited less consistent responses to increased precipitation intensity than shrubs, with both small positive and small negative responses occurring at all levels of aridity (Figure 4.5). Changes in grass transpiration tended to be most negative (minima of the curve) around 0.37 aridity (Figure 4.5).

Because plant-available soil water is the limiting resource in STEPWAT2, changes in total biomass were similar to changes in total transpiration with increased precipitation intensity (Pearson correlation coefficient = 0.87). Positive shrub biomass responses were larger in arid sites and under the 2x intensity treatment (Figure 4.6). Across sites, shrub biomass increased by a mean of 3.0% (-4.8 – 10.8%, 5^{th} – 95^{th} percentiles; 1.25x intensity treatment), 5.0% (-3.6 – 14.5%; 1.5x treatment), and 7.1% (-5.5 – 19.9%; 2x treatment) (Figure 4.7). Under the 2x intensity treatment, the maximum increase in shrub biomass (i.e., maxima of the curve) was 11.4% and occurred at an aridity index value of 0.36, and the response transitioned from positive to negative at 0.59 aridity (Figure 4.6a). The maximum decrease in shrub biomass (i.e., minima of the curve) was a -4.1% change and occurred at 0.94 aridity (Figure 4.6a).
with greater precipitation intensity.

In contrast to shrubs, herbaceous plants (grasses and forbs) did not exhibit consistent biomass responses to precipitation intensity treatments and responses varied

little with aridity (Figure 4.6). The most extreme precipitation intensity treatment (2x intensity) caused biomass across sites to change by a mean of -1.1% (-7.3 – 5.2%) for C_3 perennial grasses, -1.5% (-8.9 – 6.6%) for C_4 perennial grasses, and -0.6% (-13.5 – 15.6%) for forbs (Figure 4.7, Appendix S4.5). As a result, the shrub to C_3 perennial grass ratio increased with precipitation intensity, signaling a shift toward greater shrub dominance (Figure 4.7a). Both annual and perennial C_3 grasses exhibited similar responses to increased precipitation intensity (Appendix S4.5). Biomass responses of all plant functional types were similar among soil textures (Appendix S4.4).

Combined effects of increased precipitation intensity and warming

All plant functional type responses to 3° C and 5° C warming were larger than responses to precipitation intensity, although the magnitude and direction of responses differed among functional types (Figure 4.7; Appendix S4.5). The 5° C warming treatment caused larger changes in biomass than the 3° C treatment (Figure 4.7, Appendix S4.5). At sites with an aridity index < 0.54 (the point where the effect of precipitation intensification on total transpiration went from positive to negative), 3 °C of warming decreased shrub biomass by a mean of -12.7% (-31.6% – 10.0%; 5^{th} – 95^{th} percentiles), which is a larger change than the mean 8.8% biomass increase caused by the 2x intensity treatment in those same sites (Figure 4.7b). By comparison, in more mesic sites (aridity > 0.54; N = 35) 3 °C of warming only changed shrub biomass by a mean of -1.5% (-22.3% – 12.1%; Appendix S4.5). When combined, the positive effects of precipitation intensity partially mitigated the negative effects of warming on shrub biomass in arid and semi-arid sites (Figure 4.7b). C_3 perennial grasses also responded negatively to warming, with 3 °C warming causing a mean reduction in biomass of -9.6%

(-19.1% – 3.2%) in more arid sites (aridity < 0.54) and -4.8% (-17.1% – 5.3%) in more mesic sites (Figure 4.7c; Appendix S4.5). Similar to C_3 perennial grasses, warming also decreased forb biomass (Appendix S4.5). Precipitation intensity did not mitigate the negative effects of warming on C_3 perennial grasses (Figure 4.7c), which is in contrast to shrubs that benefited from precipitation intensification in arid and semi-arid sites. Therefore, under the combination of increased precipitation intensity and warming, shrubs decreased less relative to C_3 perennial grasses, resulting in a higher shrub to C_3 perennial grass ratio in arid and semi-arid sites (Figure 4.7a).

Unlike other functional types, C_4 grasses had large positive responses to warming, with 3 °C warming causing a mean biomass increase of 20.0% (-3.4% – 52.3%). As a result of these positive responses, shrub to C_4 grass ratios decreased under warming, and to a lesser extent under the combination of warming and increased precipitation intensity (Appendix S4.5).

Discussion

Our simulations suggest that fewer, larger precipitation events will increase shrub relative abundance in arid and semi-arid sites (i.e., where the aridity index is less than ~ 0.5). This increase in shrub relative abundance reflects little change in herbaceous growth and an increase in shrub growth. This change occurred because larger precipitation events 'pushed' water deeper into the soil where shrubs roots were more common than grass and forb roots (Appendix S4.5). These findings provide a mechanistic understanding of how precipitation intensification might contribute to greater dominance of woody plants, a trend that has been observed in arid and semi-arid systems globally in the past 50 years (Archer et al., 2017; Zhou et al., 2021). Interestingly, we also found that in arid and semi-

arid sites warming alone decreased shrub relative abundance, but that warming and precipitation intensification generally had the opposite effect. Consequently, our results suggest that models that do not consider precipitation intensity effects might incorrectly predict ecosystem responses to future climate changes.

Under increased precipitation intensity, we simulated a decrease in evaporation from surface soils during the warm season, when evaporative demand is high, resulting in greater penetration and percolation of precipitation into deep soil layers (Figure 4.3). Precipitation in sagebrush ecosystems and many other semi-arid ecosystems is dominated by small events (< 5 mm) that typically only wet shallow soils where plant roots compete with evaporative demand from the atmosphere (Lauenroth & Bradford, 2009). Our treatments created longer times between precipitation events resulting in drier surface soils. However, when larger precipitation events occurred, water percolated deeper into the soil where it was more protected from evaporation, and where roots of woody plants are more abundant than those of grasses and forbs. The decreases in evaporation and increases in drainage we simulated are consistent with modeling studies that have examined the effects of inter-annual precipitation variability on water balance pools and fluxes (Hou et al., 2021; Sala et al., 2015).

We found that the effects of precipitation intensity on soil water fluxes varied greatly with aridity (Figure 4.4). In arid sites, increased precipitation intensity only caused small increases in water lost to drainage (i.e., below rooting zones), likely because in drier climates precipitation events are usually not large or frequent enough to saturate deep soil layers. In addition, in these arid sites, evaporation decreased more than drainage increased, resulting in more plant available water and transpiration. In contrast, in mesic

sites, larger precipitation events pushed more water below plant rooting zones, resulting in less plant available water and transpiration.

The response of total transpiration to precipitation intensification transitioned from positive to negative around an aridity index of 0.54 and a mean annual precipitation (MAP) of 515 mm (Appendix S4.3). This transition can help explain why experiments in arid sites have found positive effects of precipitation intensity on productivity whereas experiments in mesic sites have found negative effects (Liu et al., 2020; Wilcox et al., 2015; but see Zhang et al., 2016). Previous research on interannual precipitation variability suggests the transition point from positive to negative responses occurs between 300 and 380 MAP (Gherardi & Sala, 2019; Hou et al., 2021; Sala et al., 2015), but these studies mainly focused on grasslands, and intra-annual and inter-annual variability could have different transition points. Our results suggest that in sites with less than 515 mm MAP, shrubs can intercept soil water that percolates below shallow grass roots.

Our simulations indicate that, in arid and semi-arid sites shrubs, but not grasses, will benefit from increased precipitation intensity. This finding is consistent with the two-layer hypothesis because, relative to shallow-rooted grasses, deeper-rooted shrubs preferentially benefited from deeper soil water percolation caused by larger precipitation events (Walter, 1971; Ward et al., 2013). For shrubs, reduced surface soil water uptake (0 – 10 cm) was usually overcompensated by increased sub-surface soil water uptake (10 – 150 cm; Figure 4.2). This positive effect on shrubs was greatest in the most arid sites and disappeared around 0.54 aridity. Forbs and grasses also reduced water uptake from surface soils, but in contrast to shrubs, they did not consistently compensate this loss with

increased uptake from deeper soils (Figure 4.2). These results are consistent with a recent experiment which found that sagebrush growth increased, and grass and forb growth remained unchanged in response to increased precipitation intensity in a semi-arid site (Holdrege et al. 2021). Results are also consistent with experiments that increased precipitation intensity in a sub-tropical savanna (Kulmatiski & Beard, 2013), and interannual precipitation variability in a desert shrubland (Gherardi & Sala, 2015), which both found positive growth responses of woody, but not herbaceous plants.

Differences in soil texture had small effects on ecohydrological and biomass responses to increased precipitation intensity. Further, because we found that relationships between soil water fluxes and aridity were similar among soil textures, we did not find evidence to support the inverse texture effect (Knapp et al., 2008; Noy-Meir, 1973). We found that silt, which had the highest plant available water capacity of the soils we simulated, retained slightly more water from larger precipitation events without losing it to drainage (Appendix S4.4). In contrast, sand lost the most water to drainage and had the smallest increase in total transpiration. Our results might differ from recent studies emphasizing the importance of soil texture (Case & Staver, 2018; Hou et al., 2021) because winter-dominated precipitation regimes common in temperate semi-arid ecosystems, like in the western U.S., allow for deep soil water recharge regardless of soil texture (Renne et al., 2019).

Warming decreased all plant biomass (except C_4 grasses), but because precipitation intensification increased shrub, but not grass, biomass, the combined effect of warming and precipitation intensification was an increase in shrub relative abundance in arid and semi-arid sites (Figure 4.7). We simulated a wide range of precipitation

intensity that is greater than expected with climate change, yet our results showed consistent responses across this range of precipitation intensity. This robust response shows that in arid and semi-arid sites some precipitation intensification is likely to partially counteract negative effects of warming on shrubs, but not forbs or grasses. While previous studies in this system have described negative effects of warming on plant growth in arid and semi-arid sites (Palmquist et al., 2021; Renwick et al., 2018), our results show that it is important to consider the interactive effects of warming, precipitation intensity, and plant functional type. More specifically, in arid and semi-arid sites our results indicated a decrease in the shrub to C_3 perennial grass ratio with warming alone, but an increase in the shrub to C_3 perennial grass ratio with warming plus precipitation intensification (Figure 4.7).

Our results focus more on responses of C_3 than C_4 grasses, because C_3 perennial grasses are the second most dominant plant functional type (after big sagebrush) in big sagebrush ecosystems. However, understanding the C_4 grass response is also important, especially in the southern and eastern edges of the big sagebrush range where C_4 grasses are currently present (Paruelo & Lauenroth, 1996). Our results suggest that C_4 grasses will respond positively to warming, though our model did not consider dispersal limitations which are likely to slow C_4 expansion.

Shrub encroachment has been observed in drylands globally and while over-grazing, CO_2 enrichment, warming, and fire suppression can be important (Archer et al., 2017; Bestelmeyer et al., 2018), our results indicate that increased precipitation intensity also contributes to increased shrub dominance. While not simulated here, trees in arid ecosystems may exhibit similar positive responses to increased precipitation intensity.

Such responses could be impactful in sagebrush ecosystems where, for example, encroachment by juniper (*Juniperus* spp.) has resulted in changes in fire regimes and decreases in habitat quality for obligate wildlife species (Coates et al., 2017; Hamilton et al., 2019; Remington et al., 2021). More broadly, shifts in shrub and grass abundance can impact plant diversity, livestock production, and soil erosion (Anadon et al., 2014; Holthuijzen & Veblen, 2016; Lett & Knapp, 2005; Remington et al., 2021).

Increasing precipitation intensity may also have additional effects not considered in this study. Deeper percolation and reduced evaporation may have the beneficial effect of increasing aquifer recharge (Condon et al., 2020; Pascolini-Campbell et al., 2021; Seyfried et al., 2005). In contrast, in sites with steep slopes, more intense precipitation events may lead to greater runoff and erosion (Nearing et al., 2005; Yin et al., 2018).

Climate change-driven increases in precipitation intensity are likely to alter water balance pools and fluxes with important impacts for water-limited plant communities, which are most sensitive to these changes. Our results contribute to a growing body of evidence that suggests that responses to increased precipitation intensity will vary with aridity, with positive productivity responses in drier sites and negative responses in wetter sites. Additionally, as predicted by the two-layer hypothesis, we found that shrubs, but not grasses or forbs, in arid and semi-arid sites benefitted from deeper soil moisture caused by larger precipitation events 'pushing' water deeper into the soil.

References

Anadon, J. D., Sala, O. E., Turner, B. L., & Bennett, E. M. (2014). Effect of woody-plant encroachment on livestock production in North and South America. *Proceedings of the National Academy of Sciences*, *111*(35), 12948–12953.

https://doi.org/10.1073/pnas.1320585111

Archer, S. R., Anderson, E. M., Predick, K. I., Schwinning, S., Steidl, R. J., & Woods, S. R. (2017). Woody plant encroachment: Causes and consequences. In D. D. Briske (Ed.), *Rangeland systems: Processes, management and challenges* (pp. 25–84). Springer.

Bates, J. D., Svejcar, T., Miller, R. F., & Angell, R. A. (2006). The effects of precipitation timing on sagebrush steppe vegetation. *Journal of Arid Environments*, *64*(4), 670–697. https://doi.org/10.1016/j.jaridenv.2005.06.026

Berry, R. S., & Kulmatiski, A. (2017). A savanna response to precipitation intensity. *PLoS ONE*, *12*(4), 1–18. https://doi.org/10.1371/journal.pone.0175402

Bestelmeyer, B. T., Peters, D. P. C., Archer, S. R., Browning, D. M., Okin, G. S., Schooley, R. L., & Webb, N. P. (2018). The grassland–shrubland regime shift in the southwestern United States: Misconceptions and their implications for management. *BioScience*, *68*(9), 678–690. https://doi.org/10.1093/biosci/biy065

Bradford, J. B., Schlaepfer, D. R., Lauenroth, W. K., Palmquist, K. A., Chambers, J. C., Maestas, J. D., & Campbell, S. B. (2019). Climate-driven shifts in soil temperature and moisture regimes suggest opportunities to enhance assessments of dryland resilience and resistance. *Frontiers in Ecology and Evolution*, *7*, 1–16. https://doi.org/10.3389/fevo.2019.00358

Case, M. F., & Staver, A. C. (2018). Soil texture mediates tree responses to rainfall intensity in African savannas. *New Phytologist*, *219*, 1363–1372. https://doi.org/10.1111/nph.15254

Cherlet, M., Hutchinson, C., Reynolds, J., Hill, J., Sommer, S., & von Maltitz, G. (Eds.).

(2018). *World Atlas of Desertification*. Publication Office of the European Union. https://doi.org/10.2760/06292

Coates, P. S., Prochazka, B. G., Ricca, M. A., Gustafson, K. Ben, Ziegler, P., & Casazza, M. L. (2017). Pinyon and juniper encroachment into sagebrush ecosystems impacts distribution and survival of greater sage-grouse. *Rangeland Ecology & Management*, *70*(1), 25–38. https://doi.org/10.1016/j.rama.2016.09.001

Condon, L. E., Atchley, A. L., & Maxwell, R. M. (2020). Evapotranspiration depletes groundwater under warming over the contiguous United States. *Nature Communications*, *11*(1). https://doi.org/10.1038/s41467-020-14688-0

Dolby, G. A. (2021). Towards a unified framework to study causality in Earth–life systems. *Molecular Ecology*, *30*(22), 5628–5642. https://doi.org/10.1111/mec.16142

Du, H., Alexander, L. V., Donat, M. G., Lippmann, T., Srivastava, A., Salinger, J., Kruger, A., Choi, G., He, H. S., Fujibe, F., Rusticucci, M., Nandintsetseg, B., Manzanas, R., Rehman, S., Abbas, F., Zhai, P., Yabi, I., Stambaugh, M. C., Wang, S., … Wu, Z. (2019). Precipitation from persistent extremes is increasing in most regions and globally. *Geophysical Research Letters*, *46*(11), 6041–6049. https://doi.org/10.1029/2019GL081898

Epstein, H. E., Lauenroth, W. K., Burke, I. C., & Coffin, D. P. (1997). Productivity patterns of C3 and C4 functional types in the U.S. Great Plains. *Ecology*, *78*(3), 722. https://doi.org/10.2307/2266052

Gherardi, L. A., & Sala, O. E. (2015). Enhanced precipitation variability decreases grass- and increases shrub-productivity. *Proceedings of the National Academy of Sciences*, *112*(41), 12735–12740. https://doi.org/10.1073/pnas.1506433112

Gherardi, L. A., & Sala, O. E. (2019). Effect of interannual precipitation variability on dryland productivity: A global synthesis. *Global Change Biology*, *25*(1), 269–276. https://doi.org/10.1111/gcb.14480

Good, S. P., & Caylor, K. K. (2011). Climatological determinants of woody cover in Africa. *Proceedings of the National Academy of Sciences*, *108*(12), 4902–4907. https://doi.org/10.1073/pnas.1013100108

Guan, K., Good, S. P., Caylor, K. K., Sato, H., Wood, E. F., & Li, H. (2014). Continental-scale impacts of intra-seasonal rainfall variability on simulated ecosystem responses in Africa. *Biogeosciences*, *11*(23), 6939–6954. https://doi.org/10.5194/bg-11-6939-2014

Hamilton, B. T., Roeder, B. L., & Horner, M. A. (2019). Effects of Sagebrush Restoration and Conifer Encroachment on Small Mammal Diversity in Sagebrush Ecosystem. *Rangeland Ecology & Management*, *72*(1), 13–22. https://doi.org/10.1016/j.rama.2018.08.004

Holdrege, M. C., Beard, K. H., & Kulmatiski, A. (2021). Woody plant growth increases with precipitation intensity in a cold semiarid system. *Ecology*, *102*(1), 1–11. https://doi.org/10.1002/ecy.3212

Holthuijzen, M. F., & Veblen, K. E. (2016). Grazing effects on precipitation-driven associations between sagebrush and perennial grasses. *Western North American Naturalist*, *76*(3), 313–325. https://doi.org/10.3398/064.076.0308

Hou, E., Litvak, M. E., Rudgers, J. A., Jiang, L., Collins, S. L., Pockman, W. T., Hui, D., Niu, S., & Luo, Y. (2021). Divergent responses of primary production to increasing precipitation variability in global drylands. *Global Change Biology*, *27*(20), 5225–

5237. https://doi.org/10.1111/gcb.15801

Kleinhesselink, A. R., & Adler, P. B. (2018). The response of big sagebrush (Artemisia tridentata) to interannual climate variation changes across its range. *Ecology*, *99*(5), 1139–1149. https://doi.org/10.1002/ecy.2191

Knapp, A. K., Beier, C., Briske, D. D., Classen, A. T., Luo, Y., Reichstein, M., Smith, M. D., Smith, S. D., Bell, J. E., Fay, P. A., Heisler, J. L., Leavitt, S. W., Sherry, R., Smith, B., & Weng, E. (2008). Consequences of more extreme precipitation regimes for terrestrial ecosystems. *BioScience*, *58*(9), 811–821. https://doi.org/10.1641/B580908

Kulmatiski, A., & Beard, K. H. (2013). Woody plant encroachment facilitated by increased precipitation intensity. *Nature Climate Change*, *3*(9), 833–837. https://doi.org/10.1038/nclimate1904

Lauenroth, W. K., & Bradford, J. B. (2009). Ecohydrology of dry regions of the United States: precipitation pulses and intraseasonal drought. *Ecohydrology*, *2*(2), 173–181. https://doi.org/10.1002/eco.53

Lett, M. S., & Knapp, A. K. (2005). Woody plant encroachment and removal in mesic grassland: Production and composition responses of herbaceous vegetation. *The American Midland Naturalist*, *153*(2), 217–231. https://doi.org/10.1674/0003-0031

Liu, J., Ma, X., Duan, Z., Jiang, J., Reichstein, M., & Jung, M. (2020). Impact of temporal precipitation variability on ecosystem productivity. *Wiley Interdisciplinary Reviews: Water*, *7*(6), 1–22. https://doi.org/10.1002/wat2.1481

Middleton, N., & Thomas, D. S. G. (Eds.). (1997). *World atlas of desertification* (2nd ed.). Edward Arnold.

Milchunas, D. G., & Lauenroth, W. K. (1993). Quantitative effects of grazing on vegetation and soils over a global range of environments. *Ecological Monographs*, *63*(4), 327–366. https://doi.org/10.2307/2937150

Myhre, G., Alterskjær, K., Stjern, C. W., Hodnebrog, Ø., Marelle, L., Samset, B. H., Sillmann, J., Schaller, N., Fischer, E., Schulz, M., & Stohl, A. (2019). Frequency of extreme precipitation increases extensively with event rareness under global warming. *Scientific Reports*, *9*(1), 16063. https://doi.org/10.1038/s41598-019-52277-4

Nearing, M. A., Jetten, V., Baffaut, C., Cerdan, O., Couturier, A., Hernandez, M., Le Bissonnais, Y., Nichols, M. H., Nunes, J. P., Renschler, C. S., Souchère, V., & Van Oost, K. (2005). Modeling response of soil erosion and runoff to changes in precipitation and cover. *Catena*, *61*(2-3 SPEC. ISS.), 131–154. https://doi.org/10.1016/j.catena.2005.03.007

Noy-Meir, I. (1973). Desert ecosystems: environment and producers. *Annual Review of Ecology and Systematics*, *4*, 25–51.

O'Gorman, P. A., & Muller, C. J. (2010). How closely do changes in surface and column water vapor follow Clausius-Clapeyron scaling in climate change simulations? *Environmental Research Letters*, *5*(2). https://doi.org/10.1088/1748-9326/5/2/025207

Palmquist, K. A., Bradford, J. B., Martyn, T. E., Schlaepfer, D. R., & Lauenroth, W. K. (2018). STEPWAT2: an individual-based model for exploring the impact of climate and disturbance on dryland plant communities. *Ecosphere*, *9*(8). https://doi.org/10.1002/ecs2.2394

Palmquist, K. A., Schlaepfer, D. R., Renne, R. R., Torbit, S. C., Doherty, K. E., Remington, T. E., Watson, G., Bradford, J. B., & Lauenroth, W. K. (2021). Divergent climate change effects on widespread dryland plant communities driven by climatic and ecohydrological gradients. *Global Change Biology*, *27*(20), 5169–5185. https://doi.org/10.1111/gcb.15776

Paruelo, J. M., & Lauenroth, W. K. (1996). Relative abundance of plant functional types in grasslands and shrublands of North America. *Ecological Applications*, *6*(4), 1212–1224. https://doi.org/10.2307/2269602

Pascolini-Campbell, M., Reager, J. T., Chandanpurkar, H. A., & Rodell, M. (2021). A 10 per cent increase in global land evapotranspiration from 2003 to 2019. *Nature*, *593*(7860), 543–547. https://doi.org/10.1038/s41586-021-03503-5

Pendergrass, A. G. (2018). What precipitation is extreme? *Science*, *360*(6393), 1072–1073. https://doi.org/10.1126/science.aat1871

Pendergrass, A. G., & Knutti, R. (2018). The uneven nature of daily precipitation and its change. *Geophysical Research Letters*, *45*(21), 1–9. https://doi.org/10.1029/2018GL080298

Prăvălie, R. (2016). Drylands extent and environmental issues. A global approach. *Earth-Science Reviews*, *161*, 259–278. https://doi.org/10.1016/j.earscirev.2016.08.003

R Core Team. (2020). *R: A Language and Environment for Statistical Computing*. R Foundation For Statistical Computing. https://www.r-project.org/

Remington, T. E., Deibert, P. A., Hanser, S. E., Davis, D. M., Robb, L. A., & Welty, J. L. (2021). *Sagebrush conservation strategy–challenges to sagebrush conservation* (U.S. Geological Survey Open-File Report 2020-1125).

https://doi.org/10.3133/ofr20201125.

Renne, R. R., Bradford, J. B., Burke, I. C., & Lauenroth, W. K. (2019). Soil texture and precipitation seasonality influence plant community structure in North American temperate shrub steppe. *Ecology*, *100*(11), 1–12. https://doi.org/10.1002/ecy.2824

Renwick, K. M., Curtis, C., Kleinhesselink, A. R., Schlaepfer, D., Bradley, B. A., Aldridge, C. L., Poulter, B., & Adler, P. B. (2018). Multi-model comparison highlights consistency in predicted effect of warming on a semi-arid shrub. *Global Change Biology*, *24*(1), 424–438. https://doi.org/10.1111/gcb.13900

Ritter, F., Berkelhammer, M., & Garcia-Eidell, C. (2020). Distinct response of gross primary productivity in five terrestrial biomes to precipitation variability. *Communications Earth & Environment*, *1*(34), 1–8. https://doi.org/10.1038/s43247-020-00034-1

Sage, R. F. (2004). The evolution of C4 photosynthesis. *New Phytologist*, *161*(2), 341–370. https://doi.org/10.1111/j.1469-8137.2004.00974.x

Sala, O. E., Gherardi, L. A., & Peters, D. P. C. (2015). Enhanced precipitation variability effects on water losses and ecosystem functioning: differential response of arid and mesic regions. *Climatic Change*, *131*(2), 213–227. https://doi.org/10.1007/s10584-015-1389-z

Savage, M. J., Ritchie, J. T., Bland, W. L., & Dugas, W. A. (1996). Lower limit of soil water availability. *Agronomy Journal*, *88*(4), 644–651. https://doi.org/10.2134/agronj1996.00021962008800040024x

Schlaepfer, D. R., Lauenroth, W. K., & Bradford, J. B. (2012). Ecohydrological niche of sagebrush ecosystems. *Ecohydrology*, *5*(4), 453–466.

https://doi.org/10.1002/eco.238

Seyfried, M. S., Schwinning, S., Walvoord, M. A., Pockman, W. T., Newman, B. D., Jackson, R. B., & Phillips, F. M. (2005). Ecohydrological control of deep drainage in arid and semiarid regions. *Ecology*, *86*(2), 277–287. https://doi.org/10.1890/03-0568

Smith, T., & Huston, M. (1989). A theory of the spatial and temporal dynamics of plant communities. *Vegetatio*, *83*(1–2), 49–69. https://doi.org/10.1007/BF00031680

Soil Survey Staff. (2012). *Natural Resources Conservation Service, United States Department of Agriculture U.S. General Soil Map (STATSGO2)*. http://soildatamart.nrcs.usda.gov

Sturges, D. L. (1977). Soil water withdrawal and root characteristics of big sagebrush. *American Midland Naturalist*, *98*(2), 257. https://doi.org/10.2307/2424978

Thornton, P. E., Thornton, M. M., Mayer, B. W., Wei, Y., Devarakonda, R., Vose, R. S., & Cook, R. B. (2016). *Daymet: Daily Surface Weather Data on a 1-km Grid for North America, Version 3*. ORNL Distributed Active Archive Center. https://doi.org/10.3334/ORNLDAAC/1328

Trenberth, K. E. (2011). Changes in precipitation with climate change. *Climate Research*, *47*(1–2), 123–138. https://doi.org/10.3354/cr00953

U.S. Geological Survey Gap Analysis Program. (2016). *GAP/LANDFIRE National Terrestrial Ecosystems 2011: U.S. Geological Survey*. https://doi.org/10.5066/F7ZS2TM0

Walter, H. (1971). *Ecology of tropical and subtropical vegetation.* Oliver & Boyd.

Ward, D., Wiegand, K., & Getzin, S. (2013). Walter's two-layer hypothesis revisited:

Back to the roots! *Oecologia*, *172*(3), 617–630. https://doi.org/10.1007/s00442-012-2538-y

West, N. E. (ed. . (1983). *Temperate deserts and semi-deserts*. Amsterdam (Netherlands) Elsevier Scientific Pub.

Wilcox, K. R., von Fischer, J. C., Muscha, J. M., Petersen, M. K., & Knapp, A. K. (2015). Contrasting above- and belowground sensitivity of three Great Plains grasslands to altered rainfall regimes. *Global Change Biology*, *21*(1), 335–344. https://doi.org/10.1111/gcb.12673

Xu, X., Medvigy, D., & Rodriguez-Iturbe, I. (2015). Relation between rainfall intensity and savanna tree abundance explained by water use strategies. *Proceedings of the National Academy of Sciences of the United States of America*, *112*(42), 12992–12996. https://doi.org/10.1073/pnas.1517382112

Xu, X., Medvigy, D., Trugman, A. T., Guan, K., Good, S. P., & Rodriguez-Iturbe, I. (2018). Tree cover shows strong sensitivity to precipitation variability across the global tropics. *Global Ecology and Biogeography*, *27*(4), 450–460. https://doi.org/10.1111/geb.12707

Yamori, W., Hikosaka, K., & Way, D. A. (2014). Temperature response of photosynthesis in C3, C4, and CAM plants: temperature acclimation and temperature adaptation. *Photosynthesis Research*, *119*(1–2), 101–117. https://doi.org/10.1007/s11120-013-9874-6

Yin, J., Gentine, P., Zhou, S., Sullivan, S. C., Wang, R., Zhang, Y., & Guo, S. (2018). Large increase in global storm runoff extremes driven by climate and anthropogenic changes. *Nature Communications*, *9*(1). https://doi.org/10.1038/s41467-018-06765-

2

Zeppel, M. J. B., Wilks, J. V., & Lewis, J. D. (2014). Impacts of extreme precipitation and seasonal changes in precipitation on plants. *Biogeosciences*, *11*(11), 3083–3093. https://doi.org/10.5194/bg-11-3083-2014

Zhang, D. H., Li, X. R., Zhang, F., Zhang, Z. S., & Chen, Y. Le. (2016). Effects of rainfall intensity and intermittency on woody vegetation cover and deep soil moisture in dryland ecosystems. *Journal of Hydrology*, *543*, 270–282. https://doi.org/10.1016/j.jhydrol.2016.10.003

Zhou, Y., Tingley, M. W., Case, M. F., Coetsee, C., Kiker, G. A., Scholtz, R., Venter, F. J., & Staver, A. C. (2021). Woody encroachment happens via intensification, not extensification, of species ranges in an African savanna. *Ecological Applications*, *31*(8), 1–14. https://doi.org/10.1002/eap.2437

Figures

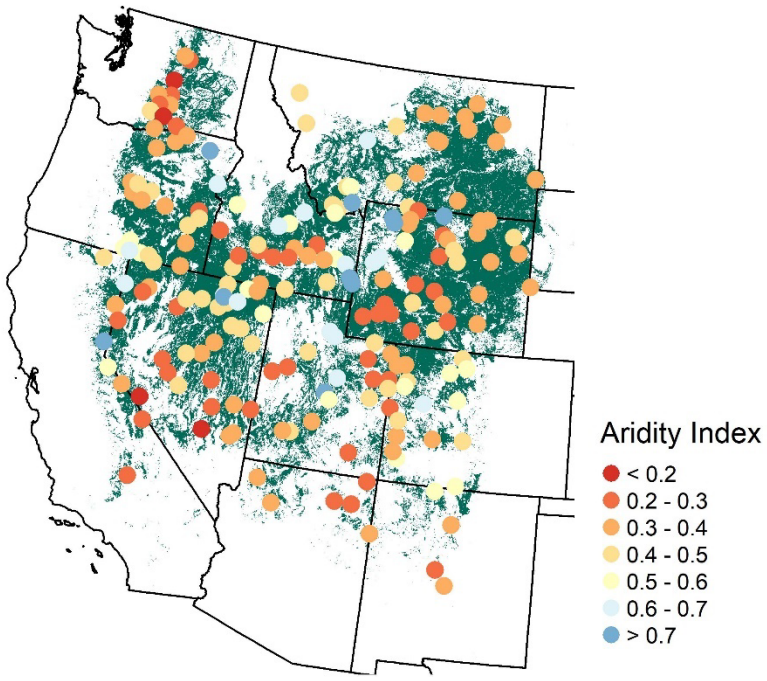

Figure 4.1 Simulations were conducted using climate data from 200 sites in the western United States that span the climate envelope of sagebrush-dominated ecosystems (aridity index = mean annual precipitation/potential evapotranspiration). The background (green shading) shows sagebrush ecosystem occurrence as defined in Schlaepfer et al. (2012b).

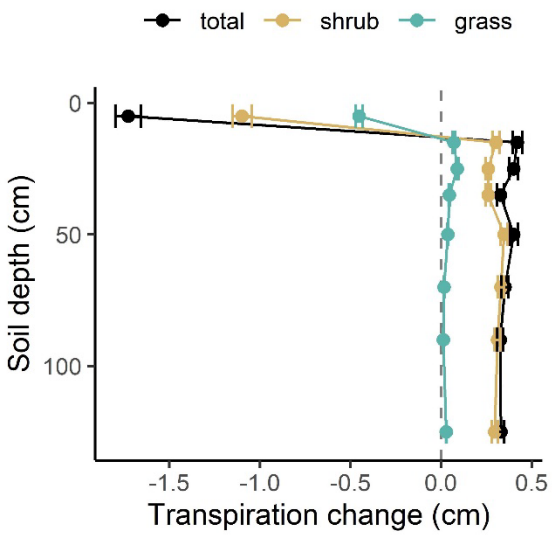

Figure 4.2 Mean changes in total annual, shrub, and grass transpiration by soil depth in response to a doubling of mean precipitation event size (2x intensity treatment). Values represent the difference between 2x intensity and ambient (control) conditions, and are the mean (± 1 SE) response across 200 sites. Values > 0 indicate that water uptake from that depth increased as a result of increased precipitation intensity.

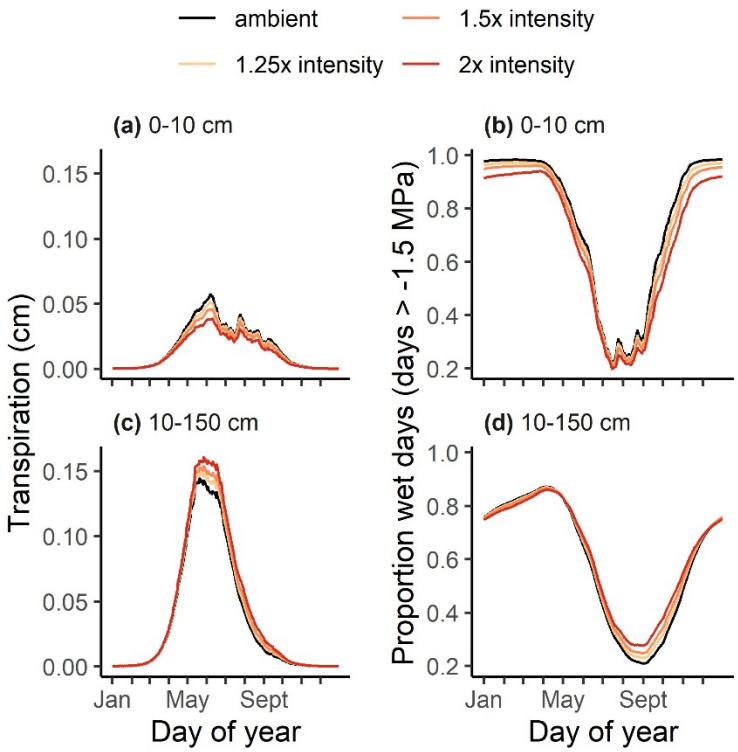

Figure 4.3 Mean daily total transpiration (a, c), and proportion of days that are wet (b, d), in surface (0 – 10 cm; panels a and b) and sub-surface soils (10 – 150 cm; panels c and d) in response to precipitation intensity treatments across sites. Precipitation intensity treatments increased precipitation event sizes by 1.25x, 1.5x, and 2x, respectively. Proportion wet days is the proportion of times when for that day of year, soil water potential at a given depth was > -1.5 MPa.

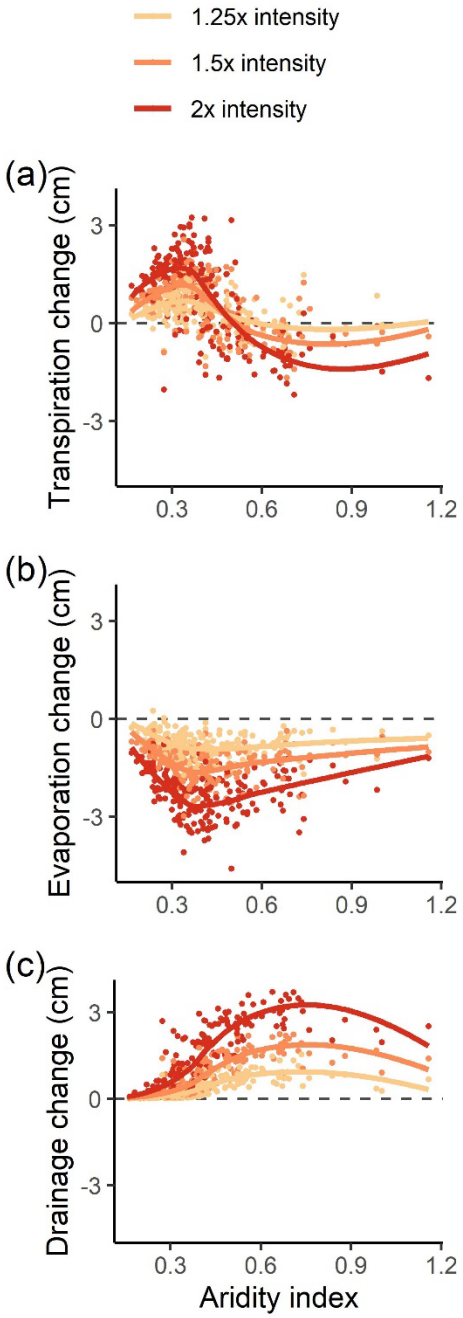

Figure 4.4 Changes in annual (a) total transpiration, (b) evaporation, and (c) deep drainage of soil water, in response to precipitation intensity treatments across a range of aridity (mean annual precipitation/potential evapotranspiration). Each point represents mean annual changes (treatment minus ambient conditions) at each of 200 sites in response to 1.25x, 1.5x, and 2x increases in precipitation event size, respectively. Lower values of aridity index represent drier conditions. Values of response variables > 0 indicate an increase with greater precipitation intensity.

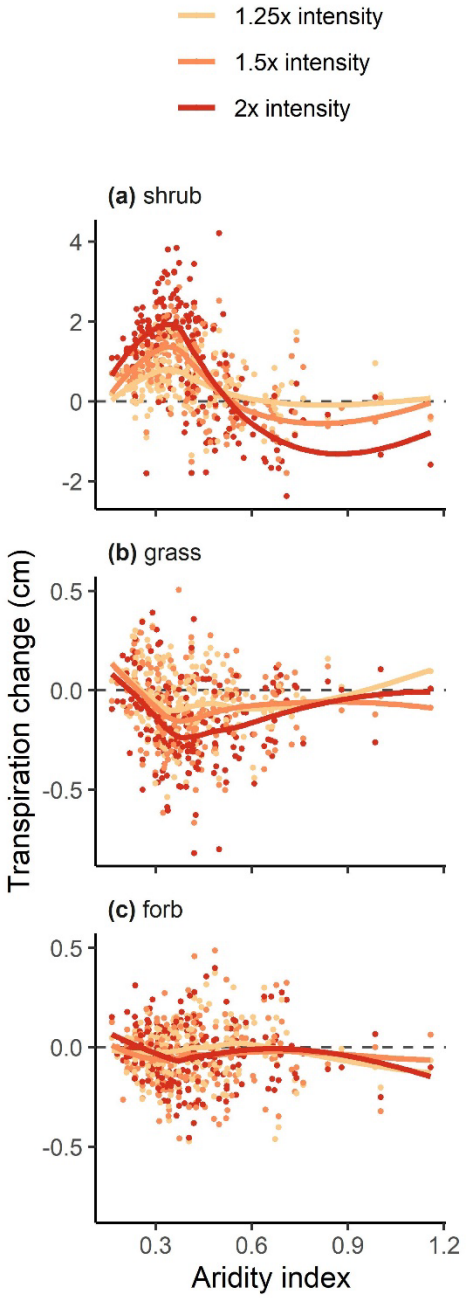

Figure 4.5 Changes in annual transpiration of (a) shrubs, (b) grasses, and (c) forbs in response to increased precipitation intensity versus aridity index (mean annual precipitation/potential evapotranspiration). Points represents mean annual changes (treatment minus ambient conditions) in water transpired by a plant functional type at each site in response to 1.25x, 1.5x, and 2x increases in precipitation event size, respectively. Note that the y-axis scale differs among panels. Values > 0 indicate an increase in transpiration with greater precipitation intensity.

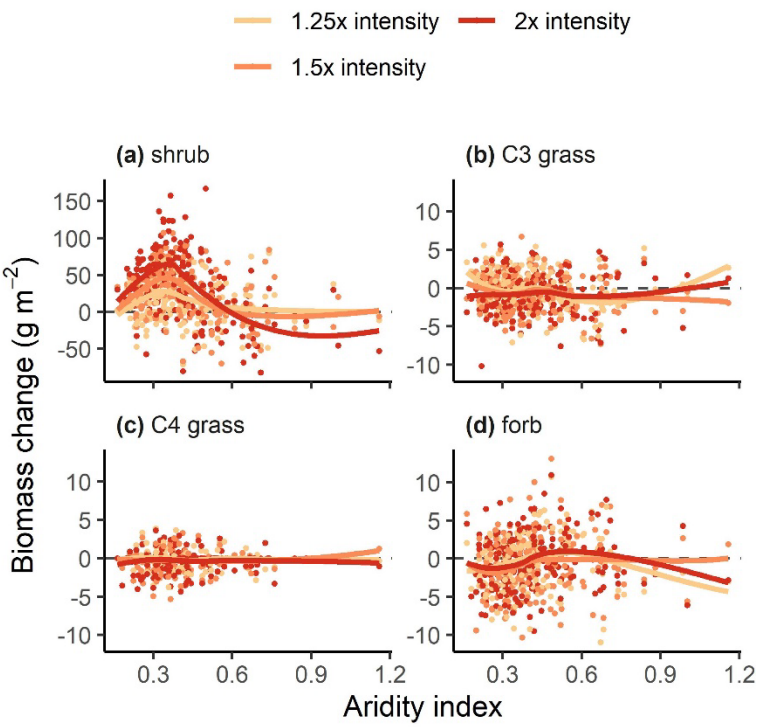

Figure 4.6 Changes in biomass of (a) shrubs, (b) C_3 perennial grasses, (c) C_4 perennial grasses, and (d) forbs in response to increased precipitation intensity across an aridity gradient (mean annual precipitation/potential evapotranspiration). Points are changes in mean plant functional type biomass (treatment minus ambient conditions) at each site, in response to 1.25x, 1.5x, and 2x increases in precipitation event size, respectively. Note that the y-axis scale differs among panels. Values > 0 indicate an increase in biomass with greater precipitation intensity.

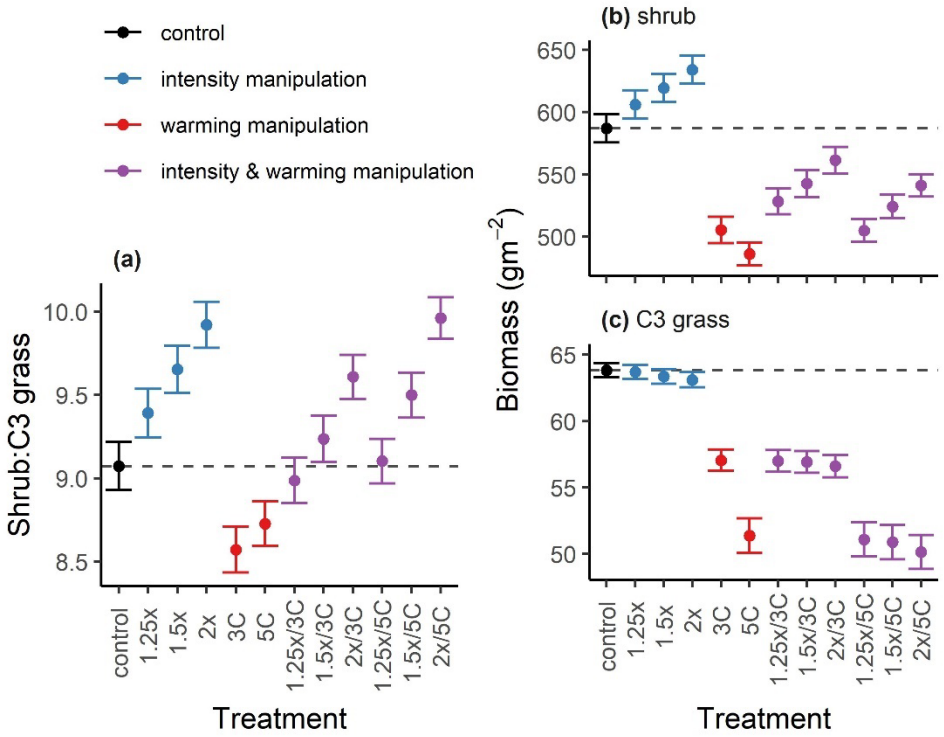

Figure 4.7 (a) Ratio of shrub to C_3 perennial grass biomass, and biomass of (b) shrubs and (c) C_3 perennial grasses, in response to precipitation intensity and warming treatments. Values in panels are means (± 1 SE) across sites with an aridity index < 0.54 (N = 165). Data from sites with aridity values > 0.54 are reported in Appendix S4.5. Precipitation intensity treatments increased precipitation event sizes by 1.25x, 1.5x, and 2x. Warming treatments raised temperatures by 3 °C and 5 °C. The dashed lines show the mean value under control conditions. Note that the y-axis scale differs between panels (b) and (c).

CHAPTER 5

CONCLUSIONS

Overview

Here I briefly summarize the findings of my research on the effects of increased precipitation intensity described in the main chapters of this dissertation, and put these results in the context of what I see as some of the main uncertainties present in the current state of knowledge on this topic. Chapters 2, 3, and 4 provide results from original research conducted on the impacts of increased precipitation intensity in dryland ecosystems of the western United States. My collaborators and I conducted two field experiments, one in a natural big sagebrush dominated site (Chapter 2), and the second in a dryland agricultural site (Chapter 3). We also employed an ecohydrological model to simulate responses of big sagebrush dominated ecosystems across the western United States (Chapter 4).

The ecosystems studied are in temperate climates that have winter-dominated precipitation regimes, but despite the vast areas they cover they have largely been excluded from previous studies on precipitation intensity. Both our experimental and ecohydrological modeling results suggest that, at least in arid and semi-arid sites, fewer large precipitation events can increase soil water availability with water percolating more deeply into the ground where it can escape evaporation and be used by plants. Growth responses to these soil moisture changes varied with plant type. In big sagebrush-dominated ecosystems, shrubs tended to have positive growth responses, while growth of more shallow-rooted grasses and forbs did not change appreciably (Chapters 2 & 4). The agricultural experiment found no detectable response of winter wheat to increased

precipitation intensity (Chapter 3).

Soil moisture responses

Understanding the potential ecosystem-level impacts of increased precipitation intensity requires assessing, first, if and how soil water availability will change, and second, how plants will respond to such changes. In both field experiments, soil moisture measurements collected at multiple depths and repeated at regular time intervals showed that treatments tended to increase soil moisture. By measuring the pool size (i.e. soil moisture), we can infer that more water was available to plants, but we were not able to measure the actual changes in water fluxes (e.g., transpiration). The results from these field measurements are corroborated by results from the model simulations described in Chapter 4, which indicated that under most conditions soil moisture increased in sub-surface soil layers and this resulted in an increase in the total amount of water transpired, especially later in the growing season.

Plant growth responses

Both direct field measurements of stem-growth (Chapter 2) and simulations of biomass (Chapter 4), suggest that sagebrush will respond positively to increased precipitation intensity, at least in arid and semi-arid sites. These results are in agreement with Walter's two layer hypothesis (Walter, 1971; Ward et al., 2013), which suggests that increases in deeper soil water should preferentially benefit more deeply rooted woody plants, relative to more shallowly rooted grasses. The positive sagebrush growth responses have important implications for sagebrush-dominated ecosystems and also for shrublands more broadly. Large scale declines in sagebrush habitat have occurred across

the western United States due to a host of potential factors, including over-grazing, anthropogenic development, invasive annual grasses, tree encroachment, and changes in fire regimes (Connelly et al., 2011; Davies et al., 2011; Finch et al., 2016). Thus, the direct positive effect of increased precipitation intensity on sagebrush could counteract these changes to some degree, and thereby act as stabilizing force. However, with the exception of simulations described in Chapter 4 that included warming treatments, literature is lacking on the magnitudes of the effects of increased precipitation intensity relative to the effects of other changes in climate, management, and the plant community. An additional factor that has not been addressed is how increased precipitation intensity may impact sagebrush through competition with trees. Trees, especially junipers (*Juniperus* spp.), have steadily invaded sagebrush habitats and can have negative effects on wildlife (Coates et al., 2017; Davies et al., 2011; Hamilton et al., 2019). If increased precipitation intensity also benefits these deeply rooted trees, it is unclear whether the competitive effect on sagebrush would outweigh the direct benefits of increased deep soil moisture.

In the two field experiments (Chapters 2 & 3), no change in grass growth (including winter wheat) was detected in response to increased precipitation intensity, and similarly the simulations showed no consistent changes in grass growth (Chapter 4). These results run counter to the findings of experiments conducted in semi-arid shortgrass steppe sites that have tended to find positive productivity responses to increased precipitation intensity (Heisler-White et al., 2008, 2009; Li et al., 2019; Wilcox et al., 2015). Differences in phenology of winter wheat compared to grasses in those ecosystems may help explain why winter wheat did not respond to increased precipitation

intensity. At the agricultural site we studied, the effects of the treatments on soil moisture were evident in mid- to late summer. This is after winter wheat, which is planted the previous fall, has completed its growth. These soil moisture results are corroborated by simulations (Chapter 4), which showed that treatments primarily increased transpiration in mid- to late summer. This is the time of year when potential evapotranspiration is highest, and the benefits of larger precipitation events pushing water into sub-surface layers to escape evaporation should be greatest. Therefore, compared to the ecosystems studied here, which are dominated by cool season precipitation and largely rely on storage of deeper soil water, the effects of increased precipitation intensity may be stronger in ecosystems that receive most of their soil water from short pulses during the warm-season. In such ecosystems dominated by warm-season precipitation, most of the annual precipitation is exposed to strong evaporative demands, and the soil water usually cannot not penetrate deeply (Lauenroth et al., 2014; Sala et al., 1992).

Perennial grasses, especially C_4 species, that grow in the short-grass steppe of North America can grow later into the summer (Bork & Irving, 2015; Moore & Lauenroth, 2017). These differences in phenology may help explain why studies in these ecosystems have tended to find positive grass growth response from fewer larger precipitation events, and why we did not detect such responses in the earlier senescing winter wheat. However, differences in phenology do not fully explain why both our experimental (Chapter 2) and simulation (Chapter 4) results found no evidence of consistent perennial grass responses to increased intensity in sagebrush-dominated ecosystems, because the perennial grasses in these systems can also continue growing into the summer. When shrubs are the dominant functional type, direct competition with

shrubs may help explain the lack of grass responses. In our simulations, grass roots were present in the deeper soil layers, but only represented a small fraction of total root biomass at those depths. Therefore, these findings suggest that when present, the additional deep soil water will go to shrubs, not grasses. To address this hypothesis, one could estimate grass responses in simulations using the same climate data but with shrubs removed from the model.

The challenge of forecast horizons

The simulation results (Chapter 4) provide a mechanistic explanation for measurements of sagebrush responses (Chapter 2) to increased precipitation intensity. However, the results of these two approaches are not directly comparable. In the field we were able to detect changes in sagebrush growth using point dendrometer measurements of stem diameter, but not with visual surveys of cover, possibly because of the high sensitivity (0.01 mm) of the dendrometer measurements. Increases in stem diameter are a reasonable proxy for increases in biomass (Brown, 1976), but these were responses to three years of precipitation intensity treatments, which is a period during which only short-term processes, such as changes in growth rate, should predominate. By comparison, simulations (Chapter 4) were run for 150 years, over which time a given precipitation intensity treatment was applied, and biomass was able to reach a stable state. Therefore, the simulations are analogous to a space-for-time substitution, where the effects of climate are assessed by comparing locations with different climates, and where plant communities have had a long time to adjust to local conditions through processes such immigration and extinction.

A serious challenge with predicting how plant communities will respond to

climate change is understanding over what time horizons these short- and long-term responses predominate (Adler et al., 2020). Studies relying on time-series observations (more analogous to our field experiment) tend to find lower sensitivity to climate than space-for-time substitutions, and this may be the leading source of uncertainty in ecological forecasts (Felton et al., 2021). Both results from Chapter 2 and Chapter 4 agree on the direction of the effect of increased precipitation intensity on sagebrush. However, in addition to very real limitations on how well ecohydrological models can represent reality, neither our modeling results or field experiment can fully resolve uncertainty regarding how fast sagebrush ecosystem will respond to increases in precipitation intensity in an ever-changing climate over, say, the next 30 years.

These concerns about uncertainty in the rate of ecological change appear less salient in an agricultural context. For example, in the winter wheat cropping system studied, the recent history of climatic conditions should matter only in so much that they change stored soil water or soil chemistry. Because the crop is harvested, the ground tilled and then re-planted, slower processes such as mortality of perennial species are irrelevant. Therefore, manipulative field experiments of crop responses such as the one described in Chapter 3, may provide better estimates of future changes than those in less intensively managed perennial ecosystems, where many more sources of uncertainty exist.

Uncertainty in precipitation changes

General consensus exists that extreme (rare) daily precipitation events will increase in size and frequency more than mean event sizes; in other words, the distribution of individual precipitation event sizes will become more right skewed

(Fischer & Knutti, 2016; Pendergrass, 2018; Pendergrass & Knutti, 2018). The degree to which the 'shape' of the distribution will change is uncertain, but could have important ecological ramifications. For example, an increase in mean precipitation event sizes and decrease in frequency, with no change in total precipitation, may have different effects depending on how that change is created. Small precipitation events (e.g., 2 mm) are of little value to plants because most of the water is intercepted and evaporates. Alternatively, very large precipitation events (perhaps several cm) may be inefficient in providing water to plants if a high percentage of the water is lost to deep drainage or run-off. Therefore, a shift in the precipitation regime that replaces many small events with fewer moderate sized events may be more beneficial than replacing medium to large events with fewer very large events.

Due to practical constraints of collecting rainwater in tanks, both field experiments re-distributed small events, but did not make large events larger. By comparison, the simulated precipitation used in the modelling study (Chapter 4) increased the size of rare events (e.g. 99^{th} percentile), more than common events (e.g. 50^{th} percentile) thus creating a more right-skewed distribution. However, even with this latter approach, increased precipitation intensity tended to increase soil water availability, and there was no evidence of a threshold existing, because in arid- and semi-arid sites the most extreme treatment (doubling mean event sizes) had the strongest positive effect. Further research is needed to determine under what conditions more severely right skewed precipitation distributions may have negative effects, which could depend on factors that affect run-off such as infiltration rate or slope.

Most research, including that described here, has focused on the impacts of

increased precipitation intensity at daily or longer time scales (e.g., Hou et al., 2021; Knapp et al., 2008; Li et al., 2021). Yet intensification of sub-daily (e.g., 1-3 h) precipitation events may be especially harmful due to greater run-off and flash flooding (Fowler et al., 2021). A heavy thunderstorm that deposits a lot of rain over an hour is different than the same amount of rain falling at a moderate rate over a period of 24 hours, during which time it can fully infiltrate the soil. Thus, our finding that even a fairly extreme intensification of daily precipitation events increased soil water availability may not apply to an intensification of sub-daily precipitation events.

Summary

The research described in this dissertation helps build understanding of the impacts of fewer larger precipitation events on soil water cycling and plant communities in temperate water limited ecosystems. Both manipulative field experiments and ecohydrological modeling have limitations, but by employing both approaches we can have more confidence in our estimated responses. Increased precipitation intensity caused deeper percolation of soil water, thereby increasing soil water availability especially during the warmest months. In shrublands, this change in the soil water benefitted more deeply rooted woody plants, and provides a mechanism for continued increases in woody dominance. Broadly, the results from this research underscore the importance of accounting for climatic variability when forecasting ecological responses to climate change.

References

Adler, P. B., White, E. P., & Cortez, M. H. (2020). Matching the forecast horizon with

the relevant spatial and temporal processes and data sources. *Ecography*, 1–11. https://doi.org/10.1890/ES14-00208.1

Bork, E. W., & Irving, B. D. (2015). Seasonal Availability of Cool- and Warm-Season Herbage in the Northern Mixed Prairie. *Rangelands*, *37*(5), 178–185. https://doi.org/10.1016/j.rala.2015.07.002

Brown, J. K. (1976). Estimating shrub biomass from basal stem diameters. *Canadian Journal of Forest Research*, *6*(2), 153–158. https://doi.org/10.1139/x76-019

Coates, P. S., Prochazka, B. G., Ricca, M. A., Gustafson, K. Ben, Ziegler, P., & Casazza, M. L. (2017). Pinyon and Juniper Encroachment into Sagebrush Ecosystems Impacts Distribution and Survival of Greater Sage-Grouse. *Rangeland Ecology & Management*, *70*(1), 25–38. https://doi.org/10.1016/j.rama.2016.09.001

Connelly, J. W., Knick, S. T., Braun, C. E., Baker, W. L., Beever, E. A., Christiansen, T. J., Doherty, K. E., Garton, E. O., Hagen, C. A., Hanser, S. E., Johnson, D. H., Leu, M., Miller, R. F., Naugle, D. E., Oyler-McCance, S. J., Pyke, D. A., Reese, K. P., Schroeder, M. A., Stiver, S. J., … Wisdorn, M. J. (2011). Conservation of greater sage-grouse- a synthesis of current trends and future management. In *Greater Sage-Grouse: Ecology and Conservation of a Landscape Species and Its Habitats* (pp. 549–563). http://pubs.er.usgs.gov/publication/70004658

Davies, K. W., Boyd, C. S., Beck, J. L., Bates, J. D., Svejcar, T. J., & Gregg, M. A. (2011). Saving the sagebrush sea: An ecosystem conservation plan for big sagebrush plant communities. *Biological Conservation*, *144*(11), 2573–2584. https://doi.org/10.1016/j.biocon.2011.07.016

Felton, A. J., Shriver, R. K., Stemkovski, M., Bradford, J. B., Suding, K. N., & Adler, P.

B. (2021). The rate of ecological acclimation is the dominant uncertainty in long-term projections of a key ecosystem service. *BioRxiv*, 2021.08.11.455579. https://doi.org/10.1101/2021.08.11.455579

Finch, D. M., Boyce, D. A., Chambers, J. C., Colt, C. J., Dumroese, K., Kitchen, S. G., McCarthy, C., Meyer, S. E., Richardson, B. A., Rowland, M. M., Rumble, M. A., Schwartz, M. K., Tomosy, M. S., & Wisdom, M. J. (2016). *Conservation and restoration of sagebrush ecosystems and sage-grouse: An assessment of USDA Forest Service Science*. https://doi.org/10.2737/RMRS-GTR-348

Fischer, E. M., & Knutti, R. (2016). Observed heavy precipitation increase confirms theory and early models. *Nature Climate Change*, *6*(11), 986–991. https://doi.org/10.1038/nclimate3110

Fowler, H. J., Lenderink, G., Prein, A. F., Westra, S., Allan, R. P., Ban, N., Barbero, R., Berg, P., Blenkinsop, S., Do, H. X., Guerreiro, S., Haerter, J. O., Kendon, E. J., Lewis, E., Schaer, C., Sharma, A., Villarini, G., Wasko, C., & Zhang, X. (2021). Anthropogenic intensification of short-duration rainfall extremes. *Nature Reviews Earth and Environment*, *2*(2), 107–122. https://doi.org/10.1038/s43017-020-00128-6

Hamilton, B. T., Roeder, B. L., & Horner, M. A. (2019). Effects of Sagebrush Restoration and Conifer Encroachment on Small Mammal Diversity in Sagebrush Ecosystem. *Rangeland Ecology & Management*, *72*(1), 13–22. https://doi.org/10.1016/j.rama.2018.08.004

Heisler-White, J. L., Blair, J. M., Kelly, E. F., Harmoney, K., & Knapp, A. K. (2009). Contingent productivity responses to more extreme rainfall regimes across a grassland biome. *Global Change Biology*, *15*(12), 2894–2904.

https://doi.org/10.1111/j.1365-2486.2009.01961.x

Heisler-White, J. L., Knapp, A. K., & Kelly, E. F. (2008). Increasing precipitation event size increases aboveground net primary productivity in a semi-arid grassland. *Oecologia*, *158*(1), 129–140. https://doi.org/10.1007/s00442-008-1116-9

Hou, E., Litvak, M. E., Rudgers, J. A., Jiang, L., Collins, S. L., Pockman, W. T., Hui, D., Niu, S., & Luo, Y. (2021). Divergent responses of primary production to increasing precipitation variability in global drylands. *Global Change Biology*, *July*, gcb.15801. https://doi.org/10.1111/gcb.15801

Knapp, A. K., Beier, C., Briske, D. D., Classen, A. T., Luo, Y., Reichstein, M., Smith, M. D., Smith, S. D., Bell, J. E., Fay, P. a., Heisler, J. L., Leavitt, S. W., Sherry, R., Smith, B., & Weng, E. (2008). Consequences of more extreme precipitation regimes for terrestrial ecosystems. *BioScience*, *58*(9), 811–821. https://doi.org/10.1641/B580908

Lauenroth, W. K., Schlaepfer, D. R., & Bradford, J. B. (2014). Ecohydrology of Dry Regions: Storage versus Pulse Soil Water Dynamics. *Ecosystems*, *17*(8), 1469–1479. https://doi.org/10.1007/s10021-014-9808-y

Li, L., Kang, X., Biederman, J. A., Wang, W., Qian, R., Zheng, Z., Zhang, B., Ran, Q., Xu, C., Liu, W., Che, R., Xu, Z., Cui, X., Hao, Y., & Wang, Y. (2021). Nonlinear carbon cycling responses to precipitation variability in a semiarid grassland. *Science of The Total Environment*, *781*(April), 147062. https://doi.org/10.1016/j.scitotenv.2021.147062

Li, L., Zheng, Z., Biederman, J. A., Xu, C., Xu, Z., Che, R., Wang, Y., Cui, X., & Hao, Y. (2019). Ecological responses to heavy rainfall depend on seasonal timing and

multi-year recurrence. *New Phytologist*. https://doi.org/10.1111/nph.15832

Moore, L. M., & Lauenroth, W. K. (2017). Differential effects of temperature and precipitation on early- vs. late-flowering species. *Ecosphere*, *8*(5). https://doi.org/10.1002/ecs2.1819

Pendergrass, A. G. (2018). What precipitation is extreme? *Science*, *360*(6393), 1072–1073. https://doi.org/10.1126/science.aat1871

Pendergrass, A. G., & Knutti, R. (2018). The uneven nature of daily precipitation and its change. *Geophysical Research Letters*, 1–9. https://doi.org/10.1029/2018GL080298

Sala, O. E., Lauenroth, W. K., & Parton, W. J. (1992). Long-term soil water dynamics in the shortgrass steppe. *Ecology*, *73*(4), 1175–1181. https://doi.org/10.2307/1940667

Walter, H. (1971). *Ecology of tropical and subtropical vegetation.* Oliver & Boyd.

Ward, D., Wiegand, K., & Getzin, S. (2013). Walter's two-layer hypothesis revisited: Back to the roots! *Oecologia*, *172*(3), 617–630. https://doi.org/10.1007/s00442-012-2538-y

Wilcox, K. R., von Fischer, J. C., Muscha, J. M., Petersen, M. K., & Knapp, A. K. (2015). Contrasting above- and belowground sensitivity of three Great Plains grasslands to altered rainfall regimes. *Global Change Biology*, *21*(1), 335–344. https://doi.org/10.1111/gcb.12673

APPENDICES

Appendix S2.1: Shelter effects

Air temperature was measured at a height of 1.5 m at two locations in each plot (iButtons; Maxim Integrated, San Jose, CA, USA). Relative humidity (HOBO Pro v2, Onset Computer Corp., Bourne, MA, USA), wind speed (Sensor 014a, Met One Instruments, Inc, Grants Pass, OR, USA), and net radiation (NR-Lite sensor, Zipp and Konen, Delft, Netherlands) were measured hourly at a 1.5 m height on the inside and outside of one shelter (CR1000 data loggers, Campbell Scientific, Logan, UT).

Shelters were warmer (5.6 °C vs 5.0 °C; Fig. S2.1), drier (56.6% vs 58.5% relative humidity; Fig. S2.2), less windy (0.9 m s^{-1} vs 1.2 m s^{-1}) and less bright than ambient conditions (mean of daily maximum net radiation was 544 in the shelter compared to 582 W m^{-2} under ambient conditions) (Fig. S2.3). At night, the shelters reduced energy loss, with mean daily minimum net radiation of -36 W m^{-2} in the shelter and -96 W m^{-2} under ambient conditions (Fig. S2.3). This is presumably because the acrylic roofing of shelters blocked some incoming short-wave radiation during the day and reduced some longwave radiation loss at night. Some of these factors (higher temperature, lower humidity and higher night time net radiation in shelters) taken by themselves would lead to greater evapotranspiration in shelters. However, others (less wind and lower daily maximum net radiation in shelters) would lead to lower evapotranspiration in shelters. Taken in combination these factors caused little effect of the shelters on reference evapotranspiration (4.3 mm day^{-1} in shelters versus 4.1 mm day^{-1} under ambient conditions).

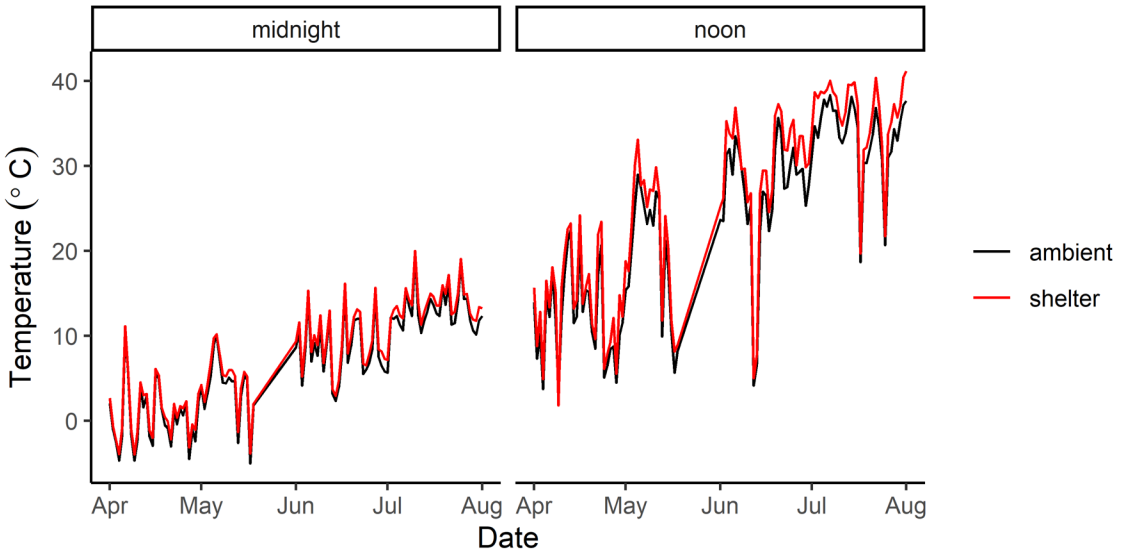

Figure S2.1 Temperature at midnight and noon (mid-day) under ambient conditions and in shelters during the 2017 growing season. Temperatures are the mean values from iButton sensors in ambient (shelter-less) plots and sheltered plots.

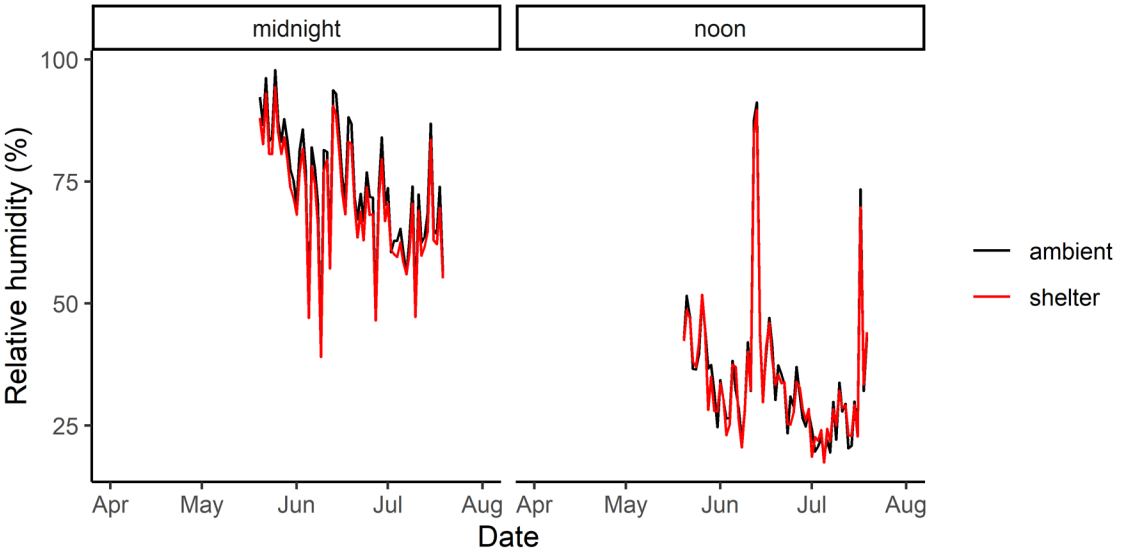

Figure S2.2 Relative humidity at midnight and noon (mid-day) from one sensor measuring ambient humidity and one sensor located in a sheltered plot during the 2017 growing season. Data from the beginning of the 2017 growing season is missing due to sensor failure.

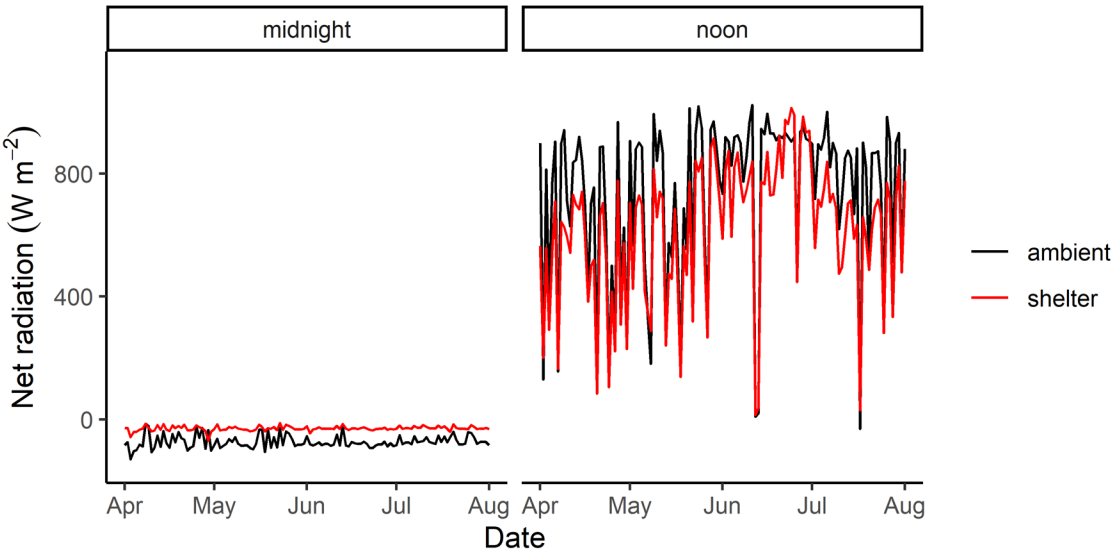

Figure S2.3 Net radiation at midnight and noon (mid-day) under ambient and shelter conditions during the 2017 growing season. Values are means from two sensors measuring ambient net radiation and two sensors located in sheltered plots.

Appendix S2.2: Description of precipitation intensity treatments

Water was applied to plots via a sprinkler system once enough water was collected in the tanks to create a precipitation event of a certain size (which varied by treatment). The target precipitation event sizes (i.e., tank sizes) were calculated using historical precipitation data and the Clausius-Clapeyron relation. For example, for the 2 mm treatment associated with 1 °C of warming, the following steps were used to calculate the target tank size:

1. Historical observed daily precipitation was put in descending order.
2. A curve was fit to this distribution of historical precipitation events to create a model of the precipitation distribution.
3. Precipitation events in this generalized distribution were multiplied by 1.07 to create a new distribution of larger events.
4. Enough of the smallest precipitation events were removed from this new distribution so that the sum of annual precipitation was equal to the sum of the original distribution (since all events were increased by 7%, if the smallest events were not 'removed' then total annual precipitation would necessarily also increase by 7%). This created a new distribution with fewer larger precipitation events, but the same total annual precipitation.
5. The smallest precipitation event size from this new distribution was used as the tank size for the treatment.

The above sequence of steps was repeated to calculate tank sizes for the treatments meant to reflect increased precipitation intensity associated with 2 °C, 3 °C, 5 °C and 10 °C of warming.

Rain water was applied to the plots in a way that can be described as a tipping bucket model. That is, once the 'bucket' (a water tank in our case) filled from water collected off the shelter roof it would 'tip' (in our case that means water would be applied to the plot via an electric pump and sprinklers). Because a tank can fill and empty multiple times during a storm this tipping bucket model was applied to historical precipitation to calculate the mean daily precipitation event size that results from the treatments. That is, the mean amount of precipitation received on days when there was > 0 mm of precipitation. The mean daily event sizes were calculated using only precipitation data from April to November because those are snow-free months when our pumps would be installed and running, and therefore they are the months during which the tipping bucket model most accurately represents the way treatments were applied. However, when year-round precipitation data is used results remain very similar. Mean event size of the treatment in which additional 1 mm precipitation events were added, were calculated by 'removing' 1 mm of precipitation from larger natural events and re-depositing it on days no natural precipitation occurred. This led to a range of mean daily event sizes of 4.8, 5.3, 6.2, 7.2, 8.4, 10.8, and 19.4 mm, for the 1, control, 2, 3, 4, 8, and 18 mm treatments, respectively. These mean daily event sizes are used in our regression analysis of vegetation cover, NDVI, and shrub stem radius (Fig. 5b).

Note that the mean precipitation event size for a given treatment varies from year to year (Figure 2 in the manuscript) and these numbers are the mean event sizes across years in the historical record. The mean daily event sizes for the 1 mm, control, 2, 3, 4, 8 and, 18 mm treatments fall into the 43rd, 61st, 81st, 96th, 100th, 100th, and 100th percentiles of historical annual daily mean precipitation event sizes. This means that no year on

record had mean daily event sizes as large as the mean daily event sizes of the 4, 8 and, 18 mm treatments. The mean daily event size of the control plots (61st percentile) was above the 50th percentile because a small amount of water needed to be collected in the tanks before the float switches would automatically trigger. While the mean event sizes of the extreme treatments were outside the historical range of annual mean precipitation event sizes, they were within the range of precipitation event sizes that can occur on any given day. Meaning, the treatments didn't receive more water on a single day than can naturally occur. The mean daily event sizes for the 1 mm, control, 2, 3, 4, 8 and, 18 mm treatments fall into the 66th, 69th, 73rd, 77th, 81st, 86th, and 96th percentiles of historical daily precipitation event sizes. For example, this means that historically on days with precipitation, about 4% of days received more than 19.4 mm (the mean event size of the 18 mm treatment). Note that the distribution of daily precipitation events is strongly right skewed (many small events, few large) causing even the 1 mm and control treatments to have mean event sizes well above the 50th percentile of daily event sizes.

In addition to increasing precipitation event sizes, the treatments also increased the coefficient of variation of daily precipitation (Figure S2.4). The increase in the coefficient of variation reflects the fact that treatments increased the number of days with zero precipitation, and increased the amount of precipitation on the remaining days it did rain, thus increasing the standard deviation of daily precipitation. The coefficient of variation of daily precipitation in the 1, control, 2, 3, 4, 8, and 18 mm treatments were 321, 326, 327, 330, 337, 359, and 446%, respectively.

The target number of snow events to be applied for a given treatment was calculated using a similar methodology described above for rain. However, for snow,

instead of calculating a target ‘tank size’, the target number of snow events for the winter was calculated. The actual number of snow events for a given treatment varied depending on the actual number of natural snow events in that winter. That is, if there were fewer naturally occurring snow events during a given winter, all treatments received fewer snow additions.

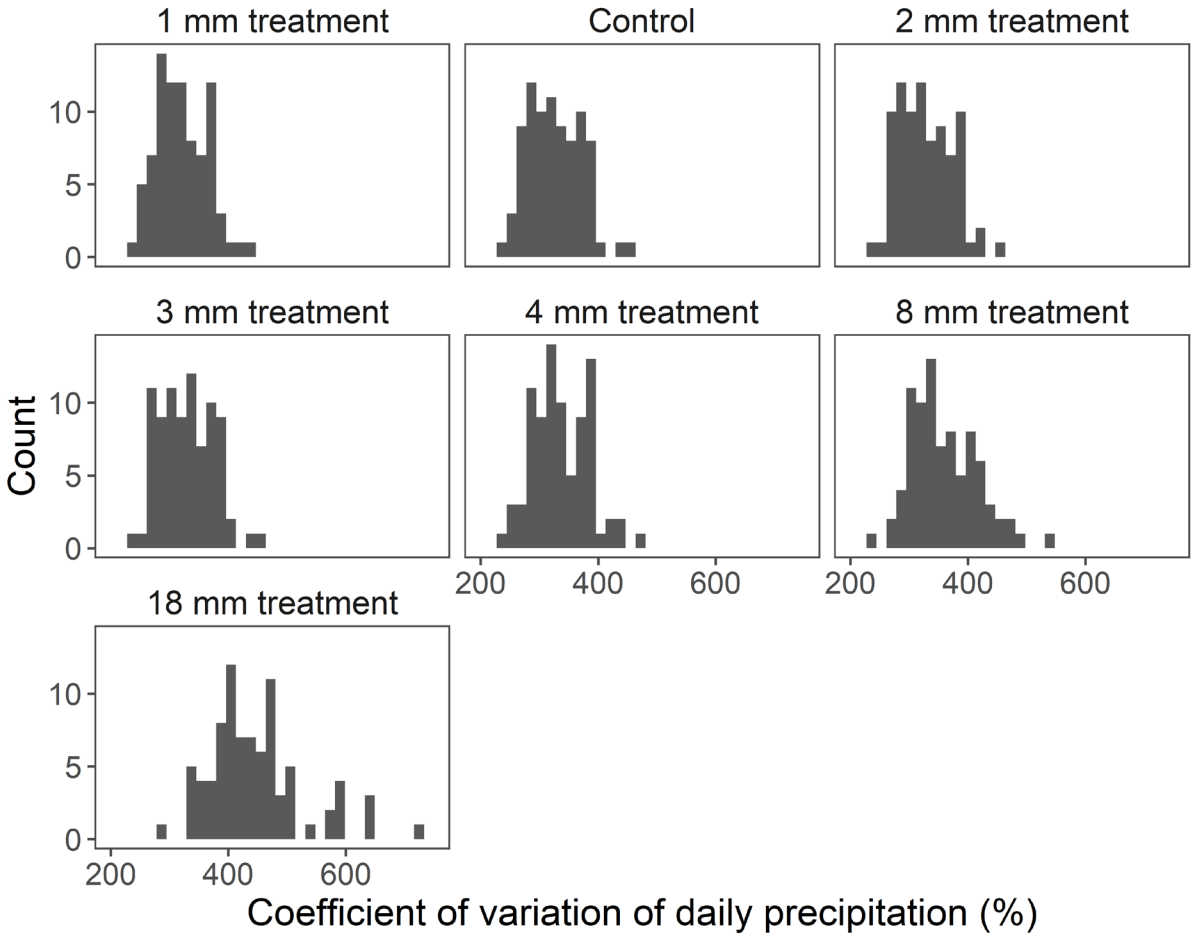

Figure S2.4 Coefficient of variation (CV) of daily precipitation by treatment. Each panel is a histogram of the CV of daily precipitation event size for a given treatment. A tipping bucket model was applied to the historical precipitation record to calculate daily precipitation for each treatment. That is, for each year on record the CV of daily precipitation event size was calculated as if treatments had been applied for each of those years, and the resulting histogram shows how CV varies between years.

Appendix S2.3: Soil moisture responses to treatments.

Table S2.1 AIC table for models of volumetric soil water content in treated and control plots. Separate models fit to each of three depths. For the null model, measurements in different plots were not distinguished. For the 'All Separate' model, measurements were associated with one of seven treatment levels. For the 'Low vs. High' model, measurements from the 1 mm, control, 2 mm and 3 mm treatments were grouped and compared to measurements in the 4 mm, 8 mm and 18 mm treatments.

Depth	Model	logLik	AIC	ΔlogLik	ΔAIC	df	Weight
10-30 cm							
	Low vs. High*	1085	-2157	0	0	7	0.98
	All Separate	1081	-2149	4.1	8.1	7	0.02
	Null	1013	-2013	72.8	143.6	6	<0.001
40-60 cm							
	All Separate *	1213	-2411	0	0	7	0.59
	Low vs. High *	1212	-2410	0.3	0.7	7	0.41
	Null	1181	-2350	31.4	60.8	6	<0.001
70-100 cm							
	Low vs. High *	1216	-2419	0	0	7	0.60
	All Separate *	1216	-2418	0.4	0.8	7	0.40
	Null	1185	-2358	31.3	60.5	6	<0.001

Abbreviations: logLik, log likelihood; AIC, Akaike's information criterion; df, degrees of freedom. *Indicates top model based on ΔAIC < 2 criteria.

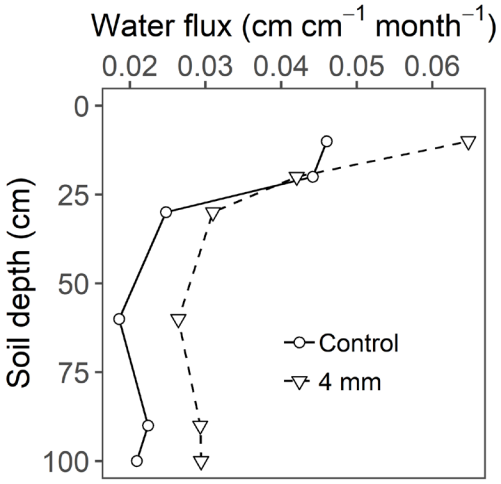

Figure S2.5 Water flux in one control plot and one 4 mm treatment plot, which received fewer, larger precipitation events. Soil moisture data from January 2016 (start of treatments) through July 2018 from 10 cm to 100 cm soil depths. Water flux was approximated by calculating the summed positive increment of daily mean volumetric soil moisture content. Data is from one treated and one control plot and is not tested statistically.

Table S2.2 AIC table for models of water potential in one control and one 4 mm treatment plot. Models were separately fit to data from shallow (10-30 cm) and deep (60-100 cm) soils. For the null models, measurements in the two plots were not distinguished. For the 'Separate' models, water potential from the two plots was able to follow different trends with time.

Model	**logLik**	**AIC**	**ΔlogLik**	**ΔAIC**	**df**	**Weight**
Shallow (10 – 30 cm)						
Separate	-7885.9	15785.8	0	0	7	>0.99
Null	-8091.5	16195	205.6	409.1	6	<0.001
Deep (60 – 100 cm)						
Separate	-8012.5	16039	0	0	7	>0.99
Null	-8277.4	16566.8	264.9	527.8	6	<0.001

Abbreviations: logLik, log likelihood; AIC, Akaike's information criterion; df, degrees of freedom.
*Indicates top model based on ΔAIC < 2 criteria.

Table S2.3 Number of 'dry days' in one control plot and one 4 mm treatment plot, which received fewer larger precipitation events. Here 'dry days', for a given depth, are days when the water potential was below -1.5 MPa, which is approximately wilting point. Dates where either plot had a missing value were excluded.

Depth (cm)	Treatment	Dry days	Total days	Percent dry days
10	Control	301	771	39
10	4 mm	212	771	28
20	Control	276	771	36
20	4 mm	201	771	26
30	Control	355	771	46
30	4 mm	308	771	40
60	Control	552	771	72
60	4 mm	263	771	34
90	Control	610	771	79
90	4 mm	378	771	49
100	Control	615	771	80
100	4 mm	372	771	48

Appendix S2.4: Stem growth responses to increased precipitation intensity treatments

Table S2.4 Shrub stem radius responses to precipitation intensity treatments. The null model did not distinguish between treatments, the high versus low treatments model separated high (18, 8, 4 mm) and low (3, 2, 1 mm and control) precipitation intensity treatments, and the all treatments separate model separated all treatments.

Model	logLik	AIC	ΔlogLik	ΔAIC	df	Weight
All treatments separate*	21637.7	-43261.3	0	0	7	>0.99
High vs. low treatments	21615.1	-43216.2	22.6	45.1	7	<0.001
Null	21613.8	-43215.6	23.9	45.7	6	<0.001

Abbreviations: logLik, log likelihood; AIC, Akaike's information criterion; df, degrees of freedom.

*Indicates top model based on ΔAIC < 2 criteria.

Appendix S2.5: Normalized difference vegetation index responses to increased precipitation intensity treatments

Table S2.5 GAMMs of twice monthly NDVI values measured in all plots. For the null model, measurements in different plots were not distinguished. For the 'All Separate' model, measurements were associated with one of seven treatment levels. For the 'Low vs. High' model, measurements from the 1 mm, control, 2 mm and 3 mm treatments were grouped and compared to measurements in the 4 mm, 8 mm and 18 mm treatments.

Model	logLik	AIC	ΔlogLik	ΔAIC	df	Weight
Null*	271.7	-531.3	0	0	6	>0.999
Low vs. High	243.9	-473.8	27.8	57.6	7	<0.001
All Seperate	193.9	-373.8	77.8	157.6	7	<0.001

Abbreviations: logLik, log likelihood; AIC, Akaike's information criterion; df, degrees of freedom.
*Indicates top model based on ΔAIC < 2 criteria.

Figure S2.6 Daily Normalized Difference Vegetation Index (NDVI) in low versus high intensity treatment plots. The lines show the predicted values from the GAMM, and the shaded regions are 95% confidence intervals. While the null model outperformed this model (Table S2.5), it illustrates our NDVI data.

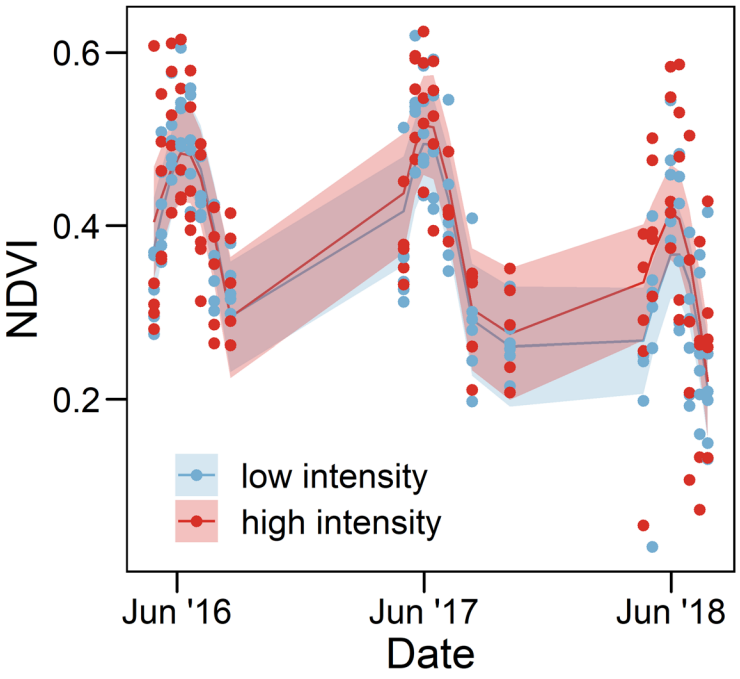

Table S2.6 GAMMs of daily NDVI measured in one control plot and one 4 mm treatment plot which received fewer larger precipitation events (data shown in Fig. S2.7). For the null model, measurements in the two plots were not distinguished. The separate model allowed the non-linear relationship of NDVI with time to differ between the two plots.

Model	logLik	AIC	ΔlogLik	ΔAIC	df	Weight
Separate*	3854.8	-7695.6	0	0	7	>0.99
Null	3842.7	-7673.5	12	22.1	6	<0.001

Abbreviations: logLik, log likelihood; AIC, Akaike's information criterion; df, degrees of freedom.
*Indicates top model based on ΔAIC < 2 criteria.

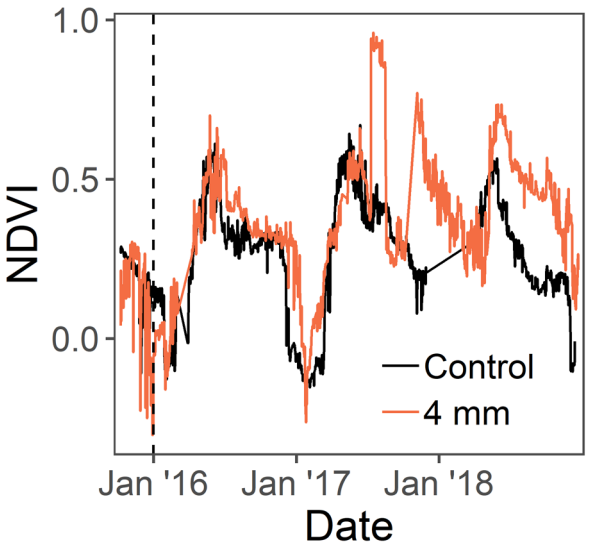

Figure S2.7 Daily Normalized Difference Vegetation Index (NDVI) in a control and a 4 mm treatment plots which received fewer larger precipitation events.

Appendix S2.6: Root growth responses to increased precipitation intensity treatments

Table S2.7 New root growth and root area responses to precipitation intensity. For the null models, no treatments were distinguished, meaning a single spline was fit to depth. The low vs. high treatments model separated low (3, 2, 1 mm and control) and high (18, 8, 4 mm) precipitation intensities; and the all treatments model separated all treatment levels.

Model	logLik	AIC	ΔlogLik	ΔAIC	df	Weight
New roots						
Low vs. high treatments*	-264.8	541.5	0.0	0.0	6	0.97
All treatments separate	-268.6	549.2	3.8	7.7	6	0.02
Null	-270.7	551.4	6.0	9.9	5	0.01
Root area						
Null*	-307.4	626.7	0	0	6	0.89
All treatments separate	-308.7	631.3	1.3	4.6	7	0.09
Low vs. high treatments	-309.9	633.9	2.6	7.2	7	0.02

Abbreviations: logLik, log likelihood; AIC, Akaike's information criterion; df, degrees of freedom.
*Indicates top model based on ΔAIC < 2 criteria.

Appendix S3.1: Effects of rainout shelters

Shelter effects on temperature and humidity

Air temperature and relative humidity were measured at a height of 1.5 m on the inside and outside of one shelter (HOBO Pro v2, Onset Computer Corp., Bourne, MA, USA). Sensors were installed 19 May 2017, and hourly measurements were collected until the end of the experiment (3 August 2019). Shelters were in place during this entire period.

Shelters had a negligible impact on temperature and humidity. Shelters had very slightly higher mean daily maximum temperature (15.8 vs. 15.7 °C) and the same daily minimum temperature (2.7 °C) as ambient conditions (Figure S3.1). Shelters had slightly lower mean daily maximum relative humidity (79.4% vs. 80.3%) and daily minimum relative humidity (43.4% vs. 43.8%) than ambient conditions (Figure S3.2).

Shelter effects on vegetation

Shelter effects on vegetation were analyzed using mixed-effects models to compare vegetation in the three shelterless-control plots and the three sheltered-control plots. Four models were fit, with the respective response variables being wheat height, aboveground wheat biomass, wheat grain yield, and aboveground weed biomass ("lme4" package [45]). In all cases, the fixed effects were shelter (i.e., sheltered vs. shelterless) and year (treated as a categorical variable). Plot was treated as a random effect.
No significant shelter effects of wheat height, wheat biomass, grain yield, or weed biomass were detected (Table S3.1). However, in all four models, there was a significant effect of year (Table S3.1).

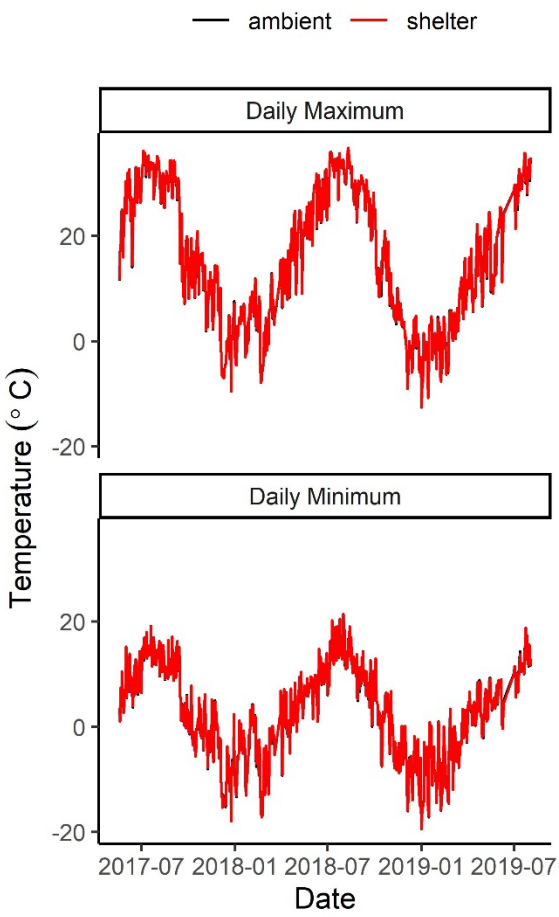

Figure S3.1 Daily maximum and minimum temperatures under ambient and shelter conditions. Ambient temperatures are mostly not visible in figure due to over-plotting because ambient and shelter temperatures were very similar.

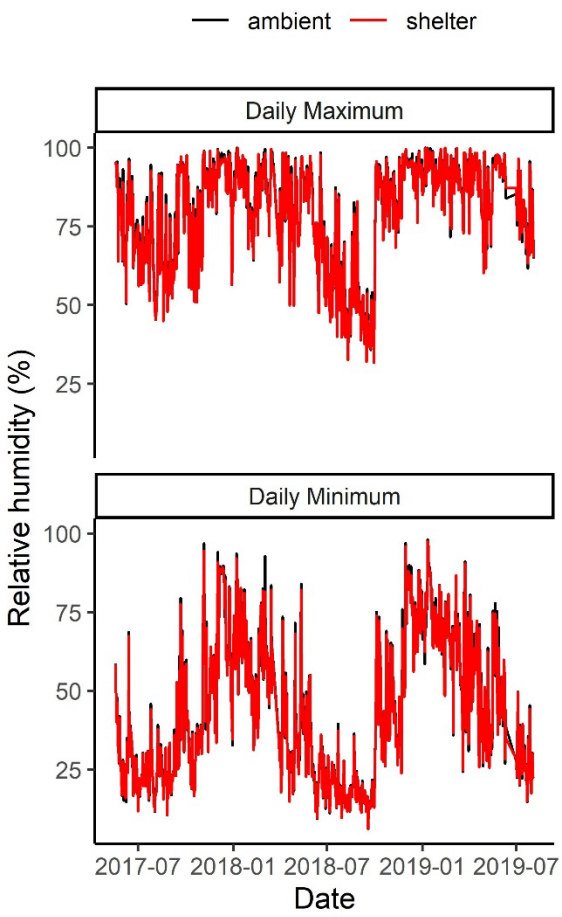

Figure S3.2 Daily maximum and minimum relative humidity under ambient and shelter conditions. Ambient humidity values are mostly not visible in figure due to over-plotting because ambient and shelter values were very similar.

Table S3.1 Results of four mixed models that tested shelter effects on wheat and weed growth. Models included fixed effects of shelter (i.e. sheltered vs. shelter-less control) and year (treated as a factor).

Model	Predictor	SS	DF_{num}	DF_{den}	F-value	P-value
Wheat height						
	shelter	3.1	1	4	0.27	0.63
	year	192.0	1	5	16.6	0.01
Wheat biomass						
	shelter	16647.6	1	4	2.1	0.22
	year	81072.0	1	5	10.4	0.02
Gain yield						
	shelter	1276.9	1	4	0.51	0.52
	year	40064.7	1	5	16.0	0.01
Weed biomass						
	shelter	1.7	1	4	0.006	0.94
	year	4167.6	1	5	15.3	0.01

Abbreviations: SS, sum of squares; DF_{num}, numerator degrees of freedom; DF_{den}, denominator degrees of freedom.

Appendix S3.2: Description of precipitation intensity treatments

Holdrege et al. [10] used the same experimental design as was employed here (but in a shrubland with different plot sizes, snow treatments, and methods of water application). For the convenience of the reader, descriptions of the precipitation treatments are also included here.

1. Water was applied to plots via drip irrigation lines once enough water was collected in the tanks to create a precipitation event of a certain size (which varied by treatment). The target precipitation event sizes were calculated using historical precipitation data and the Clausius–Clapeyron relation. For example, for the 2 mm treatment associated with 1 °C of warming, the following steps were used to calculate the target event size: historical observed daily precipitation was put in descending order.
2. A curve was fit to this distribution of historical precipitation events to create a model of the precipitation distribution.
3. Precipitation events in this generalized distribution were multiplied by 1.07 to create a new distribution of larger events.
4. Enough of the smallest precipitation events were removed from this new distribution so that the sum of annual precipitation was equal to the sum of the original distribution (since all events were increased by 7%, if the smallest events were not “removed,” then total annual precipitation would necessarily also increase by 7%). This created a new distribution with fewer larger precipitation events, but the same total annual precipitation.

The smallest precipitation event size from this new distribution was used as the event size for the treatment. In the case of the 2 mm treatment, this smallest event size was 2 mm; this means that 2 mm of water was collected in tanks before being redistributed. The above sequence of steps was repeated to calculate event sizes for the treatments meant to reflect increased precipitation intensity associated with 2, 3, 5, and 10 °C of warming.

Rainwater was applied to the plots in a way that can be described as a tipping bucket model. That is, once the "bucket" (a water tank in our case) filled to the target level (e.g., 2 mm for the 2 mm treatment) with water collected off the shelter roof, it would "tip" (in our case, that means the floating outlet would sink and water would drain onto the plots via drip irrigation lines). Because a tank could fill and empty multiple times during a storm (i.e., multiple events in one day), this tipping bucket model was applied to observed precipitation data to calculate the mean daily rainfall that resulted from the treatments, that is, the mean amount of rain received on days when there was >0 mm of rain. For the 1 mm treatment (which unlike the other treatments had lower precipitation intensity than the control), 1 mm of precipitation from larger natural events was "removed" and redeposited on days no natural precipitation occurred. The tipping bucket model was applied to precipitation data from the period of the experiment (April 2016–August 2019), but only data from the months of April to November were used because those were snow-free months when our floating outlets were operational, and therefore, the time during which the tipping bucket model most accurately represented the way treatments were applied. The distributions of daily rainfall for each treatment are shown in Figure S3.3. Mean daily rainfall values were 4.9, 5.6, 6.9, 8.3, 9.1, 11.5, and 20.5 mm, for the 1 mm, control, 2 mm, 3 mm, 4 mm, 8 mm, and 18 mm treatments,

respectively. These mean daily rainfall values were used in our regression analyses of wheat biomass, grain yield, wheat height, and weed biomass (Figure 3.5).

Mean daily rainfall of the treatments was within the range of historical daily precipitation. Meaning, the treatments did not receive more water on a single day than can naturally occur. Mean daily rainfall values for the 1 mm, control, 2 mm, 3 mm, 4 mm, 8 mm and, 18 mm treatments fall into the 67th, 72nd, 77th, 81st, 84th, 89th, and 97th percentiles of historical daily precipitation, respectively. This means, for example, that historically on days with precipitation, about 3% of days received more than 20.5 mm (which is the mean daily rainfall of the 18 mm treatment). Note that the distribution of daily rainfall is strongly right-skewed (many small events, few large), causing even the 1 mm and control treatments to have mean daily rainfall well above the 50th percentile of daily rainfall.

The target number of snow events to be applied for a given treatment was calculated using a similar methodology as described above for rain. However, for snow, instead of calculating a target event size, the target number of snow events for winter months was calculated. Snow from around the plots was shoveled onto plots to achieve the target number of snow events. All plots received an equal amount of snow water equivalent. If additional snow drifted into plots, it was removed.

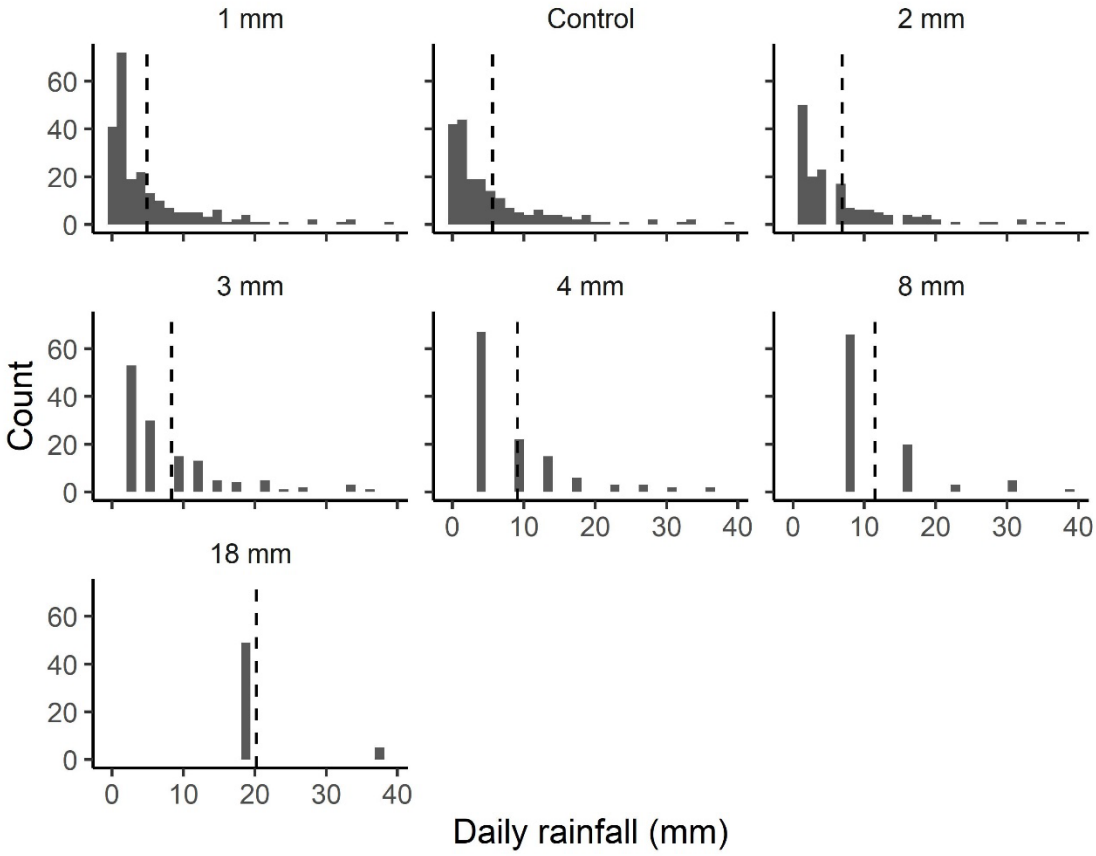

Figure S3.3 A tipping bucket model was applied to precipitation data to simulate the effects of the treatments on daily rainfall. Each panel shows the distribution of daily rainfall during the months of April to November for a given treatment during the period of the experiment. The dotted line shows mean daily rainfall on days that received rain (i.e., the distribution mean). Total rainfall was the same in each treatment. Note that distributions are not continuous, this occurred for the 18 mm treatment, for example, because water was only deposited once enough had accumulated in the tank to create an 18 mm event, on rare occasions it rained enough on one day for water to be deposited a second time (i.e., for a daily total of 36 mm).

Appendix S3.3: Model results

Table S3.2 Model results from shallow and deep soil water potential over time in a 4 mm treatment plot and a control plot. Separate sets of generalized additive mixed models (GAMMs) were fit to monthly mean water potential from sensors in shallow (10-30 cm) and deep soils (60-100 cm). Null models did not distinguish between treatments, fitting a single spline to month. The 'separate' models, separated the treated and control plot (i.e. fit separate splines for each plot; Figure S4).

Soil Depth	Model	logLik	AIC	ΔlogLik	ΔAIC	df	Weight
10-30 cm							
	Separate*	-94.8	205.6	0.0	0.0	8	0.99
	Null	-101.1	214.1	6.2	8.5	6	0.01
60-100 cm							
	Separate*	-92.5	201.0	0.0	0.0	8	0.98
	Null	-98.3	208.6	5.8	7.7	6	0.02

Abbreviations: logLik, log likelihood; AIC, Akaike's information criterion; df, degrees of freedom.

*Indicates top model based on $\Delta AIC < 2$ criteria.

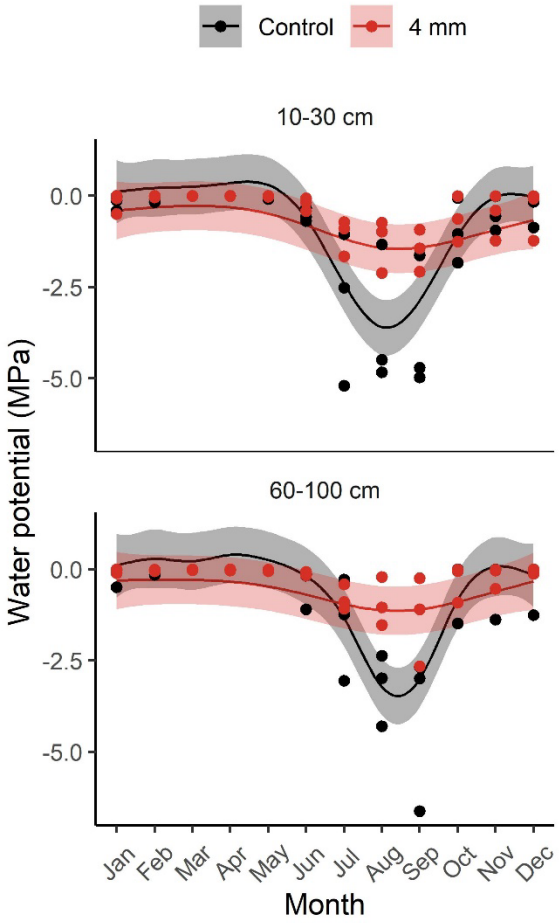

Figure S3.4 Monthly mean shallow (10-30 cm; top panel) and deep (60-100 cm; bottom panel) soil water potential over time in a treated and control plot. Water potential was measured separately with three sensors for each depth category in one control plot and one treated plot in which all precipitation events were 4 mm or greater. The lines show the predicted values from the GAMM ('separate' model; Table S2), the shaded regions are 95% confidence intervals.

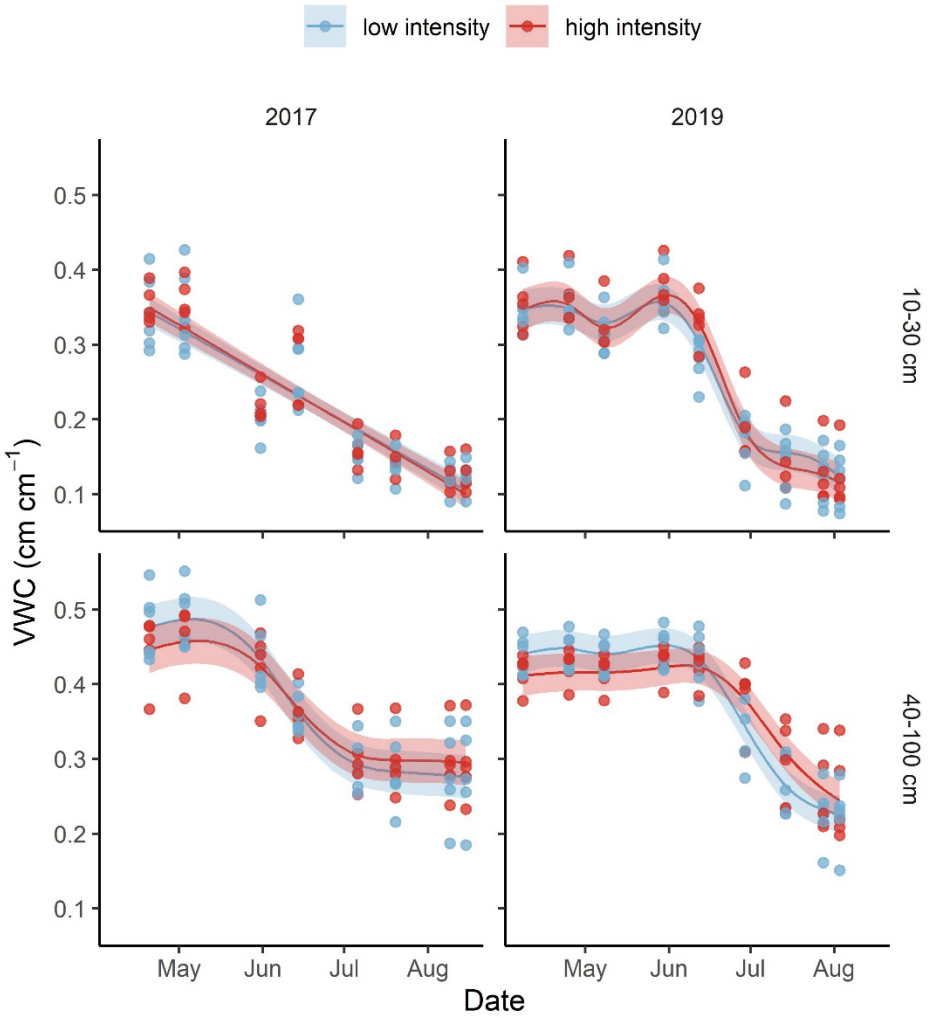

Figure S3.5 Shallow (10-30 cm; top panels) and deep (40-100 cm; bottom panels) volumetric water content (VWC) in 2017 (left panels) and 2019 (right panels). Volumetric water content was measured in all plots approximately twice monthly during the growing season. Measurements were taken in 10 cm increments and then averaged into two depth categories (10-30 cm and 40-100 cm). Lines show the predicted values from the GAMMs, the shaded regions are 95% confidence intervals. While the null models outperformed the 'low vs. high' models presented here (Table S3), they are shown to illustrate our data.

Table S3.3 In each year separate sets of GAMMs were fit to volumetric water content in shallow and deep soils. Null models did not distinguish between treatments, fitting a single spline to day of year. The 'low vs. high' treatments model separated low (3, 2, 1 mm and control) and high (18, 8, 4 mm) precipitation intensity treatments (Figure S5). The 'all separate' model separated all treatments (i.e. fitting a separate spline to day of year for each treatment). Volumetric water content was measured in all plots approximately twice monthly during the growing season. Measurements were taken in 10 cm increments and then averaged into two depth categories (10-30 cm and 40-100 cm).

Year	Soil Depth	Model	logLik	AIC	ΔlogLik	ΔAIC	df	Weight
2017	10-30 cm							
		Null*	176.4	-340.9	0.0	0.0	6	0.99
		Low vs. high	158.5	-301.1	17.9	39.8	8	<0.01
		All separate	139.6	-247.3	36.8	93.6	16	<0.01
2017	40-100 cm							
		Null*	201.4	-390.8	0.0	0.0	6	0.99
		Low vs. high	195.7	-375.5	5.7	15.3	8	<0.01
		All separate	194.3	-356.6	7.1	34.3	16	<0.01
2019	10-30 cm							
		Null*	212.6	-413.1	0.0	0.0	6	0.99
		Low vs. high	204.3	-392.6	8.3	20.5	8	<0.01
		All separate	164.2	-296.4	48.3	116.7	16	<0.01
2019	40-100 cm							
		Null*	228.0	-443.9	1.9	0.0	6	0.52
		Low vs. high*	229.9	-443.8	0.0	0.1	8	0.48
		All separate	204.9	-377.8	25.0	66.1	16	<0.01

Abbreviations: logLik, log likelihood; AIC, Akaike's information criterion; df, degrees of freedom.

*Indicates top model based on ΔAIC < 2 criteria.

Table S3.4 For each response variable, separate sets of generalized additive mixed models (GAMMs) were fit to growing season data from 2017 and 2019. Null models did not distinguish between treatments, fitting a single spline to day of year. The low versus high treatments models ('low vs. high') separated low (3, 2, 1 mm and control) and high (18, 8, 4 mm) precipitation intensity treatments (Figure 4 in manuscript). The 'all separate' model separated all treatments (i.e. fitting a separate spline to day of year for each treatment).

Response Variable	Model	logLik	AIC	ΔlogLik	ΔAIC	df	Weight
NDVI (2017)							
	Null*	127.3	-242.6	0.0	0.0	6	>0.99
	Low vs. high	113.4	-210.9	13.9	31.7	8	<0.01
	All separate	55.5	-79.1	71.8	163.6	16	<0.01
NDVI (2019)							
	Null*	97.2	-182.3	0.0	0.0	6	0.99
	Low vs. high	88.0	-160.0	9.2	22.3	8	0.01
	All separate	71.0	-110.0	26.2	72.3	16	<0.01
LAI (2017)							
	Null*	35.0	-58.0	0.0	0.0	6	>0.99
	Low vs. high	29.4	-42.8	5.6	15.2	8	<0.01
	All separate	16.9	-1.8	18.1	56.1	16	<0.01
LAI (2019)							
	Null*	38.4	-64.8	0.0	0.0	6	>0.99
	Low vs. high	33.6	-51.2	4.8	13.6	8	<0.01
	All separate	11.3	9.4	27.1	74.1	16	<0.01
PRI (2017)							
	Null*	190.9	-369.8	0.0	0.0	6	0.99
	Low vs. high	185.5	-355.1	5.4	14.7	8	0.01
	All separate	186.9	-341.7	4.0	28.1	16	<0.01
PRI (2019)							
	Null*	198.2	-384.3	0.0	0.0	6	>0.99
	Low vs. high	194.6	-373.3	3.5	11.0	8	<0.01
	All separate	185.2	-338.4	12.9	45.9	16	<0.01
T_c-T_a (2017)							
	Null*	-144.9	301.8	0.0	0.0	6	>0.99
	Low vs. high	-151.3	318.7	6.4	16.8	8	<0.01
	All separate	-154.0	340.1	9.1	38.2	16	<0.01
T_c-T_a (2019)							
	Null*	-119.7	251.5	0.0	0.0	6	>0.99
	Low vs. high	-125.7	267.3	5.9	15.9	8	<0.01
	All separate	-133.0	298.1	13.3	46.6	16	<0.01

Abbreviations: logLik, log likelihood; AIC, Akaike's information criterion; df, degrees of freedom; NDVI, Normalized Difference Vegetation Index; LAI, Leaf Area Index; PRI,

Photochemical Reflectance Index; T_c-T_a, difference between canopy temperature (T_c) and air temperature (T_a).
*Indicates top model based on ΔAIC < 2 criteria.

Table S3.5 Root responses to precipitation intensity treatments. Separate sets of generalized additive mixed models (GAMMs) were fit to data from 2017 and 2019. Response variables were mean growing season root area (mm^2 cm^{-2}) and mean growing season new root growth rate (new roots cm^{-2} $week^{-1}$). Null models did not distinguish between treatments, fitting a single spline to day of year. The low versus high treatments models ('low vs. high') separated low (3, 2, 1 mm and control) and high (18, 8, 4 mm) precipitation intensity treatments (Figure 6 in manuscript). The 'all separate' model separated all treatments (i.e. fitting a separate spline to day of year for each treatment).

Response Variable	Model	logLik	AIC	ΔlogLik	ΔAIC	df	Weight
Root area (2017)							
	Null*	-48.2	108.5	0.0	0.0	6	0.96
	Low vs. high	-49.5	115.0	1.3	6.6	8	0.04
	All separate	-50.5	137.0	2.3	28.6	18	<0.01
Root area (2019)							
	Null*	17.6	-23.3	3.5	0.0	6	0.98
	Low vs. high	15.5	-15.0	5.6	8.3	8	0.02
	All separate	21.1	-6.2	0.0	17.1	18	<0.01
New roots (2017)							
	Null*	71.5	-131.1	0.0	0.0	6	0.98
	Low vs. high	69.8	-123.6	1.7	7.5	8	0.02
	All separate	70.4	-104.9	1.1	26.2	18	<0.01
New roots (2019)							
	Null*	100.8	-189.6	5.6	0.0	6	0.76
	Low vs. high	101.7	-187.3	4.7	2.3	8	0.24
	All separate	106.4	-176.7	0.0	12.9	18	<0.01

Abbreviations: logLik, log likelihood; AIC, Akaike's information criterion; df, degrees of freedom.

*Indicates top model based on ΔAIC < 2 criteria.

Appendix S4.1: Species list

Table S4.1 Species and corresponding plant functional types for which biomass was simulated in the STEPWAT2 model.

Species	**Plant Functional Type**
Artemisia tridentata	Sagebrush
Cryptantha sp.	Annual cool season forb
Chenopodium sp.	Annual warm season forb
Phlox hoodii	Perennial cool season forb
Artemisia frigida	Perennial warm season forb
Bromus tectorum	Annual grass (C_3)
Pseudoroegnaria spicata	Perennial C_3 grass
Bouteloua gracilis	Perennial C_4 grass
Chrysothamnus viscidiflorus	Other shrub
Opuntia polyacantha	Succulent

Appendix S4.2: Description of precipitation intensity manipulations

Weather generator inputs

STEPWAT2 uses a first-order Markov weather generator (Palmquist et al., 2018). For each day of the year there are two probabilities, the probability of precipitation given the previous day received precipitation (P_W_W) and probability of precipitation given the previous day was dry (P_W_D). These transition probabilities are then used by the weather generator to determine if a given day receives precipitation (i.e., is 'wet'). If a day is 'wet', then the quantity of precipitation is determined using a draw from a normal distribution. For the ambient precipitation intensity treatment, the mean and standard deviation of the normal distribution were calculated using precipitation data from the given day of year during the 30-year observational record. If the draw from the normal distribution returns a negative number, it is replaced with 0 (in effect this makes it a truncated normal distribution). To adjust precipitation intensity, we adjusted P_W_D. However, P_W_W was not adjusted, as a result, the mean length of multi-day (i.e., consecutive days) precipitation events was not altered. For example, for the 2x intensity treatment, the P_W_D for a given day of year was reduced such that the unconditional probability of precipitation intensity was halved, and the mean and standard deviation of precipitation event size was doubled. These adjustments to weather generator inputs were done within the R program rSFSTEP2 using the 'adjust_coeffs' function from the 'precipr' R package (https://github.com/MartinHoldrege/precipr). The version of rSFSTEP2 used for these simulations, including input parameters, is hosted on Zenodo (https://doi.org/10.5281/zenodo.5661688).

Change event size distribution

Within the weather generator, precipitation event sizes were drawn from a truncated normal distribution and the mean and standard deviation were increased by the same multiplier (e.g., doubling mean and standard deviation for the 2x intensity treatment). Therefore, the value of each percentile roughly increased by that multiplier. For example, across sites the 90th and 95th percentiles of precipitation event size (on days with non-zero precipitation) were 1.23 cm and 1.52 cm, respectively, under the ambient intensity (control) treatment, and were 2.46 cm (90th percentile) and 3.04 cm (95th percentile) under the 2x intensity treatment. Meaning that under the 2x intensity treatment on average across sites, the 90th percentile event size increased by 1.23 cm and the 95th percentile event size increased by 1.52 cm. By comparison, the mean event size under the ambient treatment was 0.66 cm and increased to 1.32 cm under the 2x intensity treatment. This means that extreme (rare) precipitation events increased by a larger amount than less extreme (smaller and more common) events (Figure S2.1). Put another way, the right tails of the distributions were pulled to the right more than the means of the distributions (Figure S2.1), which roughly approximates the way precipitation distributions are expected to change with climate change (Fischer & Knutti, 2016; Pendergrass & Hartmann, 2014; Pendergrass & Knutti, 2018). The method we used to manipulate precipitation intensity (i.e. adjusting daily precipitation probabilities and event sizes) also caused an increase in inter-annual variability of annual precipitation. Across sites, the standard deviation of annual precipitation increased on average by 18%, 34%, and 61% for the 1.25x, 1.5x, and 2x intensity treatments, respectively.

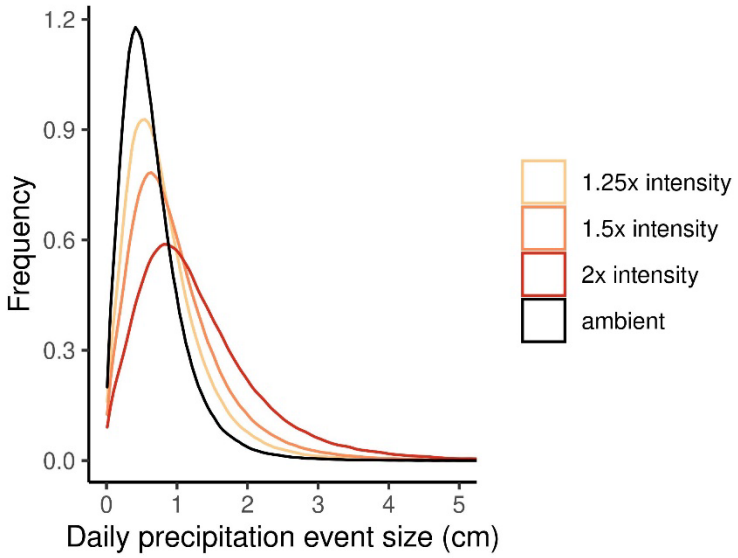

Figure S4.1 Distribution of daily precipitation event sizes, across the 200 sites for which simulations were run. Precipitation regimes differed between sites, so this figure shows the 'average' distribution. The treatments increased mean precipitation event sizes by 25% ('1.25x intensity'), 50% ('1.5x intensity'), and 100% ('2x intensity'), relative to the ambient (control) precipitation intensity treatment. Distributions shown are based on days that received > 0 cm precipitation. Treatments did not alter total (monthly or annual) precipitation.

References

Fischer, E. M., & Knutti, R. (2016). Observed heavy precipitation increase confirms theory and early models. *Nature Climate Change*, *6*(11), 986–991. https://doi.org/10.1038/nclimate3110

Palmquist, K. A., Bradford, J. B., Martyn, T. E., Schlaepfer, D. R., & Lauenroth, W. K. (2018). STEPWAT2: an individual-based model for exploring the impact of climate and disturbance on dryland plant communities. *Ecosphere*, *9*(8). https://doi.org/10.1002/ecs2.2394

Pendergrass, A. G., & Hartmann, D. L. (2014). Changes in the distribution of rain frequency and intensity in response to global warming. *Journal of Climate*, *27*(22), 8372–8383. https://doi.org/10.1175/JCLI-D-14-00183.1

Pendergrass, A. G., & Knutti, R. (2018). The uneven nature of daily precipitation and its change. *Geophysical Research Letters*, 1–9. https://doi.org/10.1029/2018GL080298

Appendix S4.3: Relationships between responses to increased precipitation intensity and mean annual precipitation

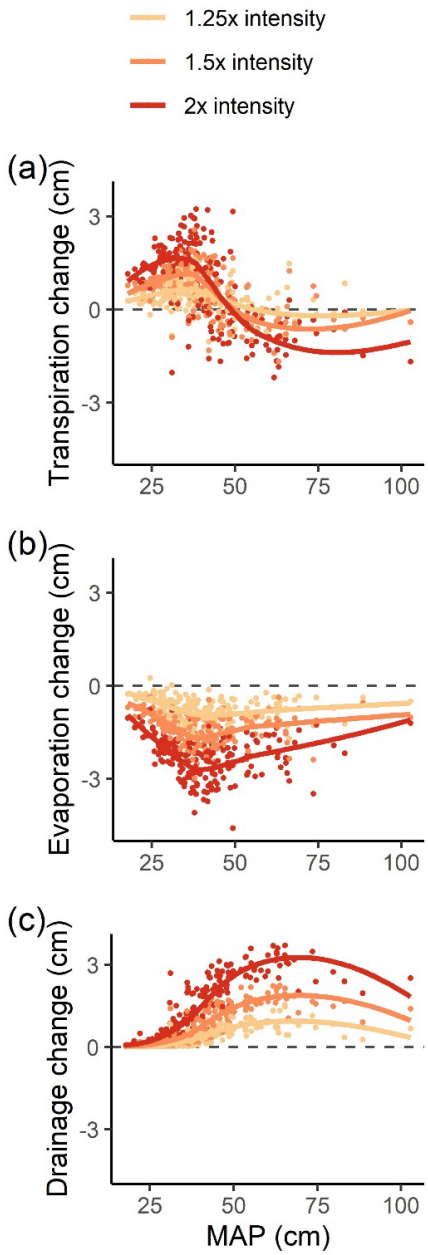

Figure S4.2 Changes in (a) total transpiration across plant functional types, (b) evaporation, and (c) deep drainage of soil water, versus mean annual precipitation (MAP). Points are changes in mean annual values (treatment minus ambient conditions) at each of 200 sites in response to 1.25x, 1.5x, and 2x increases in mean precipitation event size, respectively.

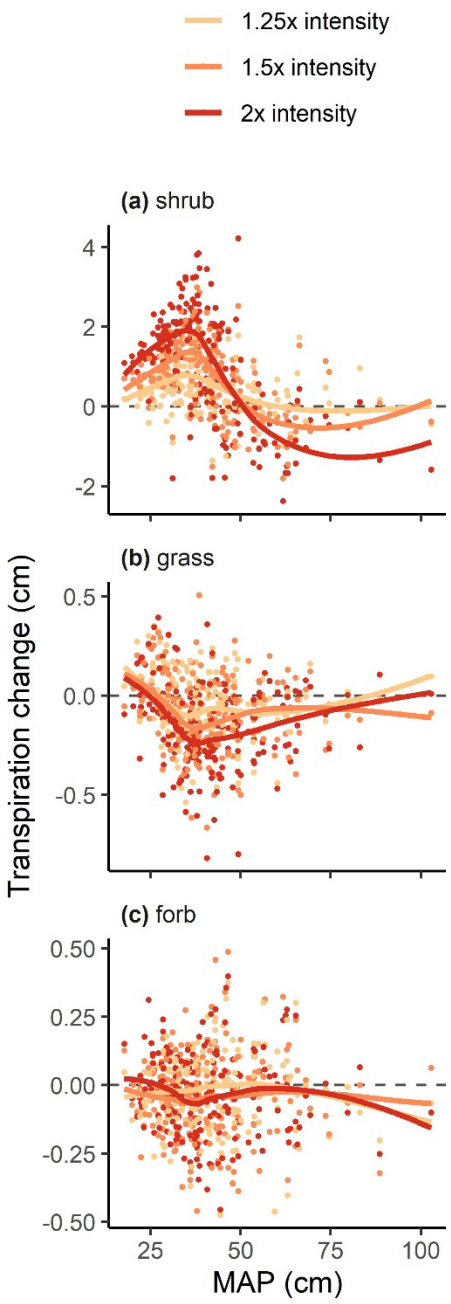

Figure S4.3 Changes in annual transpiration of (a) shrubs, (b) grasses, and (c) forbs in response to increased precipitation intensity versus mean annual precipitation intensity (MAP). Points are changes in mean annual amounts (treatment minus ambient conditions) of water transpired by a plant functional type at each of 200 sites in response to 1.25x, 1.5x, and 2x increases in precipitation event size, respectively.

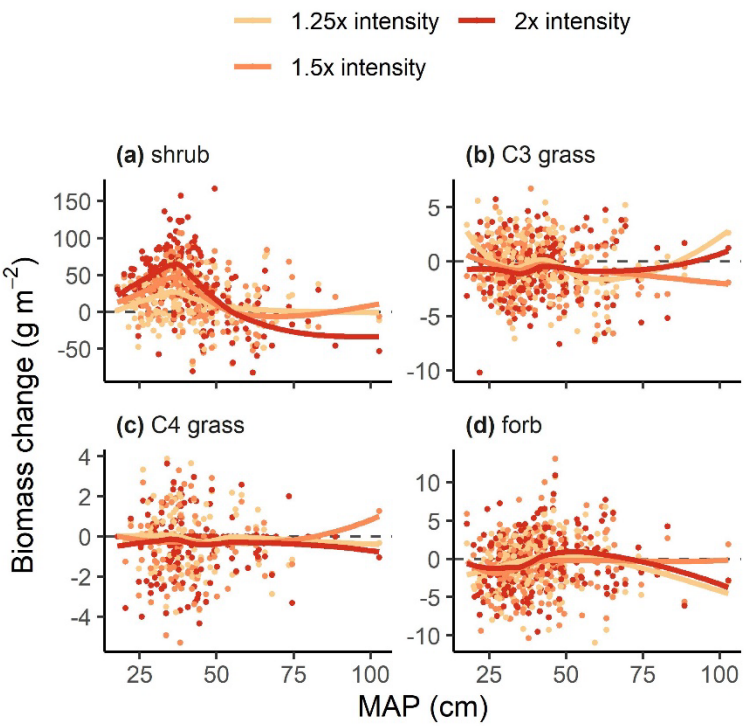

Figure S4.4 Changes in biomass of (a) shrubs, (b) perennial C_3 grasses, (c) perennial C_4 grasses, and (d) forbs in response to increased precipitation intensity versus mean annual precipitation (MAP). Points are changes in mean biomass by a plant functional type (treatment minus ambient conditions) at each of 200 sites, in response to 1.25x, 1.5x, and 2x increases in mean precipitation event size, respectively.

Appendix S4.4: Influence of soil texture on responses to increased precipitation intensity

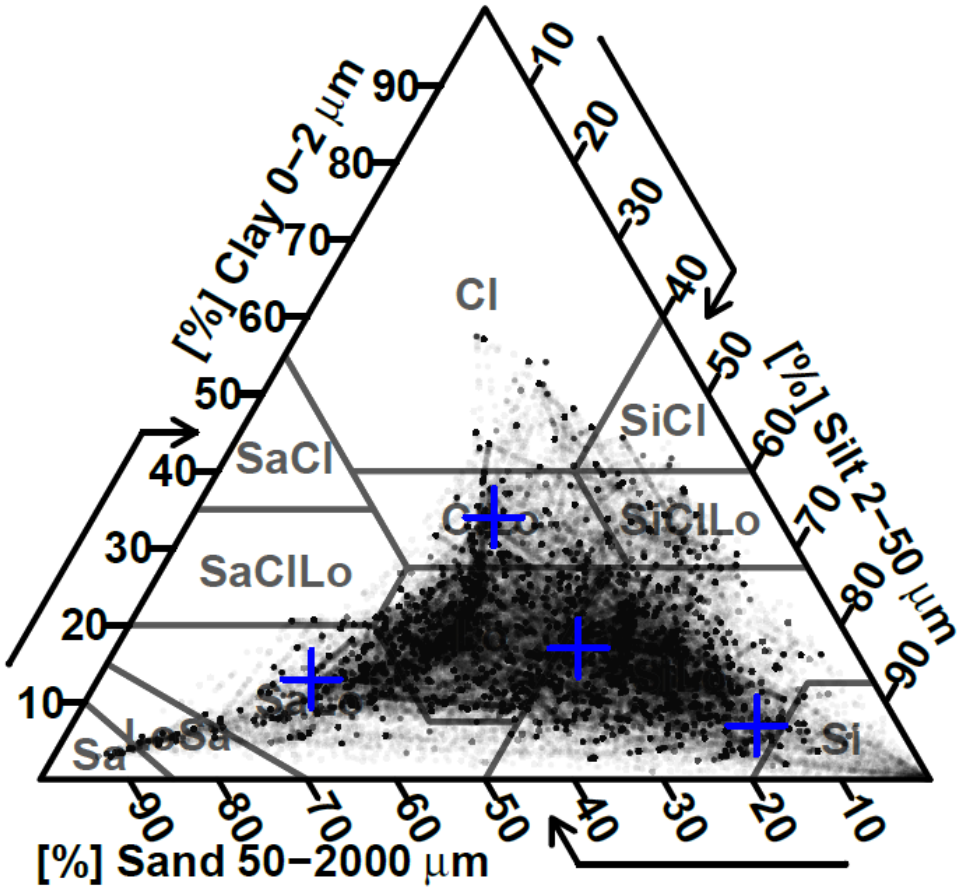

Figure S4.5 Soil textures in all NRCS STATSGO 1 km^2 grid cells that contained > 66% sagebrush and were within Sage-grouse Management Zones (black points). The blue crosses show the soil textures for which simulations were run. The center cross is a silt loam chosen by calculating the median sand and clay content across grid cells. The other three soil textures were selected by calculating the 95th percentile of sand, silt, and clay content, respectively, and by calculating the expected value of another texture class conditional on the 95th percentile of the selected class. For example, for the sandy soil the 95th percentile of sand was calculated (63%) and the conditional expected value of clay (13%) was calculated using an empirical joint probability density function of the percent sand and percent clay content in the grid cells.

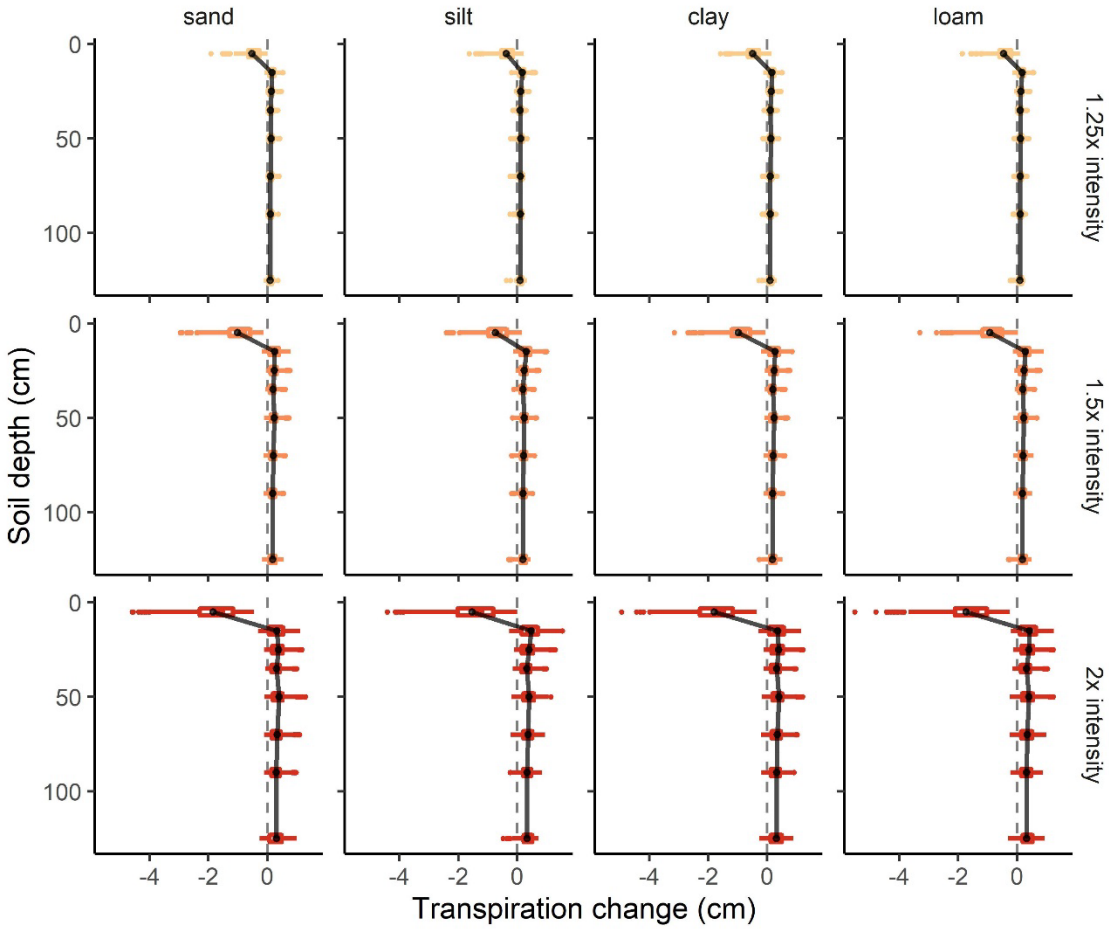

Figure S4.6 Boxplots and mean (solid black line) change in amount of water transpired annually from eight soil depths for three precipitation intensity treatments (rows: 1.25x, 1.5x and 2x) across 200 sites. Simulations were run on each of four soil textures (columns: sand, silt, clay, and loam). For each site and treatment, the mean amount of water transpired annually from each soil layer was calculated. Values shown are differences between treatment and ambient (control) conditions, values greater than zero indicate an increase in water uptake from that depth with increased precipitation intensity.

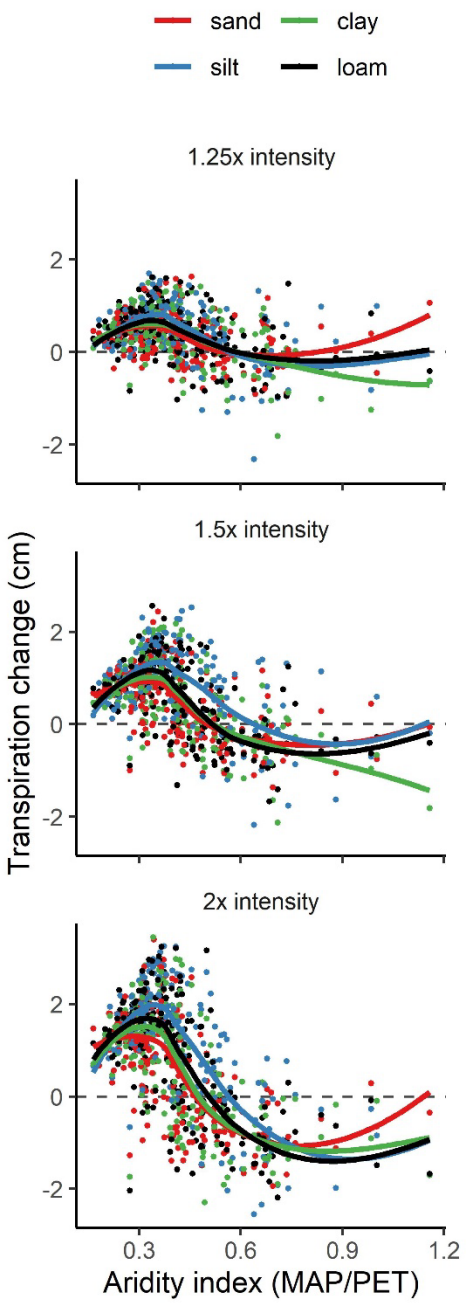

Figure S4.7 Changes in total transpiration across plant functional types versus aridity index (mean annual precipitation/potential evapotranspiration) for simulations run using each of four soil textures. Points are mean annual changes (treatment minus ambient conditions) at each of 200 sites in response to 1.25x (top panel), 1.5x (middle panel), and 2x (bottom panel) increases in mean precipitation event size, respectively.

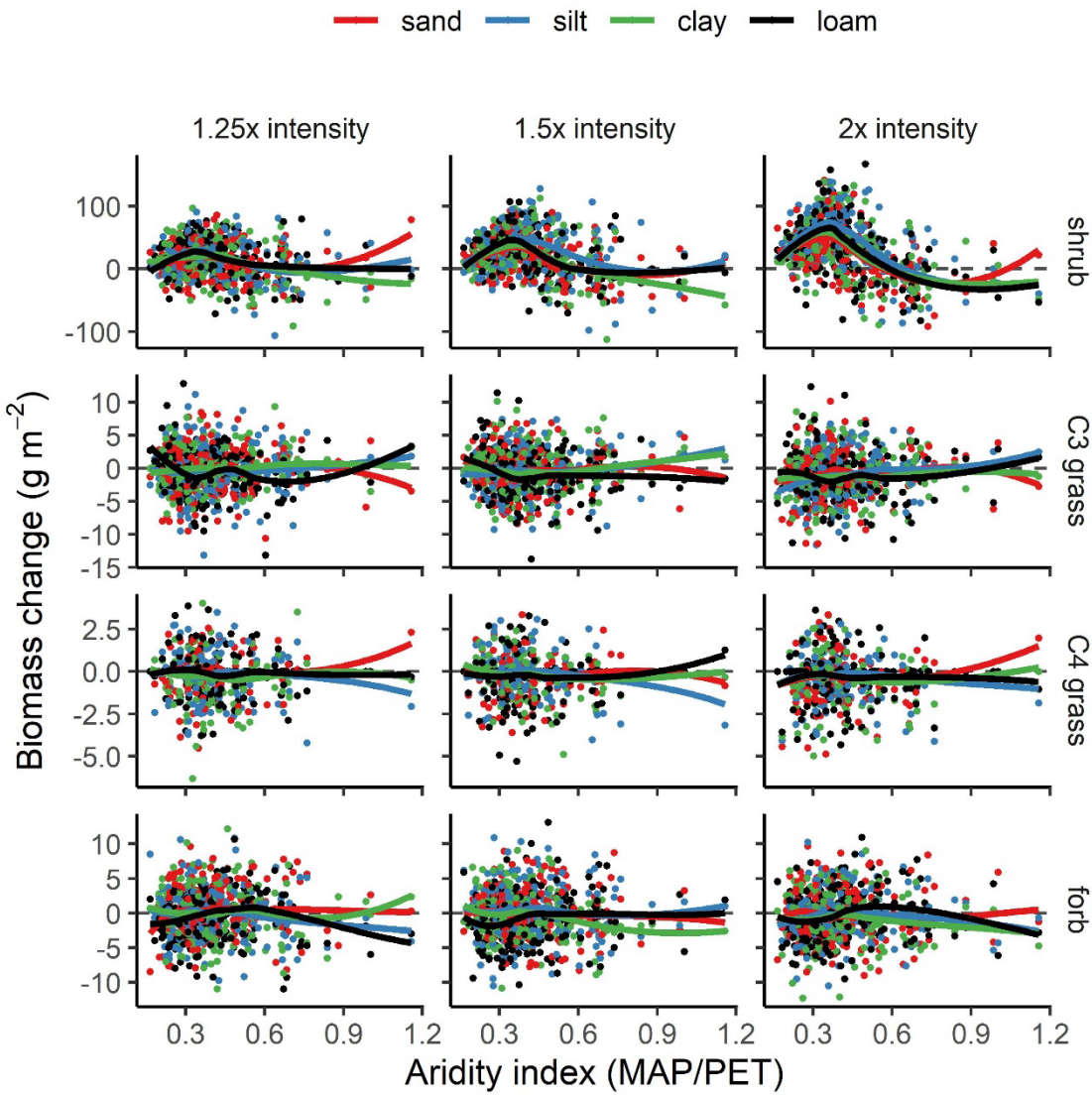

Figure S4.8 Changes in biomass of shrubs, perennial C_3 grasses, perennial C_4 grasses, and forbs in response to increased precipitation intensity versus aridity index (mean annual precipitation/potential evapotranspiration). Simulations were run using four soil textures. Points are changes in mean biomass of a plant functional type (treatment minus ambient conditions) at each of 200 sites, in response to 1.25x, 1.5x, and 2x increases in mean precipitation event size, respectively.

Appendix S4.5: Treatment responses by plant functional type

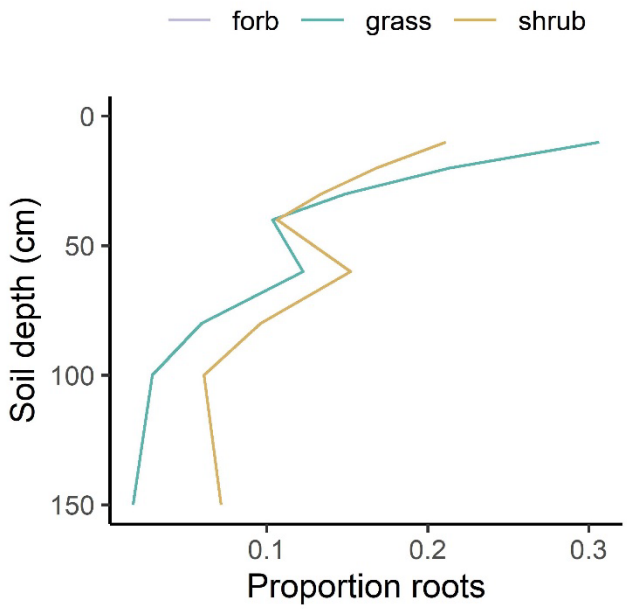

Figure S4.9 Root profiles of shrubs, grasses, and forbs used in model runs. The forb root profile used was the same as the grass root profile so does not appear on the figure due to over-plotting. 'Proportion roots' is the proportion of total root biomass for that plant functional type that is present in each of eight soil layers.

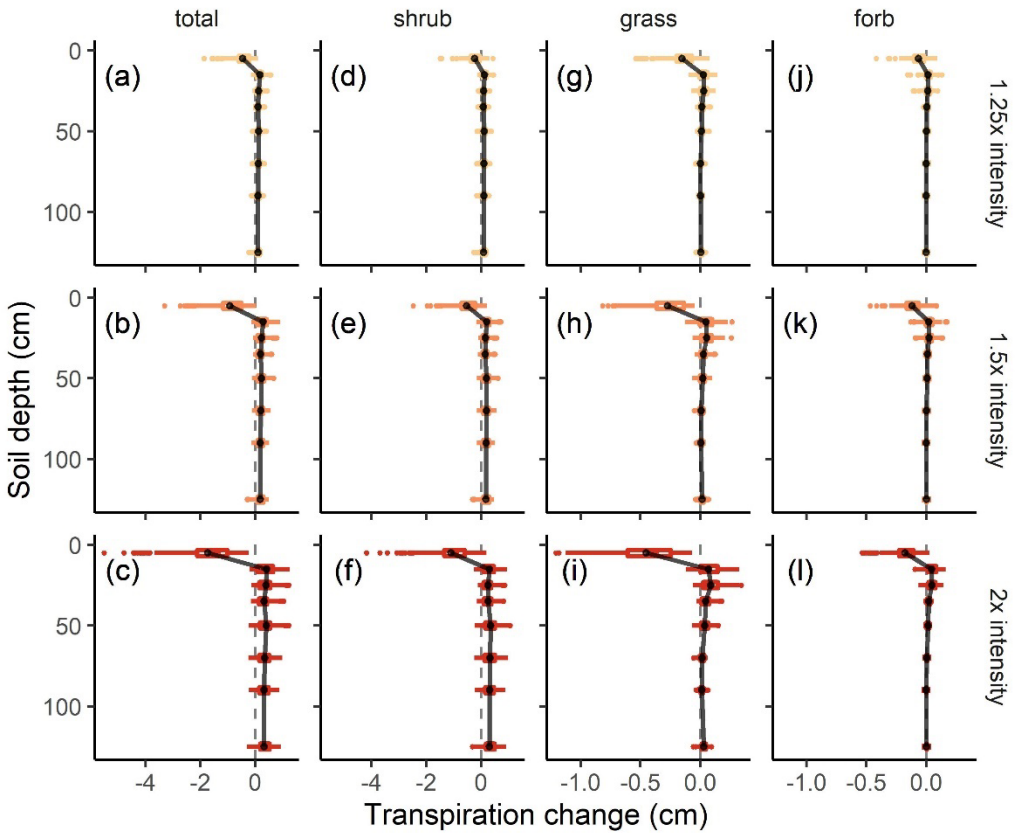

Figure S4.10 Boxplots and mean (black line) change in amount of water transpired annually from eight soil depths for three precipitation intensity treatments (1.25x, 1.5x and 2x) across 200 sites. Changes in total transpiration (across plant functional types) are shown in separate panels from changes in shrub, grass, and forb transpiration. For each site and treatment, the mean amount of water transpired annually from each soil layer was calculated. Values shown are differences between treatment and ambient (control) conditions. Values greater than zero (dashed line) indicate an increase in water uptake from that depth with increased precipitation intensity.

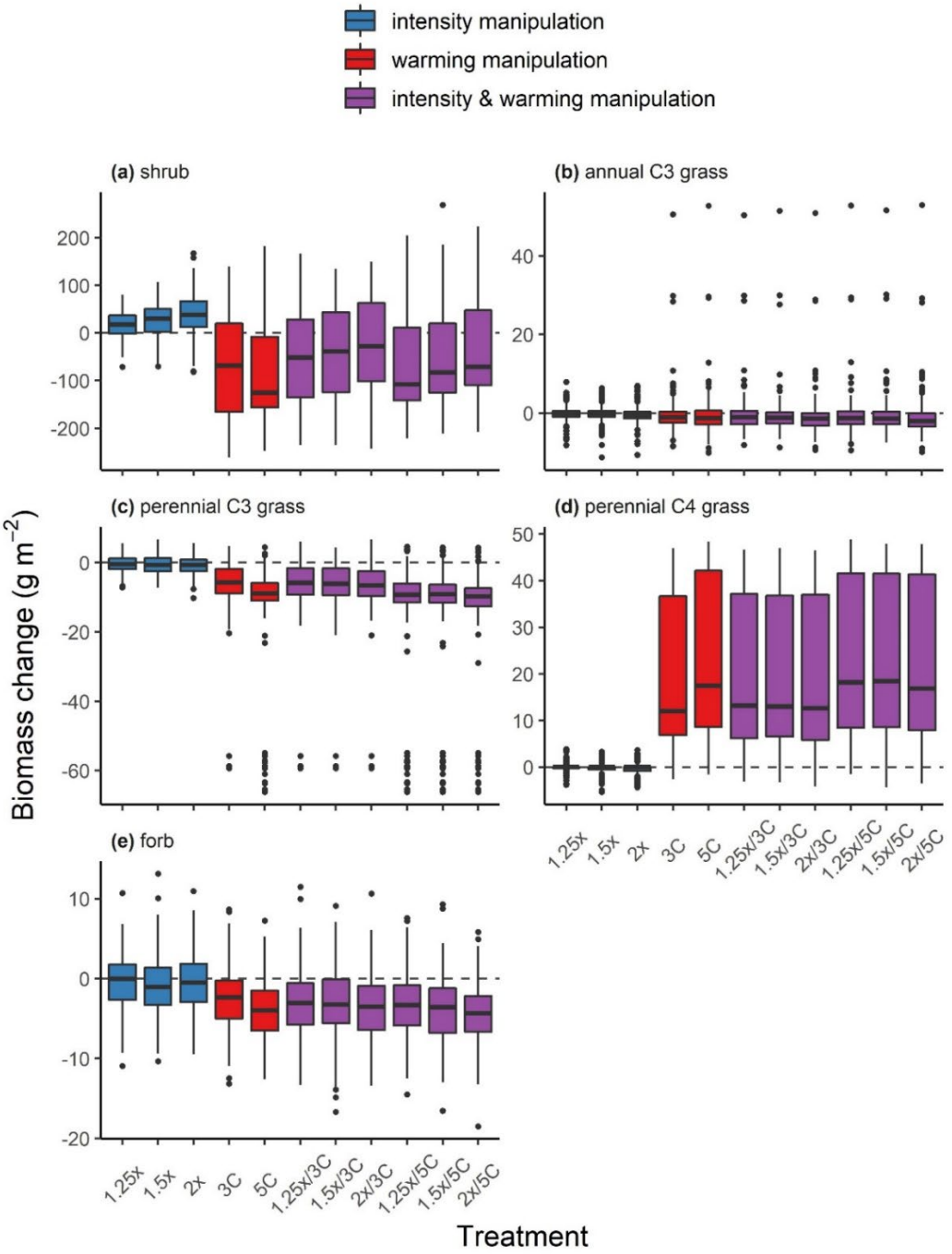

Figure S4.11 Boxplots of biomass responses to increased precipitation intensity and warming treatments, of (a) shrubs, (b) C_3 annual grasses, (c) C_3 perennial grasses, (d) C_4 perennial grasses, and (e) forbs. Biomass response was calculated as the change in biomass of a plant functional type between treatment and ambient (control) conditions at each of 200 sites. Precipitation intensity treatments increased precipitation event sizes by 1.25x, 1.5x, and 2x. Warming treatments raised temperatures by 3 °C and 5 °C. Values > 0 indicate an increase in biomass as a result of the given treatment. Note that y-axis scales differ between panels.

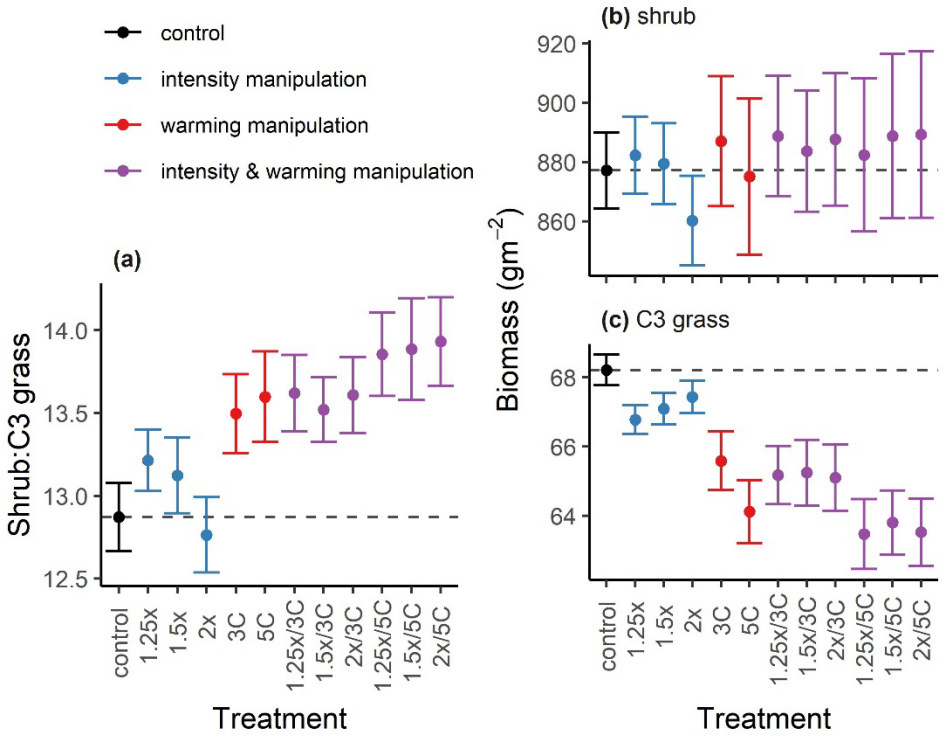

Figure S4.12 (a) Ratio of shrub to C_3 perennial grass biomass, and biomass of (b) shrubs and (c) C_3 perennial grasses, in response to precipitation intensity and warming treatments. Values in panels are means (± 1 SE) across sites with an aridity index > 0.54 (N = 35). Precipitation intensity treatments increased precipitation event sizes by 1.25x, 1.5x, and 2x. Warming treatments raised temperatures by 3 °C and 5 °C. The dashed lines show the mean value under control conditions. Note that the y-axis scale differs between panels (b) and (c). This figure compliments Figure 4.7 in Chapter 4 which shows data from sites with an aridity index < 0.54.

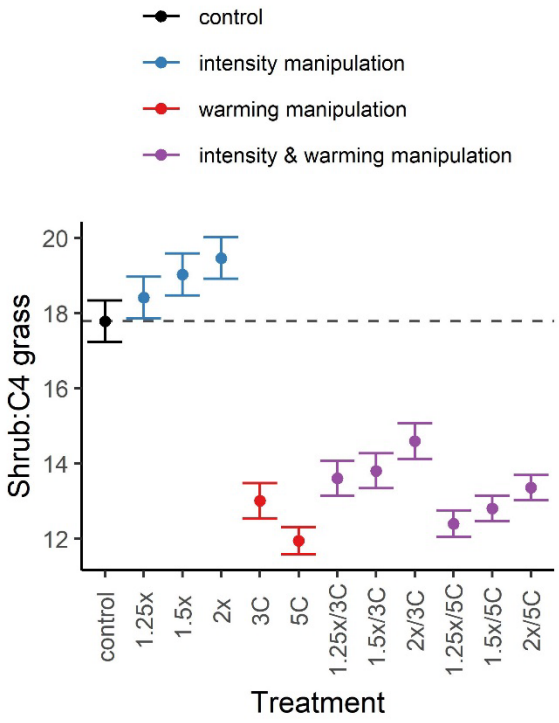

Figure S4.13 Mean (± 1 SE) ratios of shrub to C_4 perennial grass biomass. Precipitation intensity treatments increased precipitation event sizes by 1.25x, 1.5x, and 2x. Warming treatments raised temperatures by 3 °C and 5 °C. The dashed line shows the mean ratio under control (ambient) conditions. Simulations were conducted for 200 sites. However, due to differences in climate between sites, C_4 grasses were only present at 102 sites under ambient (control) conditions. Values shown in this figure are based on those 102 sites.

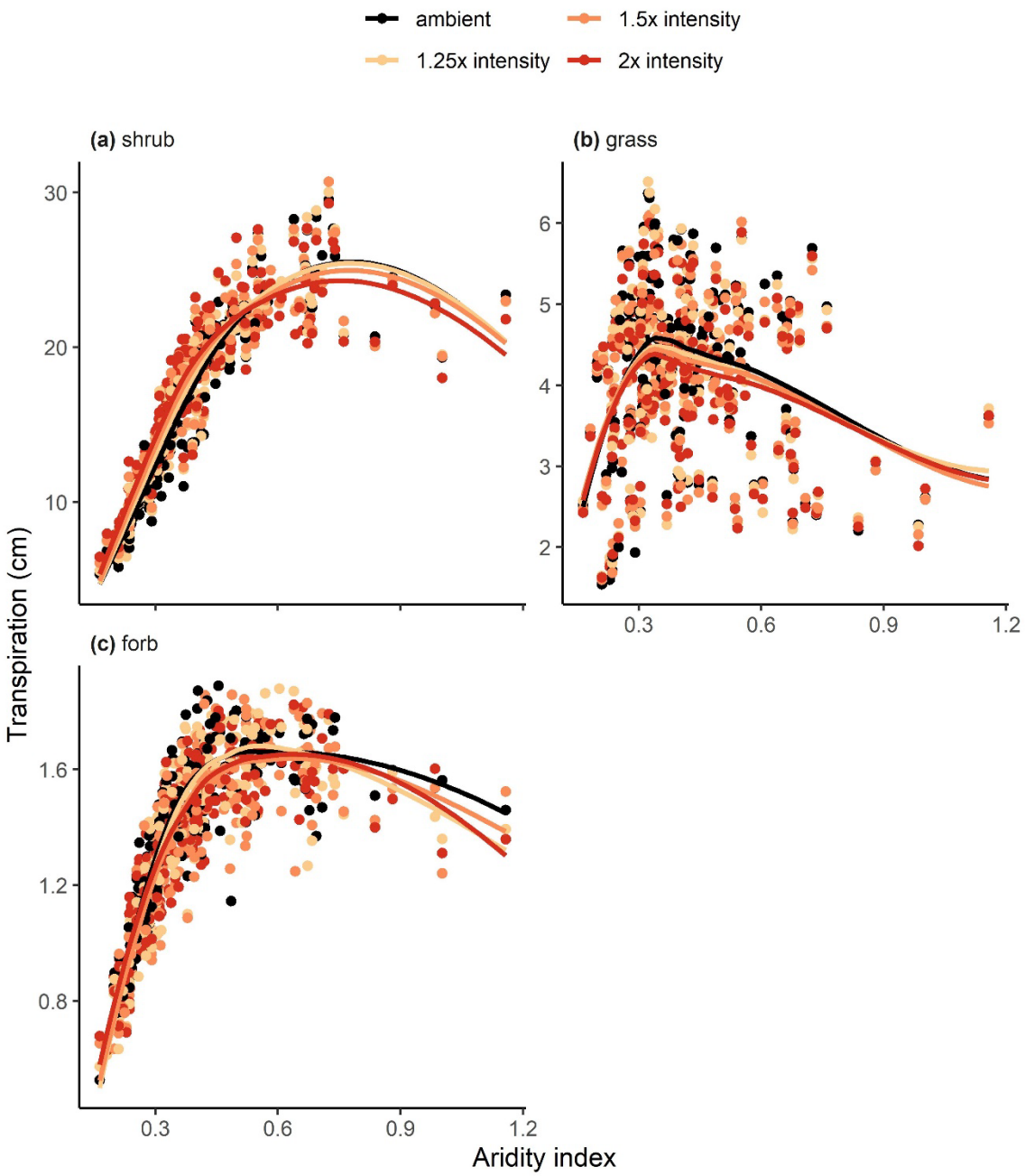

Figure S4.14 Annual transpiration of (a) shrubs, (b) grasses, and (c) forbs in response to increased precipitation intensity versus aridity index (mean annual precipitation/potential evapotranspiration). Points are mean annual values at each site in response to ambient (control) conditions and 1.25x, 1.5x, and 2x increases in mean precipitation event size, respectively. Note that the y-axis scale differs among panels. This figure compliments Figure 4.5 in Chapter 4 where differences in these values between control and treatment conditions are shown for each site.

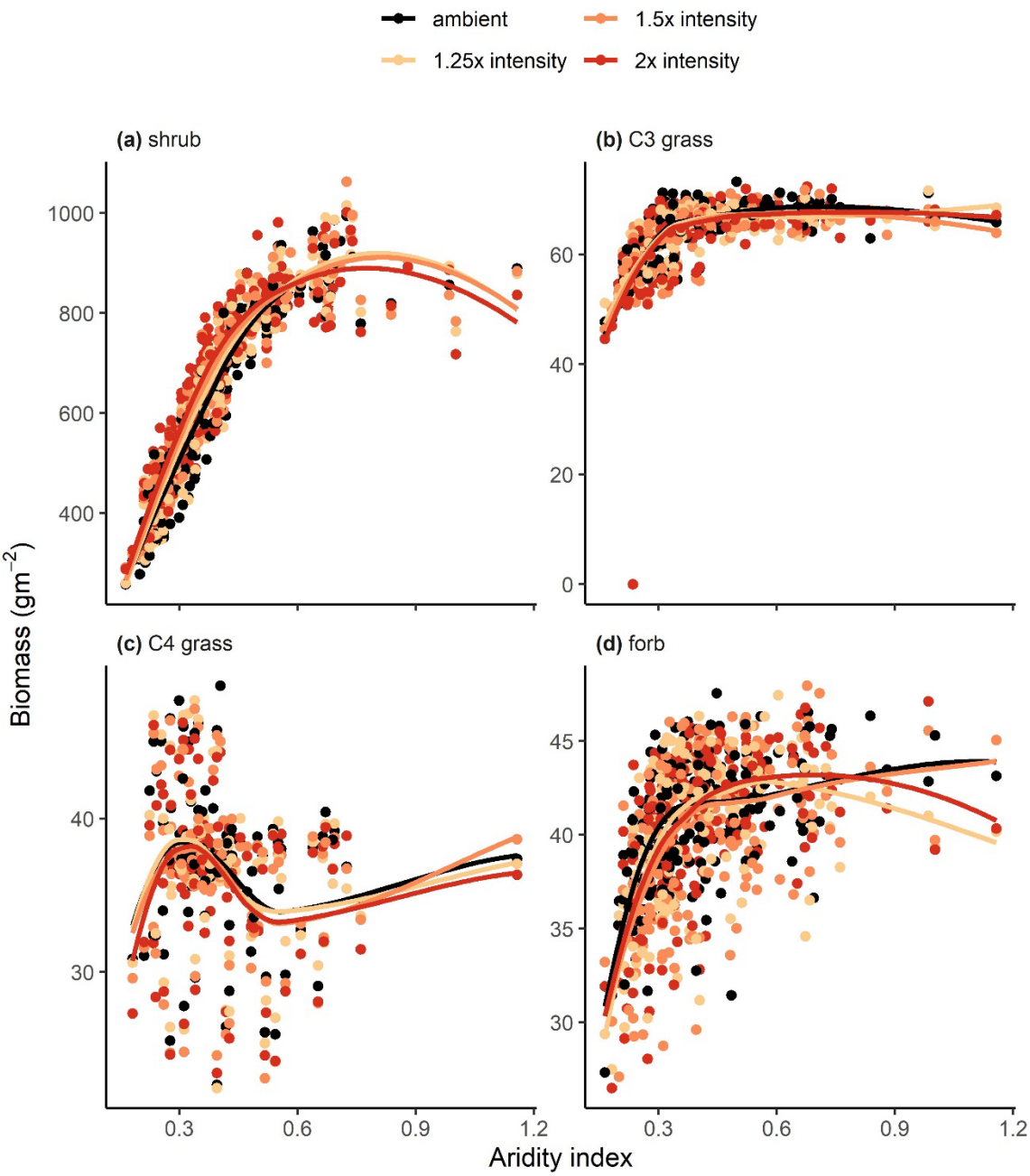

Figure S4.15 Biomass of (a) shrubs, (b) C_3 perennial grasses, (c) C_4 perennial grasses, and (d) forbs in response to increased precipitation intensity across an aridity gradient (mean annual precipitation/potential evapotranspiration). Points are mean biomass values at each site in response to ambient (control) conditions and 1.25x, 1.5x, and 2x increases in mean precipitation event size, respectively. Note that the y-axis scale differs among panels. C_4 grasses were only present at 102 sites under ambient (control) conditions, and panel (c) only shows data from those sites. This figure compliments Figure 4.6 where differences in these values between control and treatment conditions are shown for each site.

Appendix S4.6: Responses of total transpiration, evaporation, and drainage to increased precipitation intensity

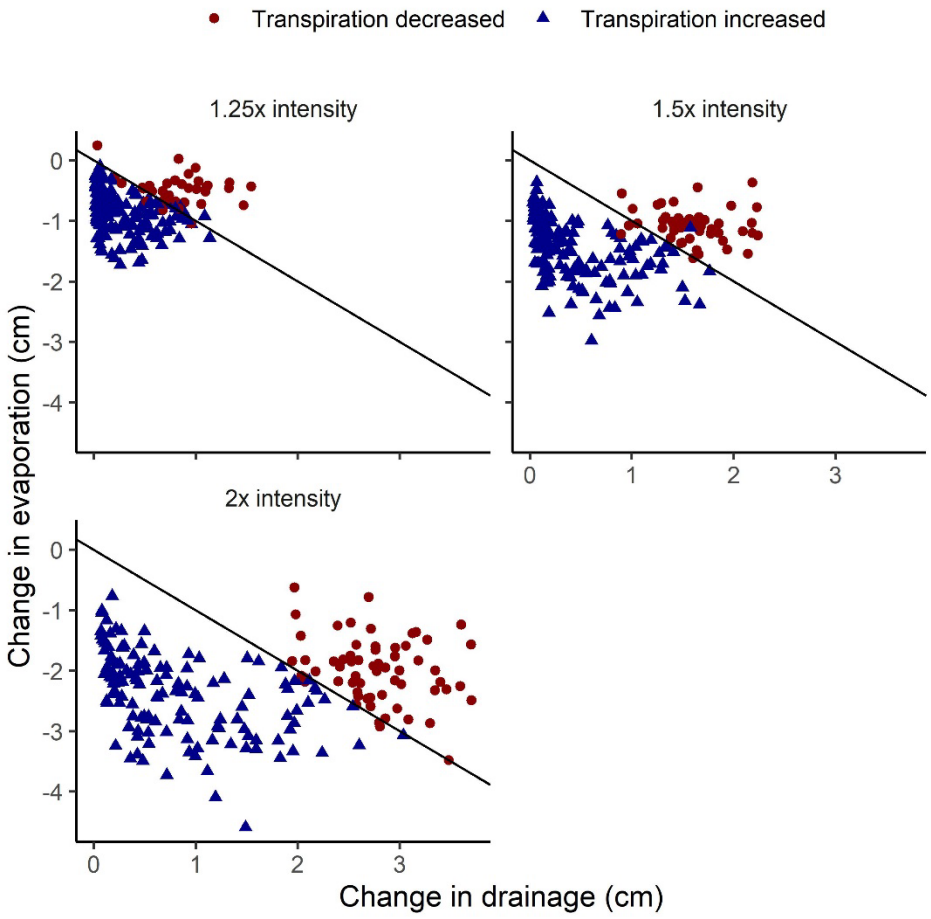

Figure S4.16 Changes in drainage vs. changes in evaporation in response to 1.25x, 1.5x, and 2x increases in mean precipitation event size, respectively. Values shown are differences between ambient (control) and treatment conditions. Red circles indicate sites where total transpiration decreased and blue triangles indicate sites where total transpiration increased in response to the treatments. The black -1:1 line shows the location where decreases in evaporation equal increases in water lost to drainage.

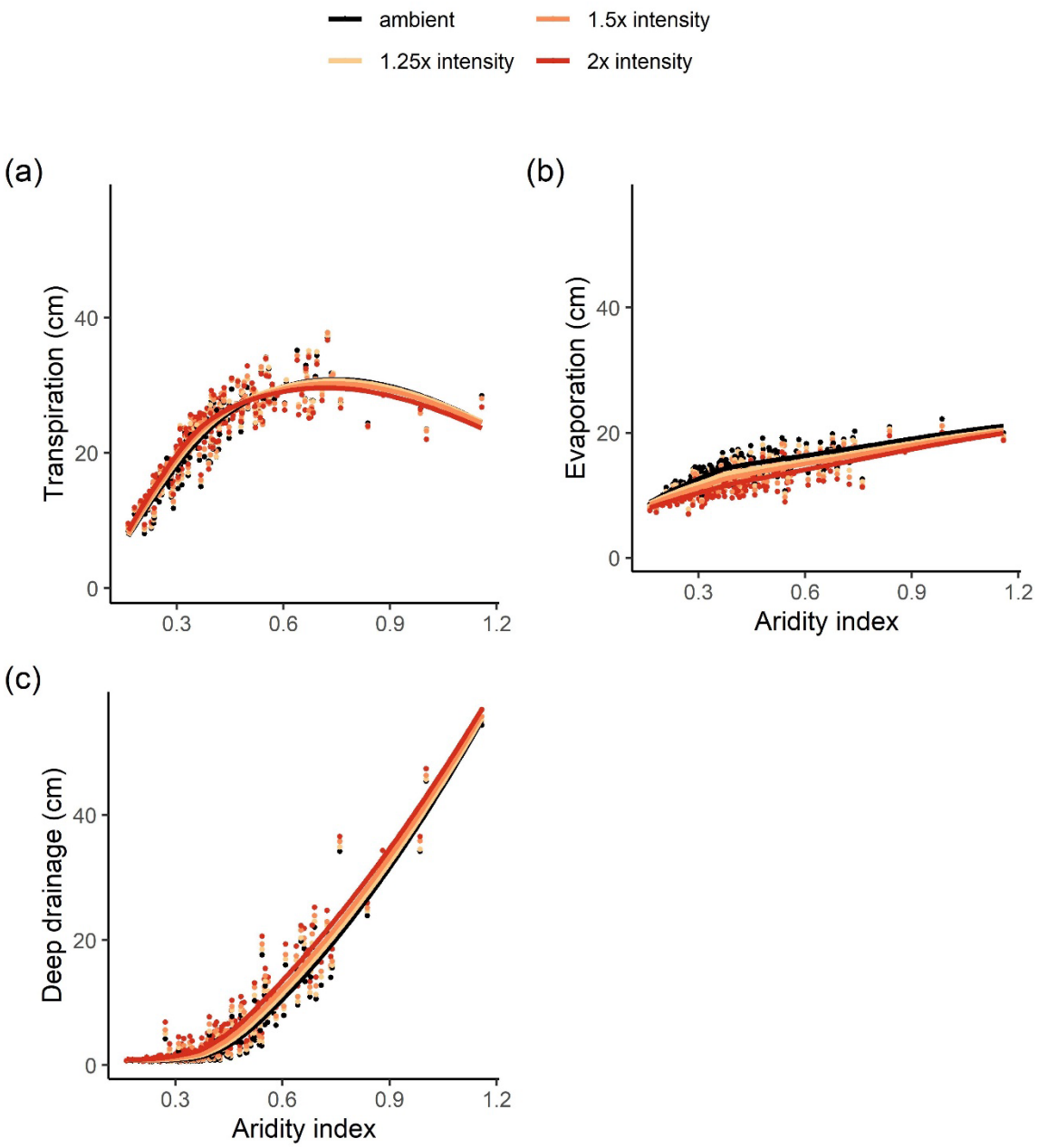

Figure S4.17 (a) Total transpiration across plant functional types, (b) evaporation, and (c) deep drainage of soil water, versus aridity index (mean annual precipitation/potential evapotranspiration). Points are mean annual values at each of 200 sites in response to ambient (control) conditions and 1.25x, 1.5x, and 2x increases in mean precipitation event size, respectively. This figure compliments Figure 4.4 where differences in these values between control and treatment conditions are shown for each site.

CURRICULUM VITAE

Martin C. Holdrege

Graduate Research Assistant
Utah State University
Logan, UT
E-mail: martinholdrege@gmail.com
Phone: 518.567.8250

Education

2016 – present	**PhD Candidate, Ecology,** Utah State University, Logan, UT *Dissertation defended*: Dec. 17, 2021 *GPA*: 4.0 *Committee*: Karen Beard, Andrew Kulmatiski, Kyle Palmquist, Peter Adler, Richard Cutler
2018 – 2020	**Master of Data Analytics,** Utah State University, Logan, UT *GPA*: 4.0 *Specialization*: Statistics
2009 – 2013	**Bachelor of Science in Environmental Biology with Honors,** State University of New York, College of Environmental Science and Forestry, Syracuse, NY *GPA*: 4.0 *Minor*: Applied Statistics

Research and Field Experience

Sept 2016 – Present	Graduate Research Assistant, Utah State University, Logan, UT
Nov 2018 – Present	Data Analysis (contract), Women and Justice Project, Inc., Jackson Heights, NY
April 2020 – Mar 2021	Data Analysis (contract), BioFire Diagnostics, LLC, Salt Lake City, UT
April – Aug 2016	Project Manager, Utah State University, Logan, UT
Nov 2015 – Mar 2016	Lab Technician—entomology, Skyler Burrows, Logan, UT
May – Sept 2015	Field Technician—fire and forest ecology, Utah State University, OR, WA, UT
Jan – April 2015	Prescribed Fire Burn Crew Leader, Georgia Department of Natural Resources, Gay, GA
May – Aug 2014	Field Technician—climate change ecology, University of Alaska Anchorage, Yukon-Kuskokwim Delta, AK
Jan – May 2014	Prescribed Fire Burn Crew Member, Georgia Department of Natural Resources, Gay, GA
Oct – Nov 2013	Intern—plant community restoration, The Nature Conservancy, Geneva, GA
June – Aug 2013	Intern—climate change ecology, Pennsylvania State University, Kangerlussuaq Greenland
June – July 2012	Entomology Research—Summer Scholars Program, Cornell

	University, Geneva, NY
Sept 2010 – May 2012	Forest Ecology Research—Undergraduate Mentoring in Environmental Biology Program, SUNY-ESF, Syracuse and Newcomb, NY
June – Aug 2009	Field Technician, Farmscape Ecology Program, Ghent, NY

Publications

Holdrege, M. C., Beard, K. H., & Kulmatiski, A. (2021). Winter wheat resistant to increases in rain and snow intensity in a semi-arid system. *Agronomy*, *11*(4), 751. https://doi.org/10.3390/agronomy11040751

Holdrege, M. C., Beard, K. H., & Kulmatiski, A. (2021). Woody plant growth increases with precipitation intensity in a cold semiarid system. *Ecology*, *102*(1), 1–11. https://doi.org/10.1002/ecy.3212

Nawrocki, J., Olin, K., **Holdrege, M. C.**, Hartsell, J., Meyers, L., Cox, C., …, Ginocchio, C. C. (2021). The effects of social distancing policies on non-SARS-CoV-2 respiratory pathogens. *Open Forum Infectious Diseases*, https://doi.org/10.1093/ofid/ofab133

Klaus, N. A., Rush, S. A., Weitzel, S. L., & **Holdrege, M. C.** (2020). Changes in tree canopy, groundcover, and avian community following restoration of a montane longleaf pine woodland. *American Midland Naturalist*, *184*(2), 163–176. https://doi.org/10.1637/0003-0031-184.2.163

Kulmatiski, A., Beard, K. H., **Holdrege, M. C.**, & February, E. C. (2020). Small differences in root distributions allow resource niche partitioning. *Ecology and Evolution*, *10*(18), 9776–9787. https://doi.org/10.1002/ece3.6612

Kulmatiski, A., Yu, K., Mackay, D. S., **Holdrege, M. C.**, Staver, A. C., Parolari, A. J., … Trugman, A. T. (2020). Forecasting semi-arid biome shifts in the Anthropocene. *New Phytologist*, *226*(2), 351–361. https://doi.org/10.1111/nph.16381

Datasets

Holdrege, M. C., Beard, K. H., & Kulmatiski, A. (2021). Winter wheat responses to increased precipitation intensity, Utah, USA (2016-2019). *Knowledge Network for Biocomplexity*. doi:10.5063/0000GQ.

Presentations

Holdrege, M. C., K. A. Palmquist, K. H. Beard and A. Kulmatiski. Responses of sagebrush-dominated ecosystems to increased precipitation intensity. Ecological Society of America meeting, Online. August 2021. Oral presentation.

Holdrege, M. C. Responses of sagebrush-dominated ecosystems to increased precipitation intensity. Utah State University, Department of Wildland Resources, Symposium, Logan, UT. April 2021. Oral presentation.

Holdrege, M. C. Rangeland Responses to Increased Precipitation Intensity. Society for Range Management, Utah Section, Annual Meeting. Online. November 2020. Oral presentation.

Holdrege, M. C., Kulmatiski, A., and Beard, K. H. Woody plant growth increases with rain and snow intensity in a shrub-steppe ecosystem. Ecological Society of America meeting, Online. August 2020. Poster presentation.

Wilkins, K., Gherardi, L. A., Wilfahrt, P., **Holdrege, M. C.,** Collins, S., Dukes, J. S., Knapp, A., Phillips, R., Sala, O., and Smith, M. Terrestrial ecosystems vary globally in response to one-year of extreme drought. Ecological Society of America meeting. Online. August 2020. Oral presentation.

Holdrege, M. C., Kulmatiski, A., and Beard, K. H. Woody plant growth increases with rain and snow intensity in a shrubsteppe ecosystem. Ecological Society of America meeting, New Orleans, LA. August 2018. Poster presentation.

Henry, H. A. L., Abedi, M., Alados, C. L., Beard, K. H., Fraser, L. H., Jentsch, A., Kreyling, J., Lamb, E. G., Sun, W., Vankoughnett, M. R., Werner, C., Beil, I., Blindow, I., Dahlke, S., Dubbert, M., Effinger, A., Garris, H. W., Gartzia, M., Gebauer, T., **Holdrege, M. C.,** Arfin Khan, M. A. S., Malyshev, A. V., Paulson, J. P., Pueyo, Y., Stover, H. J., Yang, X. Snow removal versus rain-out shelters as components of reduced precipitation effects on plants: Results from a globally-coordinated distributed field experiment. Ecological Society of America meeting, Portland, OR. August 2017. Oral presentation.

Holdrege, M. C. How changing precipitation regimes impact rangeland plants in northern Utah. Utah State University, Department of Wildland Resources, Symposium, Logan, UT. April 2017. Oral presentation

Holdrege, M. C., Fok, E. J., and Nault, B. A. Potentially important natural enemies of onion thrips in onion fields. Cornell University Summer Scholars Program Undergraduate Research Poster Session, Geneva, NY. July 2012. Poster presentation.

Holdrege, M. C., Fok, E. J., and Nault, B. A. Potentially important natural enemies of onion thrips in onion fields. Sustainable Agriculture Symposium at Cayuga Community College, Auburn, NY. November 2012. Poster presentation.

Holdrege, M. C., Beier, C., and Dovciak, M. Overstory and understory tree communities and light environment in an old growth forest. Northeast Natural History Conference, Syracuse NY. April 2012. Poster presentation.

Holdrege, M. C., Beier, C., and Dovciak, M. Overstory and understory tree communities and light environment in an old growth forest. SUNY-ESF Spotlight on Student Research, Syracuse NY. April 2012. Poster presentation.

Holdrege, M. C. and Vispo, C. Preliminary findings from surveys of native bees on Columbia County, NY, Farms. Northeast Natural History Conference, Albany, NY. April 2008. Nominated top 10 student poster.

Collaborative Endeavors

2016 – Present	International Drought Experiment (DroughtNet): Collaborator/data analyst

Honors and Awards

2020	Ecology Center Student Award (USU)
2017	Ecology Center Student Award (USU)
2013	Departmental Scholar (SUNY-ESF)
2011 – 2012	Class of 1951 Scholarship (SUNY-ESF)
2011 – 2012	Alumni Association Memorial Scholarship Award, Honorable Mention (SUNY-ESF)
2010 – 2011	Alumni Educational Grant (SUNY-ESF)
2009 – 2013	Presidential Scholars Award (SUNY-ESF)

Teaching

2016	Graduate Teaching Assistant: WILD 3830, Range Plant Taxonomy and Function (USU)

Service

Peer Reviewer*: Ecology* // *Agriculture, Ecosystems & Environment*

USU Native American STEM Mentorship Program: Mentored two students for a week in both 2017 and 2018.

Skills

Programming: R (experienced), SQL (familiar), bash (familiar), python (familiar)
Software: git (proficient)
Languages: English (native speaker), German (conversational)